

**N-glycosylation of intrinsic and  
engineered N-X-S/T motifs  
by *Pichia pastoris* can be exploited to  
ligate the mannose receptor but reveals  
no gain in immunogenicity per se**

Dissertation  
zur  
Erlangung des Doktorgrades (Dr. rer. nat.)  
der  
Mathematisch-Naturwissenschaftlichen Fakultät  
der  
Rheinischen Friedrich-Wilhelms-Universität Bonn

vorgelegt von  
**Christoph Kreer**

aus  
Kaiserslautern

Bonn, 2016

Angefertigt mit Genehmigung der Mathematisch-Naturwissenschaftlichen Fakultät  
der Rheinischen Friedrich-Wilhelms-Universität Bonn

1. Gutachter: Prof. Dr. Sven Burgdorf
  2. Gutachter: Prof. Dr. Christoph Thiele
- Tag der Promotion: 07.10.2016  
Erscheinungsjahr: 2016

# Contents

<b>1</b>	<b>Abstract</b>	<b>1</b>
<b>2</b>	<b>Introduction</b>	<b>3</b>
2.1	Human health and the co-evolution of vaccination and immunology . . . . .	3
2.2	The basics of our immune system . . . . .	4
2.3	Antigen presentation links innate immunity to the adaptive immune response . . . . .	5
2.3.1	Dendritic cells sense danger signals and are capable of antigen presentation and T cell priming . . . . .	5
2.3.2	Cytotoxic T cells . . . . .	7
2.3.3	The role of MHC II-restricted presentation to CD4 <sup>+</sup> T helper cells in B cell activation . . . . .	8
2.3.4	Antigen uptake and processing by dendritic cells dictates MHC restriction and forms the basis of rational vaccine design to specifically elicit cytotoxic activity . . . . .	9
2.4	The macrophage mannose receptor (MR, CD206) . . . . .	11
2.5	Information encoded by glycans . . . . .	13
2.6	The advent of defined vaccine formulations and the challenges for modern vaccines . . . . .	15
2.7	<i>Pichia pastoris</i> and its usage in vaccine development . . . . .	16
2.8	Aims of this thesis . . . . .	18
<b>3</b>	<b>Methods</b>	<b>19</b>
3.1	Materials . . . . .	19
3.1.1	Electronic devices . . . . .	19
3.1.2	Consumables . . . . .	20
3.1.3	Antibodies . . . . .	21

3.1.4	Enzymes . . . . .	23
3.1.5	Miscellaneous biologicals, chemicals and reagents . . . . .	24
3.1.6	Kits . . . . .	27
3.1.7	Buffers and solutions . . . . .	27
3.1.8	Media . . . . .	30
3.1.9	Bacteria and yeast strains, cell lines and mice strains . . . . .	31
3.1.10	Primers and plasmids . . . . .	32
3.1.11	Software . . . . .	34
3.2	Methods . . . . .	36
3.2.1	Molecular biology . . . . .	36
3.2.2	Cell culture . . . . .	41
3.2.3	Protein expression in bacteria, yeasts and mammalian cells . . . . .	43
3.2.4	Protein purification . . . . .	46
3.2.5	Protein modification . . . . .	48
3.2.6	Protein analysis . . . . .	49
3.2.7	Cellular assays . . . . .	52
3.2.8	<i>In vivo</i> experiments . . . . .	56
<b>4</b>	<b>Results</b>	<b>58</b>
4.1	The binding of ovalbumin to the mannose receptor is mediated by N-linked glycans . . . . .	58
4.2	<i>Pichia pastoris</i> glycosylates N-glycosylation motifs incidentally present in non-glycoproteins and thereby generates mannose receptor ligands . . . . .	60
4.3	<i>Pichia pastoris</i> -derived $\beta$ -galactosidase is internalized by the mannose receptor . . . . .	65
4.4	<i>Pichia pastoris</i> -derived $\beta$ -galactosidase is delivered to early endosomal compartments . . . . .	69
4.5	<i>Pichia pastoris</i> glycosylates an artificial N-glycosylation site, which can be used as a mannose receptor-targeting strategy for proteins lacking intrinsic N-X-S/T motifs . . . . .	71
4.6	Enforced N-glycosylated proteins from <i>Pichia pastoris</i> do not exhibit immunostimulatory effects <i>in vitro</i> . . . . .	81
4.7	<i>Pichia pastoris</i> -derived N-glycans evoke converse cytotoxic activities for different antigens and are not beneficial for a humoral response <i>in vivo</i> . . . . .	84

4.8	Enforced N-glycosylation of non-glycoproteins can affect MHC class I-restricted epitopes . . . . .	87
<b>5</b>	<b>Discussion</b>	<b>90</b>
5.1	Enforced N-glycosylation by <i>Pichia pastoris</i> as a tool to glycosylate non-glycoproteins . . . . .	90
5.2	Translating enforced N-glycosylation to non-glycoproteins that lack intrinsic N-X-S/T motifs . . . . .	93
5.3	Targeting C-type lectin receptors by protein expression in <i>Pichia pastoris</i>	94
5.4	Alternative targeting approaches for C-type lectins in comparison to enforced N-glycosylation . . . . .	97
5.5	The role of high-mannose glycans as pathogen-associated molecular patterns and their immunostimulatory capacity . . . . .	99
5.6	The influence of <i>Pichia pastoris</i> -derived N-glycans on the cellular and humoral response <i>in vivo</i> . . . . .	101
5.7	Outlook and concluding remarks . . . . .	104
<b>6</b>	<b>References</b>	<b>105</b>
<b>A</b>	<b>Plasmid maps</b>	<b>I</b>
<b>B</b>	<b>Acknowledgments</b>	<b>IV</b>

# 1 Abstract

Vaccination has the power to eradicate viral diseases and is a promising approach to cure cancer. However, modern vaccination strategies repeatedly fail in inducing a robust cytotoxic CD8<sup>+</sup> T cell response, which is needed to eradicate virus-infected or malignantly transformed cells. One way to improve this induction is the targeting of C-type lectin receptors on dendritic cells (DCs) that lead to the presentation of antigens on MHC class I molecules to CD8<sup>+</sup> T cells in a process termed cross-presentation. In addition, certain C-type lectin receptors have the capacity to induce DC maturation, which provides the second crucial signal to induce cytotoxic T cell activation. Yeasts such as *Pichia pastoris* produce N-glycans that are able to ligate such C-type lectin receptors and are thus generally considered to be immunostimulatory. N-glycosylation by *P. pastoris* might hence be exploited in vaccine strategies to promote both MHC I-restricted antigen presentation and DC maturation. However, the benefit of such a vaccination approach remains elusive since the particular effect of *P. pastoris*-derived N-glycans on a cellular and humoral response *in vivo* has not been investigated so far.

Here we tested whether it is possible to introduce N-glycans on proteins that are not glycosylated in their native state by recombinant expression in *P. pastoris* in order to target C-type lectin receptors and increase antigen cross-presentation. For this purpose we expressed  $\beta$ -galactosidase ( $\beta$ -gal), a cytosolic *Escherichia coli* protein bearing several potential glycosylation sites, and a GFP-derivative with an engineered glycosylation site (NST-GFP) in *P. pastoris*. We show that both intrinsic and artificially designed N-glycosylation motifs are readily glycosylated after secretion by *P. pastoris*. We demonstrate that the attached N-glycans ligate the calcium-dependent carbohydrate recognition domains of the mannose receptor (MR), a C-type lectin receptor that mediates cross-presentation of the model antigen ovalbumin (OVA). Antigens internalized by bone marrow-derived dendritic cells (BM-DCs) were consistently routed to OVA-positive compartments related to cross-presentation. However, subsequent *in vitro* anal-

ysis revealed that *P. pastoris*-derived N-glycans had no immunostimulatory capacity on BM-DCs per se. To elucidate the impact of such enforced N-glycosylation *in vivo* we subcutaneously immunized mice with N-glycosylated or enzymatically deglycosylated  $\beta$ -gal or NST-GFP. Surprisingly, the effect of N-glycosylation on *in vivo* cross-presentation proved to be dependent on the nature of the antigen. The presence of N-glycans increased the *in vivo* cytotoxicity against  $\beta$ -gal, whereas a decrease was observed against NST-GFP fused to an immunodominant OVA-epitope. Importantly, for both antigens tested we observed a reduction of the humoral immune response in the presence of N-glycans as indicated by decreased serum IgG in comparison to the group immunized with deglycosylated proteins.

Our data demonstrate that *P. pastoris* can be used to tag non-glycoproteins with N-glycans that target the MR. However, a beneficial effect of such N-glycans on *in vivo* cross-presentation was dependent on the antigen, and the presence of N-glycans consistently decreased a humoral response. These findings have important implications on recombinant vaccines using *Pichia pastoris* as an expression system.

# 2 Introduction

## 2.1 Human health and the co-evolution of vaccination and immunology

Infectious diseases were the main causatives of death worldwide until the beginning of the 20<sup>th</sup> century, and are still important contributors to morbidity and mortality today [1–3]. With the introduction of vaccination once common infectious diseases such as measles or diphtheria were nearly eradicated in industrialized regions like North America, thus leading to a strong decrease in child-mortality in these regions and demonstrating the potential of vaccination to contribute to human health [3–5].

The development of vaccination is profoundly linked to the emergence of immunology as a natural science. Since the proof by Edward Jenner in 1798 that infection with cow-pox induces immunity against small-pox [6], vaccination strategies continuously co-evolved with both the knowledge of the immune system and the technological advances in natural sciences [7]. The introduction of genetic engineering or the identification of pattern recognition receptors as modulators of the immune system are only two examples that have promoted the development of vaccines to become more effective, to have less side-effects, and to cover more diseases [7].

From a historical point of view, vaccination was developed to fight infectious (i.e. communicable) diseases. Yet, in recent years, vaccination strategies have also been translated to non-communicable diseases (NCDs) e.g. cancer, Alzheimer’s disease or autoimmune and chronic inflammatory diseases such as diabetes [8–10]. In any case, ever since then the idea of vaccination has been to activate the host’s own immune system by a harmless vaccine, to eventually fight harmful threats like pathogens and ideally to develop an immunological memory that conveys long-lasting immunity against that certain threat.



Despite the progress in vaccine formulation and immunological research, vaccination design remains challenging as effective vaccines for major health risks like the human immunodeficiency virus (HIV), tuberculosis or malaria are still lacking [11, 12]. One major task for effective vaccination design is the consistent and strong activation of both arms of the so-called adaptive immune response [11, 13].

## 2.2 The basics of our immune system

The immune system can be divided into two interconnected parts, the innate and the adaptive immune system (Figure 2.1) [14]. The innate immune system is a general term for our body’s first line of defense mechanisms against pathogens. These include physical barriers like epithelial surfaces, several cellular components, for example phagocytic cells like macrophages (MΦs) or dendritic cells (DCs), and mechanisms based on a protein network known as the complement system. In terms of first-line-defense, the innate immune system relies on the recognition of conserved pathogen-associated molecular patterns (PAMPs) to quickly restrict the spread of pathogens and simultaneously activate the more specific adaptive immune system [15, 16]. Vaccination strategies mainly aim at the activation of the adaptive immune system with its inherent property to detect virtually any possible antigen.

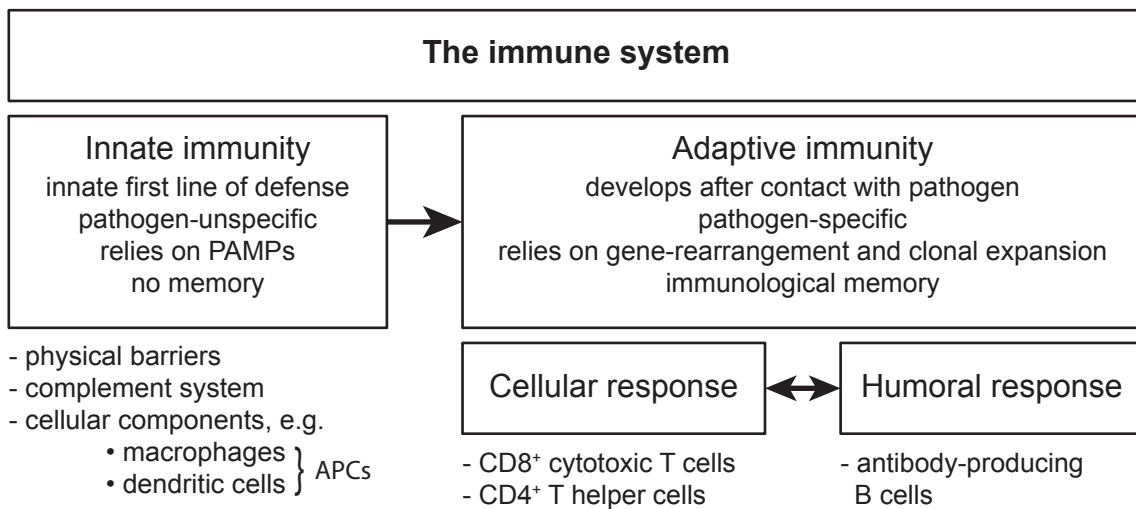


**Figure 2.1: The immune system**

The scheme gives a condensed overview of the components and their properties that constitute the immune system as described in the text.

The two pillars of the adaptive immune system are a humoral and a cellular immune response. The humoral response comprises the generation of antigen specific antibodies by specialized B lymphocytes [17, 18], whereas the cellular response consists of the activation of antigen specific T lymphocytes which are able to carry out diverse cellular functions [19–22]. A rough discrimination of certain effector T cell phenotypes is possible by their characteristic cluster of differentiation (CD) surface molecules. Effector T cells which are able to kill other cells and are hence called cytotoxic T lymphocytes (CTLs) are positive for CD8 [20]. Effector T cells which act as T helper cells ( $T_h$  cells), e.g. in helping B cells to mount an efficient humoral immune response, are positive for CD4 [23]. The key step of T cell activation (T cell priming) is mediated by so-called professional antigen presenting cells (APCs) from the innate immune system, which are mainly dendritic cells and macrophages.

In the case of viral infections, it becomes particularly obvious why it is so important for modern vaccines to activate both arms of the adaptive immune response. A humoral response will be able to neutralize free virus particles and maybe cells from which viral particles are actively budding. But many viruses, e.g. HIV or the hepatitis B virus (HBV), can hide within cells, thereby forming a resting reservoir that will lead to viral rebound if the infected cell is not eliminated directly [24, 25]. Hence, full eradication of a virus will be most likely if both the humoral and the cellular cytotoxic response are activated.

### **2.3 Antigen presentation links innate immunity to the adaptive immune response**

The key to understanding how antigens evoke either humoral or cytotoxic responses lies within the process of antigen presentation and T cell priming by professional antigen presenting cells such as dendritic cells.

#### **2.3.1 Dendritic cells sense danger signals and are capable of antigen presentation and T cell priming**

Dendritic cells are a heterogenous group of cells specialized in antigen presentation [26, 27]. Peripheral dendritic cells screen the tissues for PAMPs and take up extracellular

material by macropinocytosis and receptor-mediated endocytosis to eventually present antigen-derived peptides on major histocompatibility complex (MHC) molecules to T cells. Detection of PAMPs is carried out by a heterogeneous group of germ-line encoded receptors, named pattern recognition receptors (PRRs) [28]. PRRs comprise secreted, membrane-bound and intracellular receptors of diverse receptor classes that engage in multiple functions like complement activation, phagocytosis and DC activation. Due to their important role in innate immune cell activation, PRRs like the toll-like receptor (TLR) family became important targets not only for fine-tuning vaccines to elicit appropriate immune responses against the different types of pathogens [29] but also to inhibit unwanted inflammation [30].

The first human TLR to be characterized was TLR4 [31]. A well-known ligand of this type-1 membrane protein is lipopolysaccharide (LPS), a main cell wall component of gram-negative bacteria [32]. Signaling via TLR4 triggers diverse dose-dependent pathways in DCs that can lead to the increased surface expression of co-stimulatory molecules like CD40, CD80 and CD86, the migration towards lymph nodes and the release of cytokines [33–36]. These phenotypic changes are collectively known as DC maturation [37]. Once in the lymph node, they encounter circulating naïve T cells, which screen the incoming DCs with their unique T cell receptor (TCR) for their cognate antigen. DCs express MHC class I and II, which specifically interact with the TCRs of CD8<sup>+</sup> and CD4<sup>+</sup> T lymphocyte, respectively. However, a proper T cell activation requires more than a mere interaction of the MHC-peptide complex with the TCR. The second essential step is the activation of CD28-signaling in the T cell, which is mediated by the above-mentioned co-stimulatory molecules CD80 and CD86 on the DC. This is one of the key checkpoints in T cell activation as it guarantees tolerance to peptides in the absence of a danger signal (such as TLR-agonists). Upon activation, T cells start to proliferate and differentiate into CTLs in the case of CD8<sup>+</sup> or into T helper cells (T<sub>h</sub> cells) in the case of CD4<sup>+</sup> T lymphocytes (Figure 2.2). Proliferation is accompanied by interleukin-2 (IL-2) secretion and autocrine self-stimulation by the IL-2 receptor on T cells [38], which can be exploited to measure T cell proliferation *in vitro*.

After TLR-activation, DCs and Macrophages also secrete inflammatory cytokines such as interleukin-6 (IL-6), interleukin-12 (IL-12) or tumor necrosis factor alpha (TNF- $\alpha$ ). IL-6 and TNF- $\alpha$  are mainly known as mediators of the classical inflammation symptoms (e.g. fever) and the induction of acute phase proteins of the innate immune system [39, 40]. Besides their effects on innate immunity, cytokines further refine the appropriate

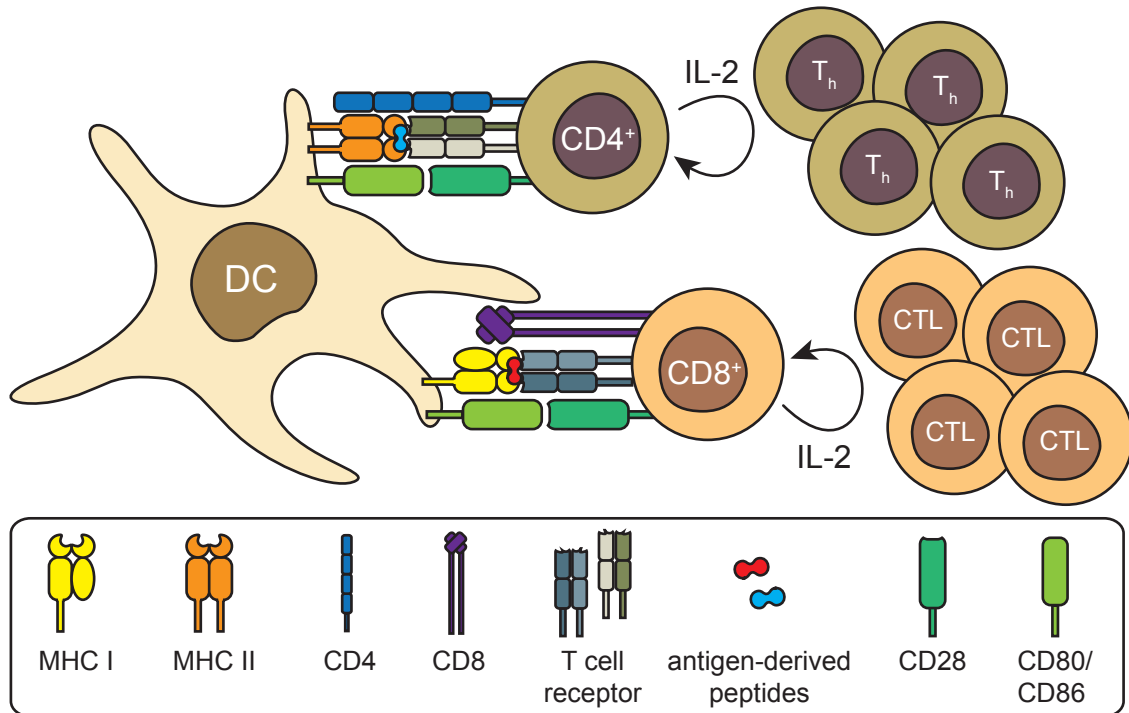


**Figure 2.2: T cell priming by dendritic cells requires antigen presentation on MHC molecules and co-stimulation**

A dendritic cell (DC) presents antigen-derived peptides to naïve  $CD4^+$  and  $CD8^+$  T lymphocytes via MHC class II and class I molecules, respectively. In addition to the interaction between the T cell receptor and the MHC-peptide complex, T cell activation requires co-stimulation of CD28 via CD80/CD86 expressed by the dendritic cell. T cell proliferation is further induced and sustained by autocrine IL-2 signaling.  $CD4^+$  T cells differentiate into  $T_h$  cells,  $CD8^+$  T cells into cytotoxic T lymphocytes (CTL).

cellular program of adaptive effector cells. IL-12 for example promotes  $CD4^+$   $T_h$  cell differentiation into a subset called  $T_{h1}$  cells, which produce Interferon gamma ( $IFN-\gamma$ ) and support macrophage activation and CTL generation [41].

### 2.3.2 Cytotoxic T cells

The  $CD8^+$  cytotoxic T lymphocyte is the major cellular effector cell of the adaptive immune response when it comes to the eradication of malignant or pathogen-infected cells. Hence, the induction of CTLs is a central goal in vaccination strategies. In contrast to MHC class II expression, which is restricted to professional APCs, MHC class I is expressed by all nucleated cells. Upon activation by DCs, CTLs are attracted to the sites of inflammation where they screen target cells for the presentation of their cognate

MHC-I-peptide complex. After recognition, the CTL can engage several mechanism for their cytotoxic activity. These include the secretion of cytokines like TNF or IFN- $\gamma$ , the induction of apoptosis through cell-contact mediated death receptor (FAS) activation on the target cell and the release of cytotoxic granules, which rely on the cytolytic activity of granzymes and perforin [20].

### 2.3.3 The role of MHC II-restricted presentation to CD4<sup>+</sup> T helper cells in B cell activation

The key player in the humoral response is the B lymphocyte. Like T cells, they express a unique receptor that is a product of gene-rearrangement [42]. This B cell receptor (BCR) is part of the immunoglobulin superfamily and represents the membrane-bound variant of the antibody, which can be secreted by the B cell after appropriate activation. In contrast to the MHC-restricted T cell receptor, the BCR directly binds native and unprocessed antigens. But similar to T cells, proper B cell activation requires more than one signal. The first signal comes from BCR cross-linking after antigen binding. For most protein antigens the second signal, however, is delivered by CD4<sup>+</sup> T<sub>h</sub> cell-activity [23]. Like macrophages and DCs, B cells express MHC II molecules which are loaded with antigen-derived peptides [43]. These MHC II-peptide complexes are then recognized by antigen-experienced (i.e. previously activated) CD4<sup>+</sup> T<sub>h</sub> cells that in turn deliver the second signal for B cell activation by cytokines release (e.g. IL-4) and membrane-bound activators like CD40L that binds to CD40 on the B-cell [23]. B cells can additionally undergo several rounds of somatic hypermutation of their BCR, followed by T<sub>h</sub> cell-dependent selection and expansion of only those clones that express a BCR with increased affinity [44]. After this affinity maturation, B cells finally differentiate into antibody secreting plasma or memory B cells [44, 45]. Moreover, class switching from immunoglobulins (Ig) IgM and IgD to IgG, IgA and IgE takes place [46], of which IgG is the most abundant antibody found in the plasma [47]. Class switching also depends on CD4<sup>+</sup> T<sub>h</sub> cells and is modulated by cytokines [46]. Hence, a strong humoral response with high affinity antibodies requires T<sub>h</sub> cell activity, and this in turn requires preceding MHC II-restricted presentation from APCs like DCs to naïve CD4<sup>+</sup> T cells.

### **2.3.4 Antigen uptake and processing by dendritic cells dictates MHC restriction and forms the basis of rational vaccine design to specifically elicit cytotoxic activity**

As described above, the activation of CD8<sup>+</sup> CTLs requires antigen presentation in the MHC class I context, whereas a potent humoral response to protein antigens requires CD4<sup>+</sup> T<sub>h</sub> cell activity, and hence MHC class II-restricted presentation. In DCs, the loading of MHC class II molecules with antigen-derived peptides occurs in late endosomes/lysosomes. The source of such antigens comprises extracellular antigens that are taken up by the cell and enter the endo/lysosomal pathway of degradation but might also include intracellular antigens, which enter lysosomes by autophagy [37]. The common MHC class I loading machinery is situated within the endoplasmic reticulum (ER) and is supplied by cytosolic proteins that were cleaved into peptides by the proteasome [48]. However, if self-synthesized cytosolic proteins were the only source of MHC class I loading, the immune system would not be able to present viral antigens from viruses that do not infect DCs, and tumor-derived antigens would never be presented to cytotoxic T lymphocytes except if a DC itself turned malignant. Fortunately, dendritic cells have developed an additional mechanism that allows the presentation of extracellular antigens on MHC class I molecules — a process termed cross-presentation [49, 50]. The determination whether an extracellular antigen is presented on MHC class II molecules or cross-presented on MHC class I molecules was shown to depend on the uptake mechanism (Figure 2.3) [51]. It could be demonstrated that the model antigen ovalbumin (OVA) enters the classical endolysosomal/MHC class II pathway if it is taken up by macropinocytosis or scavenger receptor (SR)-mediated endocytosis, whereas it is cross-presented after internalization by the mannose receptor (MR). It turned out that the MR shuttles OVA to a distinct compartment which is positive for early endosomal markers like the early endosome antigen-1 (EEA1) and transferrin (Trf), but negative for the lysosomal marker lysosomal-associated membrane protein 1 (LAMP-1) [51]. From here the antigen is exported into the cytosol, degraded by the proteasome, re-imported into the same compartment and loaded *in situ* onto MHC class I molecules by an MHC class I loading machinery spatially separated from the ER [52].

The MR is only one of several PRRs on DCs that supply the cross-presentation pathway with internalized antigens [53–60].

Coupling antigens to natural ligands or antibodies against these receptors is a promising approach to increase uptake and subsequent MHC I-restricted presentation by DCs in order to induce a cytotoxic T cell response in vaccination strategies.

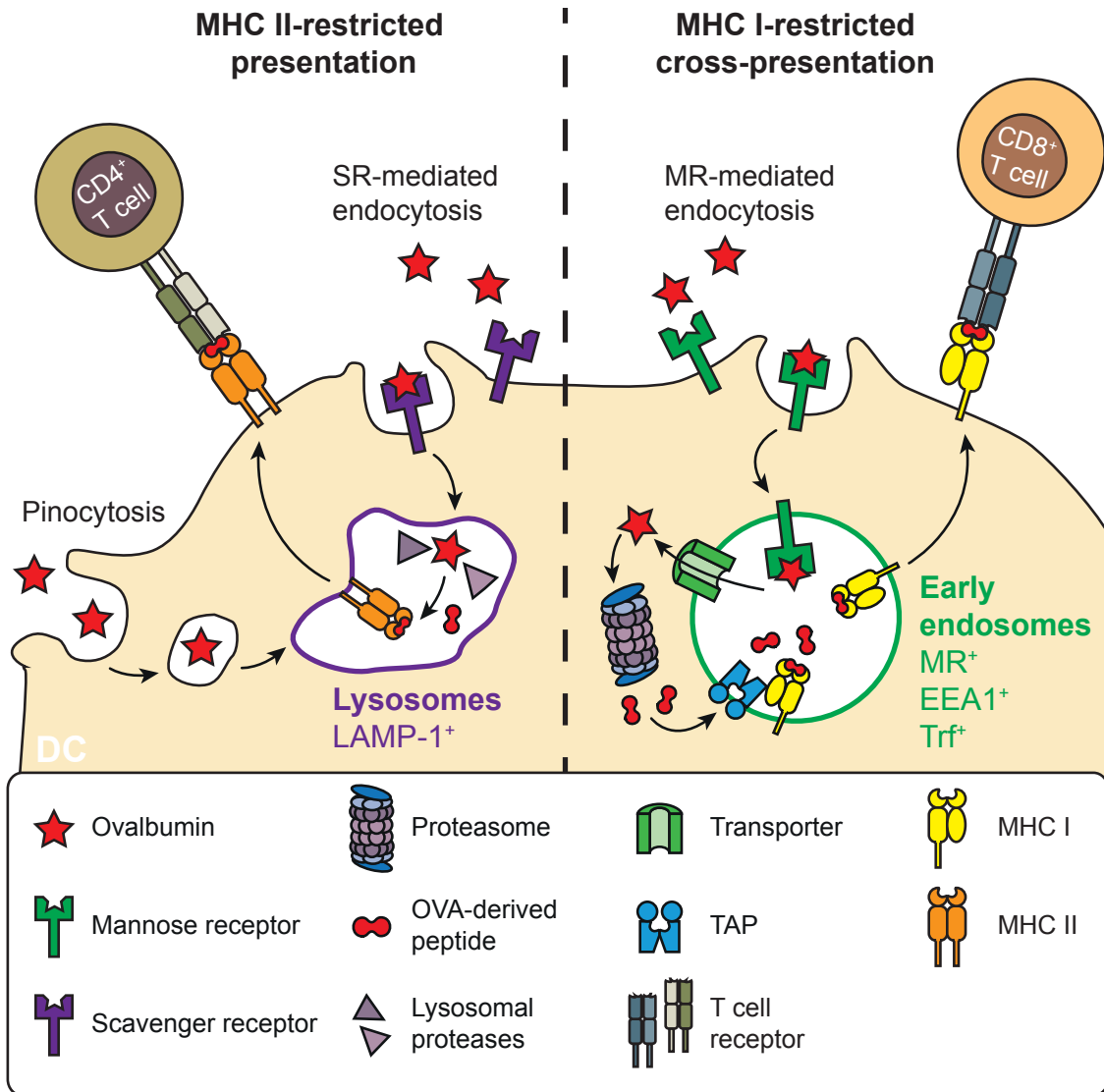


**Figure 2.3: Distinct pathways direct exogenous antigens towards MHC I- or MHC II-restricted presentation**

Ovalbumin that is taken up by scavenger receptor (SR)-mediated endocytosis or pinocytosis is directed towards lysosomal degradation and MHC class II-restricted presentation to  $CD4^+$  T cells. If ovalbumin is endocytosed by the mannose receptor (MR), it enters a distinct early endosomal compartment from where it is processed for MHC class I-restricted cross-presentation to  $CD8^+$  T cells. DC = dendritic cell, LAMP-1 = lysosomal-associated membrane protein 1, EEA1 = early endosome antigen-1, Trf = transferrin, TAP = transporter associated with antigen processing. The graphic is based on Burgdorf et al. 2007 and Kreer et al. 2012 [50, 51].

## 2.4 The macrophage mannose receptor (MR, CD206)

The mannose receptor is a multidomain type I membrane protein and belongs to the C-type lectin-like receptors. C-type lectins are a huge family of proteins [61] that have one or several conserved carbohydrate recognition domains (CRDs). CRDs bind carbohydrates in a calcium-dependent manner [62] and are also referred to as C-type lectin-like domains (CTLDs) [63]. The MR consists of an N-terminal cysteine-rich (CR) domain and a fibronectin II (FNII) domain, which are followed by 8 CRDs, a transmembrane domain and a short cytoplasmic tail (Figure 2.4). The CR domain binds to sulfated carbohydrates (SO<sub>4</sub>-(3)-galactose and SO<sub>4</sub>-(3/4)-N-Acetylgalactosamine) [64, 65], whereas the FNII domain binds to collagen (I, II, III, IV and to a much lesser degree to V) [66, 67]. The C-type lectin activity is mediated by the CRDs 4–8, whereas CRDs 1–3 do not bear carbohydrate-binding properties [68]. From the CRDs 4–8, only CRD4 shows strong binding to the monosaccharides mannose, fucose and N-Acetylglucosamine in isolation [68]. High affinity binding to multivalent ligands, however, requires the participation of the CRDs 4–7 [69]. Binding studies with isolated human MR revealed a prevalence of branched over linear mannose oligosaccharides or monosaccharides [70]. Two well-described ligands of the MR are yeast mannan and the model antigen ovalbumin (OVA). Mannan is a natural polymer derived from *Saccharomyces cerevisiae* and consists of multiple  $\alpha$ -1,2-,  $\alpha$ -1,3- or  $\alpha$ -1,6-linked mannose residues [71]. OVA, a ~45 kDa glycoprotein with high-mannose glycans attached to Asn292 [72], is the main component of hen egg white.

Upon antigen internalization, the MR enters early endosomes from where it recycles back to the cell surface [73, 74]. In the steady state, roughly 80% of the MR are present within these recycling endosomes [75]. The short cytoplasmic N-terminal tail harbors a di-aromatic motif (Tyr18-Phe19), which was reported to be essential for receptor internalization and sorting in recycling endosomes [76]. The MR lacks further signaling motifs in its cytoplasmic tail and concordantly did not induce cytokine release upon binding to mannan [77]. In the same study, however, cross-linking ligands like antibodies or mannose-capped lipoarabinomannan (ManLAM) induced anti-inflammatory cytokines [77]. In contrast, other studies reported the MR-dependent release of pro-inflammatory cytokines [78, 79]. The data are discussed controversially, and Gazi et al. suggested that the MR engages signaling-competent co-receptors which account for the diverse signaling pathways but is not able to signal on its own as shown for mannan [80].



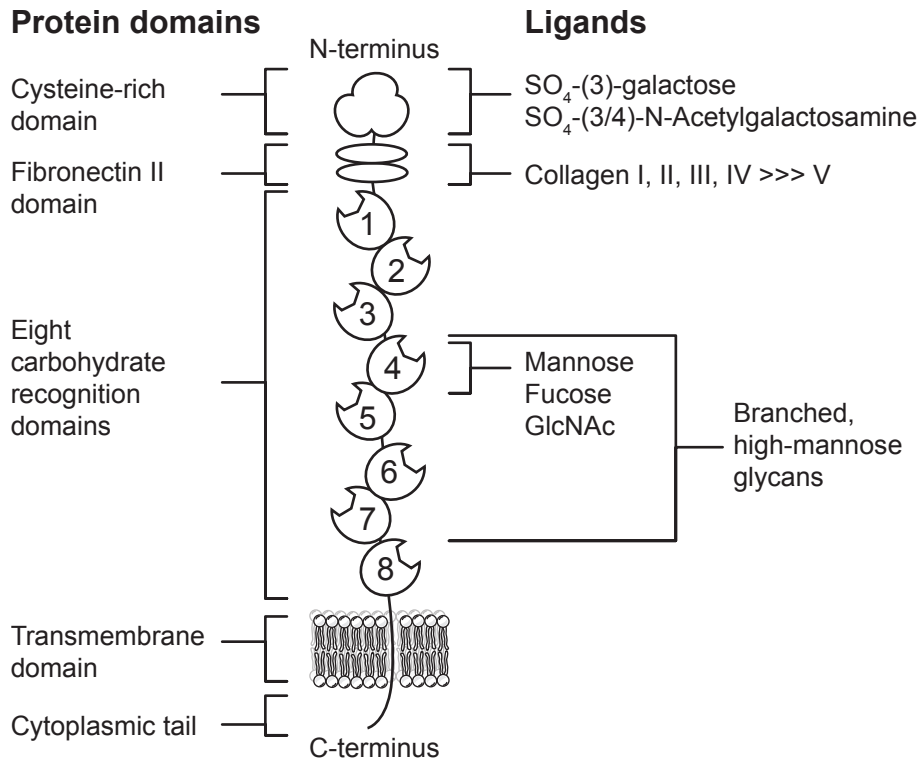


**Figure 2.4: The mannose receptor**









The MR comprises different types of protein domains that differ in their ligand specificities. GlcNAc = N-Acetylglucosamine. This modified graphic is based on Martinez-Pomares et al. 2006 [66].

The MR is expressed by subsets of several myeloid immune cells including monocytes, macrophages, dendritic cells or Langerhans cells, but also by endothelial cells like the dermal microvascular endothelial cells (DMECs) and liver sinusoidal endothelial cells (LSECs) [81, 82]. Specifically in monocytes, macrophages and dendritic cells, MR expression and engagement for antigen uptake seem to be tightly controlled by the activation state and show variations depending on whether cells were freshly isolated or generated *in vitro* [81, 83–85]. Besides its participation in antigen uptake it also plays a crucial role in collagen internalization by macrophages [86] and LSECs [87]. Additionally, the MR has been reported to regulate serum glycoprotein homeostasis [88] and to mediate cell adhesion and trafficking, for example by its expression on lymphatic vessels [89].

## 2.5 Information encoded by glycans

The natural ligands of C-type lectins like the MR are polysaccharides. One type of polysaccharides — called glycans — can be attached to other macromolecules, such as lipids (e.g. in the case of LPS) or proteins. The most important building blocks for protein associated glycans are the carbohydrates summed up in Table 2.1.

**Table 2.1: Monosaccharide building blocks of glycans**

Name	Symbol	Abbreviation
Galactose		Gal
Glucose		Glc
Mannose		Man
N-Acetylgalactosamine		GalNAc
N-Acetylglucosamine		GlcNAc
Fucose		Fuc
N-Acetylneuraminic acid (Sialic acid)		NANA
Xylose		Xyl

Glycosylation (i.e. the attachment of glycans) is a major post-translational modification on proteins in eukaryotic cells. Two types of glycosylations, N- and O-glycosylation, are distinguished due to their linkage to the protein and their side of synthesis [90]. N-glycosylation starts co-translationally in the endoplasmic reticulum. During protein synthesis, the N-glycosylation motif N-X-S/T (where X denotes any amino acid except proline) is recognized by a glycosyltransferase that transfers a pre-assembled high-mannose core-glycan to the amide nitrogen of the asparagine within that motif [91]. Core glycans can be further edited during the secretory pathway in the ER and the Golgi apparatus [92]. This occurs by several glycosidases and glycosyltransferases, which trim or add specific monosaccharides ending up in three major types of glycans in animal cells, namely high-mannose, complex or hybrid type (Figure 2.5). In contrast, O-glycosylation takes strictly place post-translationally in the Golgi apparatus by the linkage of a monosaccharide to the hydroxyle group of either serine or threonine [93] (Figure 2.5). In mammals, the first monosaccharide is typically a GalNAc, which is subsequently branched by Gal or GlcNAc at C3, and potentially by another GlcNAc at C6 to form several types of core structures. The core is then elongated by sequential addition of further monosaccharides. Up to date, there is no consensus sequence known for O-glycosylation, thus making this type of modification hardly predictable. Convenient tools for glycan analysis are specific glycosidases like Endoglycosidase H (Endo H), which cleaves between the first two

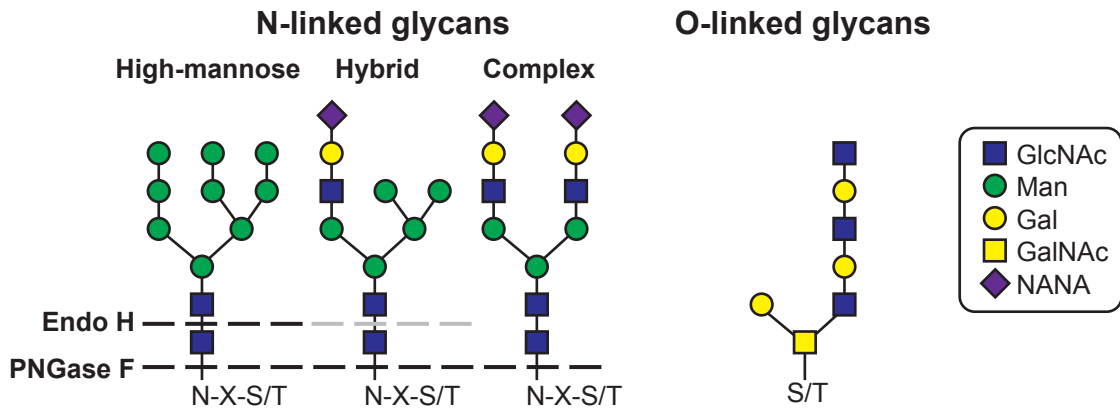


**Figure 2.5: Glycans in mammalian cells**

N-linked glycans are attached to the nitrogen of an asparagine in the N-X-S/T motif and can be separated into the three groups depicted above. O-linked glycans consist of one out of four possible core structures attached to the side-chain of either serine or threonine, which is then further elongated. All glycans depict representative examples and may vary in the total number and, except for high-mannose, in the types of the attached monosaccharides. Dashed lines indicate cleavage sites of the glycosidases Endo H and PNGase F. The O-linked glycan depicts a core 2 structure. N = asparagine, X = any amino acid except proline, S = serine, T = threonine.

GlcNAc within high-mannose and some hybrid N-glycans or Peptide-N-Glycosidase F (PNGase F), which cleaves between the first GlcNAc and asparagine (Figure 2.5).

Glycans play diverse roles *in vivo*, ranging from the rendering of protein-properties like solubility and stability to cell-adhesion and communication [94]. In terms of communication, glycans are able to decode high levels of information through their structural properties. In contrast to amino acids, which always form a backbone through the amine and carboxylic acid at the alpha carbon, monosaccharides can engage all of their free hydroxyl groups to form glycosidic bonds at several positions. The result is the formation of branched glycans which have a complex three-dimensional structure. This directly reflects in the variety and substrate specificity of C-type lectins like the MR. Several C-type lectins might have conserved CRDs that show the same affinity for a monosaccharide like mannose. However, keeping in mind that most lectins engage several CRDs to yield high affinity binding, they can still differ in their natural glycan ligand due to the three-dimensional orientation of their CRDs [95].

It seems obvious that eukaryotic glycans differ from prokaryotic glycans, as the latter lack the ER and Golgi apparatus. But also eukaryotic glycans greatly differ from each other, as glycosylation pathways have evolved differently during eukaryotic evolution

[96]. Yeasts have only a limited set of additional glycosyltransferases resulting in the formation of high-mannose glycans only [71]. Yet, differences in glycans also occur between different yeast-genera such as *Saccharomyces cerevisiae* and *Pichia pastoris* by the favored engagement of certain linkages, branching and the number of monosaccharides added to the core structure [97]. Plants can add  $\alpha$ -1,3-linked fucose and the pentose xylose to their glycan core, which are both not present in mammalian glycans and hence immunogenic [98]. Mammalian glycans, on the other hand, are often capped by sialic acid (N-Acetylneuraminic acid) [90]. Even within the same species unique glycans define subgroups of individuals, as impressively demonstrated by the human blood groups, which have strong clinical relevance in the case of transfusion and transplantation [99].

Given this high content of information encoded by glycans, it is not surprising that the mammalian immune system makes use of them to detect pathogens and discriminate non-self from self or harmful from harmless. Immunologists realized the role of non-self glycans as targets of the immune system early, and in the late 70s of the 20<sup>th</sup> century the first polysaccharide based vaccine was published, which was derived by purification from meningococci [100, 101].

## 2.6 The advent of defined vaccine formulations and the challenges for modern vaccines

The earliest vaccines followed the principle of attenuation, where live, attenuated pathogens were administered to convey immunity against a severe pathogen [7]. The prototype attenuated vaccine by Edward Jenner was a pathogen-related virus that is less harmful [6]. Later, attenuation was achieved by cell culture methods yielding mutated viruses that had lost their virulency, yet kept their immunogenicity [102, 103]. Another approach that was quickly translated into vaccination was the killing or inactivation of pathogenic bacteria and viruses [104]. Both approaches have their drawbacks. The first includes mainly the risk of unintentional regain of the pathogen's virulency after administration [105]. The second approach, though safer in general, often shows reduced immunogenicity, thus leading to the requirement of additional adjuvants [106]. Both have in common that they are highly empirical approaches. Though the genome of a pathogen might be fully sequenced these days, the precise amount of each of the thousands of different macromolecule and their individual and composite influence on the immune-response

are hardly predictable. Hence, the trend has shifted towards defined vaccine formulations that contain subunits of the pathogens as antigens [3, 105, 107]. Historically, this strategy started with the purification of pathogen-derived macromolecules such as the polysaccharides of meningococci [100]. In terms of pathogen-derived proteins, this approach was then strongly promoted by the advent of recombinant protein technologies. Nowadays, potential subunit vaccines are produced in the whole spectrum of available prokaryotic and eukaryotic expression systems [7, 105, 108].

Sole administration of proteinaceous subunit vaccines, however, is often ineffective in eliciting CD8<sup>+</sup> T cell responses and will, if at all, primarily induce humoral immunity [105]. This is likely to be attributed to several factors. First, to be efficiently presented to T cells, antigens have to be taken up by DCs and processed towards MHC class I- or class II-restricted presentation. Depending on the vaccine administration route, however, unspecific pinocytosis by DCs might compete with other cells that contribute to *in vivo* clearance. Furthermore, the uptake of antigens by pinocytosis favors MHC II-restricted presentation [51], thereby skewing the immune response towards humoral immunity. Second, proteinaceous vaccines without any PAMP are not able to induce DC maturation and will rather induce tolerance than immunity [53]. Therefore, current subunit vaccines have to be supplied with adjuvants to activate TLRs or other receptors that induce DC maturation [53, 109, 110].

Taken together these weak points illustrate the strong need for strategies that on the one hand specifically target receptors on DCs that mediate cross-presentation and on the other hand simultaneously activate the DCs to eventually induce a strong CD8<sup>+</sup> T cell response.

## **2.7 *Pichia pastoris* and its usage in vaccine development**

Yeast expression systems combine the advantages of prokaryotic expression systems like the simple and cost-efficient high yield production of recombinant proteins with the potential to add eukaryotic post-translational modifications. Among all possible yeasts, *Pichia pastoris* (*P. pastoris*) has recently gained increasing popularity in the production of recombinant subunit vaccines [108]. *P. pastoris* was introduced as an expression system in 1985 [111]. This yeast strain is special in that it can grow on methanol as the sole carbon source. Commercial expression vectors like the pPICZ vectors (Life Technologies, Thermo Fisher Scientific) make use of the methanol induced alcohol oxi-

dase 1 promotor to drive strong protein expression which is precisely controllable [112]. The yeast is capable of growing at high cell densities, thus allowing the production of large biomass cultures, which results in high protein yields (up to 14.8 g/L have been reported [113]). Accordingly, several studies have used *P. pastoris* to yield high amounts of recombinant subunit vaccines [114–116]. Like other yeasts, *P. pastoris* is only capable of adding high-mannose glycans to its glycoproteins. In comparison to *S. cerevisiae* it tends less to hypermannosylation, which is the repetitive addition of an  $\alpha$ -1,6-linked mannose moiety to one antennary that can be elongated with further mannose-residues in  $\alpha$ -1,2-linkages [117]. Due to their potential recognition by C-type lectin receptors of the immune system, yeast-derived high-mannose glycans have repeatedly been considered to be immunogenic [112, 117, 118], and a lot of effort has been put in the humanization of glycosylation pathways, especially in terms of human therapeutic proteins [119]. On the other hand, an intrinsic adjuvancy and the potential to target C-type lectin receptors related to cross-presentation represent two valuable properties for subunit vaccines as described above. Accordingly, glycoproteins like ovalbumin [120] or the P-selectin glycoprotein ligand-1 [121] were intentionally expressed in *P. pastoris* with the goal to increase their immunogenicity, and *in vitro* studies prove that such glycoproteins are indeed recognized by C-type lectins including the MR and dendritic cell-specific ICAM-3 grabbing non-integrin (DC-SIGN) [122, 123]. This suggests that the addition of yeast-derived glycans to any protein could be used as a strategy to target C-type lectin receptors for improved cross-presentation and eventually eliciting a cytotoxic T cell response *in vivo*. Such an approach would be especially valuable if it could be translated to subunit vaccines that are not glycosylated in their native state. N-glycosylation by *P. pastoris* is initiated by the N-X-S/T amino acid sequon that could be exploited as a glycosylation tag for such subunit vaccines. However, the precise impact of *P. pastoris*-derived N-glycans on the *in vivo* response remains unclear, as none of the available studies directly compared N-glycosylated versus deglycosylated proteins *in vivo*. Furthermore, the concept that yeast-derived mannosylation per se increases immunogenicity remains controversial, as mannose-specific receptors like the MR were also reported to act in homeostasis [124], and MR-targeting on monocyte-derived DCs even led to the secretion of anti-inflammatory cytokines [77].

## 2.8 Aims of this thesis

A potent cytotoxic T cell response is a prerequisite for an efficient anti-viral or anti-tumor immune response and remains a challenging task in today's vaccine design. C-type lectin receptors like the MR are involved in antigen cross-presentation and are hence promising targets for vaccines that aim at evoking such cytotoxic responses. Glycoproteins expressed in *P. pastoris* have been shown to bind C-type lectin receptors including the MR, thus demonstrating that glycosylation by *P. pastoris* is a potential targeting strategy for the MR.

The primary goal of the present work was to investigate whether N-glycosylation by *P. pastoris* is a convenient way to target C-type lectins like the MR in order to improve cross-presentation in vaccination strategies. In this respect it was of particular interest to develop a strategy to N-glycosylate proteins that lack glycans in their native state. The binding of such proteins to MR subdomains and the uptake and subcellular localization in DCs were to be carefully characterized, since cross-presentation of OVA requires the C-type lectin activity of the MR and its subsequent localization in distinct early endosomal compartments. Finally, the applicability of the developed targeting strategy for vaccine design was to be critically evaluated. Therefore, the immunostimulatory capacity of the *P. pastoris*-derived N-glycans and their impact on the cellular and humoral immune response were to be determined.

# 3 Methods

## 3.1 Materials

### 3.1.1 Electronic devices

Device Name	Manufacturer	Category	Specifications
5417R	Eppendorf	Centrifuge	F45-30-11 rotor
5810R	Eppendorf	Centrifuge	A-4-81 rotor
Allegra X-15R	Beckmann Coulter	Centrifuge	SX4730 rotor
ARE	VELP Scientifica	Heating magnetic stirrer	Multi-purpose stirrer
Avanti J-26XP	Beckmann Coulter	Centrifuge	JA-14, JA-25.50, JLA-8.100 rotor
BioLogic LP	Bio-Rad	low-pressure chromatography system	LP chromatography, operated with Model 2110 fraction collector
CB 210	Binder	CO2 Incubator	Cell culture
ChemiDoc MP	Bio-Rad	Imaging system	Gel and WB detection
FluoroMax-4 Spectrofluorometer	Horiba	Fluorescence spectrometer	Fluorescence spectroscopy
FiveEasy	Mettler Toledo	pH Meter	Operated with LE409 glasselectrode
Gauva easyCate	Merck Millipore	Flow cytometer	Flow cytometry
Infinite® 200 PRO	Tecan	Multimode plate reader	Fluorescence measurement 96-well format, ELISA
Innova 40 and 44	New Brunswick	Incubator shaker	Bacteria/Yeast incubation

*Continued on next page*



*Continued from previous page*

<b>Device Name</b>	<b>Manufacturer</b>	<b>Category</b>	<b>Specifications</b>
LSR II	BD Bioscience	Flow cytometer	Partially operated with HTS system, flow cytometry
Mini-PROTEAN Tetra Cell	Bio-Rad	Vertical electrophoresis system	SDS-PAGE
Mini-Sub Cell GT Cell and Wide Mini-Sub Cell GT Cell	Bio-Rad	Horizontal gelelectrophoresis system	DNA-gel electrophoresis
Multiskan Plus Type 355	Thermo Scientific	Microplate Reader	ELISA
NanoDrop 2000	Thermo Scientific	Spectrophotometer	UV-Vis spectroscopy
NanoVue Plus	GE Healthcare	Spectrophotometer	OD measurement
PowerPac Basic and PowerPac HC	Bio-Rad	Power Supply	Power supply for Bio-Rad electrophoresis and Trans-Blot cells
Sonopuls HD 2070	Bandelin	Sonicator	Operated with MS 37 sonotrode
Trans-Blot SD	Bio-Rad	Semi-Dry Transfer Cell	Semi-Dry WB
Universal Oven UN-55	Memmert	Incubator	Bacteria/Yeast incubation
Vortex mixer ZX3	VELP Scientifica	Vortex mixer	Sample mixing

### 3.1.2 Consumables

<b>Consumable*</b>	<b>Manufacturer</b>
24-well plate, tissue culture treated (PS)	TPP
48-well plate, tissue culture treated (PS)	TPP
96-well plate, tissue culture treated (PS)	TPP
96-well plate, round bottom (PS)	Sarstedt
96-well Microlon ELISA plate, flat bottom, high binding (PS)	Greiner
96-well FLUOTRAC plate, black, flat bottom, high binding (PS)	Greiner

*Continued on next page*

*Continued from previous page*

<b>Consumable*</b>	<b>Manufacturer</b>
Amersham Protran 0.2 NC western blotting membrane (0.2 µm pore size, nitrocellulose)	GE Healthcare
Amicon Ultra-4 and -15 centrifugal filter units (10, 30 and 50 kDa MWCO)	Merck Millipore
BD Plastipak Syringe (1, 10 and 5 mL, PP/PS/rubber)	BD
Erlenmyer flasks, baffled (5 L, borosilicate glass 3.3)	Labomedic
Beaker (0.1 – 1 liter, borosilicate glass 3.3)	Duran
Blotting paper (1.5 mm)	Carl Roth
Bottle-top 1 L vacuum filters (0.22 µm pore size, CA)	Corning
Conical tubes (15 and 50 mL, PP)	Sarstedt
Econo-Column Chromatography Column (1.5 × 75 cm, glass)	Bio-Rad
Electroporation cuvettes (0.2 cm, PC)	Bio-Rad
Laboratory bottle (0.1 – 2 L, borosilicate glass 3.3)	Duran
Measuring cylinder (0.5, 1 L borosilicate glass 3.3)	Duran
PCR tubes (0.2 mL, PP)	Bio-Rad
Petri dishes (92 × 16 mm, PS)	Sarstedt
Reaction tubes (0.5, 1.5 and 2 mL, PP)	Sarstedt
Serological pipettes (5, 10 and 25 mL, PS)	Sarstedt
Syringe filter, sterile (0.2 µm, CA/PVDF)	VWR
Tissue culture flask T75, Standard with ventilation cap (75 cm <sup>2</sup> , PS)	Sarstedt
Tissue culture dish, Standard (10 × 2 mm and 15 × 2 mm, PS)	Sarstedt
Vivaflow 200 crossflow cassette (30 kDa MWCO, Hydrosart)	Sartorius

\*CA - cellulose acetate, PC - polycarbonate, PP - polypropylene, PS - polystyrene, PVDF - polyvinylidene fluoride

### 3.1.3 Antibodies

<b>Antibody</b>	<b>Species</b>	<b>Clone or Cat. No.</b>	<b>Vendor</b>	<b>Conjugate</b>	<b>Stock</b>	<b>Application*</b>
Anti-EEA1 (H-300)	Rabbit	sc-33585	Santa Cruz	-	0.2 mg/mL	IF
Anti-FLAG	Rabbit	F7425	Sigma-Aldrich	-	0.8 mg/mL	ELISA, WB
Anti-His	Mouse	AD1.1.10	AbD Serotec	-	1 mg/mL	ELISA, WB

*Continued on next page*

### 3 METHODS

*Continued from previous page*

<b>Antibody</b>	<b>Species</b>	<b>Clone or Cat. No.</b>	<b>Vendor</b>	<b>Conjugate</b>	<b>Stock</b>	<b>Application*</b>
Anti-Human CD206 (MMR)	Mouse	15-2	BioLegend	Biotin	0.5 mg/mL	FC
Anti-Human IgG	Rabbit	sc-2769	Santa Cruz	HRP	0.4 mg/mL	ELISA, WB
Anti-Human IgG AP	Goat	sc-2454	Santa Cruz	AP	0.4 mg/mL	ELISA
Anti-Mouse CD4	Rat	GK1.5	BioLegend	PerCP/ Cy5.5	0.2 mg/mL	FC
Anti-Mouse CD8 $\alpha$	Rat	53-6.7	eBioscience	PerCP/ Cy5.5	0.2 mg/mL	FC
Anti-Mouse CD40	Rat	1C10	eBioscience	PE	1 mg/mL	FC
Anti-Mouse CD80 (B7-1)	Armenian Hamster	16-10A1	eBioscience	PE	0.5 mg/mL	FC
Anti-Mouse CD86	Rat	PO3	AbD Serotec	Alexa Fluor 488	0.05 mg/mL	FC
Anti-Mouse CD107a (LAMP-1)	Rat	1D4B (RUO)	BD Biosciences	-	0.5 mg/mL	IF
Anti-Mouse CD206	Rat	MR5D3	AbD Serotec	Alexa Fluor 488	0.05 mg/mL	IF
Anti-Mouse IgG	Goat	sc-2005	Santa Cruz	HRP	0.4 mg/mL	ELISA, WB
Anti-Mouse IL-2	Rat	JES6-1A12	eBioscience	-	0.5 mg/mL	ELISA (Capture)
Anti-Mouse IL-2 Biotin	Rat	JES6-5H4	eBioscience	Biotin	0.5 mg/mL	ELISA (Detection)
Anti-Mouse IL-6	Rat	MP5-20F3	eBioscience	-	0.5 mg/mL	ELISA (Capture)
Anti-Mouse IL-6 Biotin	Rat	MP5-32C11	eBioscience	Biotin	0.5 mg/mL	ELISA (Detection)
Anti-Mouse IL-12p40	Rat	C15.6	eBioscience	-	0.5 mg/mL	ELISA (Capture)
Anti-Mouse IL-12p40 Biotin	Rat	C17.8	eBioscience	Biotin	0.5 mg/mL	ELISA (Detection)
Anti-Mouse IFN- $\gamma$	Rat	AN-18	eBioscience	-	0.5 mg/mL	ELISA (Capture)
Anti-Mouse IFN- $\gamma$ Biotin	Rat	R496A2	eBioscience	Biotin	0.5 mg/mL	ELISA (Detection)

*Continued on next page*

### 3 METHODS

*Continued from previous page*

<b>Antibody</b>	<b>Species</b>	<b>Clone or Cat. No.</b>	<b>Vendor</b>	<b>Conju-gate</b>	<b>Stock</b>	<b>Applica-tion*</b>
Anti-Mouse MHC class I	Mouse	28-14-8	eBioscience	-	1 mg/mL	FC
Anti-Rabbit IgG	Goat	sc-2030	Santa Cruz	HRP	0.4 mg/mL	ELISA, WB

\*ELISA - Enzyme-linked immunosorbent assay, FC - Flow cytometry, IF - Immunofluorescence, WB - Western blot

#### 3.1.4 Enzymes

All enzymes were used with included buffers (not listed) from the manufacturers.

<b>Type</b>	<b>Enzyme</b>	<b>Vendor</b>
DNA modifying enzymes	Phusion High-Fidelity DNA Polymerase	NEB
	T4 DNA Ligase	NEB
Miscellaneous enzymes	Collagenase P	Roche
	RNAse A	Macherey-Nagel
Protein modifying enzymes	Endoglycosidas H (Endo H)	NEB
	Peptide-N-glycosidase F (PNGase F)	NEB
Restriction enzymes	BglII	NEB
	ClaI	NEB
	EcoRI	NEB
	KpnI	NEB
	NcoI	NEB
	NheI	NEB
	NotI	NEB
	Sall	NEB
	XbaI	NEB
XhoI	NEB	

### 3.1.5 Miscellaneous biologicals, chemicals and reagents

#### Cell culture stock media and additives

Product	Vendor
$\beta$ -gal <sub>497-504</sub> peptide	PSL Peptide
$\beta$ -gal <sub>96-103</sub> peptide	PSL Peptide
Fetal calf serum (FCS) clone	GE Healthcare
FCS standard	GE Healthcare
Dulbecco's Modified Eagle's medium (DMEM), high glucose (4.5 g/L), with L-Glutamine	PAN-Biotech
Iscove's Modified Dulbecco's medium (IMDM) with L-Glutamine	PAN-Biotech
L-Glutamine 200 mM	GE Healthcare
Mannan from <i>Saccharomyces cerevisiae</i>	Sigma-Aldrich
Mouse serum	PAN-Biotech
Non-essential amino acids 100x	GE Healthcare
OptiMem	Thermo Fisher Scientific
Ovalbumin Alexa Fluor 488 and 647-conjugate	Thermo Fisher Scientific
OVA <sub>257-264</sub> peptide	Tebu-Bio
OVA <sub>323-339</sub> peptide	Tebu-Bio
Penicillin-Streptomycin 100x (10.000 U/mL Penicillin, 10 mg/mL Streptomycin)	GE Healthcare
Recombinant human GM-CSF	Immunotools
Recombinant human IL-4	Immunotools
Recombinant human M-CSF	Immunotools
Roswell Park Memorial Institute (RPMI) 1640 medium without L-Glutamine, with HEPES	PAN-Biotech
Sodium Pyruvate Solution 100 mM	GE Healthcare
Transferrin Alexa Fluor 647-conjugate	Thermo Fisher Scientific
Trypsin 0.05 % / EDTA 0.02 %	GE Healthcare

#### General chemicals, biologicals and solvents

Product	Vendor
3-(N-Morpholino) propane sulphonic acid (MOPS)	Carl Roth
2-Mercaptoethanol $\geq 99$ %, p.a.	Carl Roth

*Continued on next page*

### 3 METHODS

*Continued from previous page*

<b>Product</b>	<b>Vendor</b>
Acetic acid 100 %, p.a.	Carl Roth
Bromphenol blue	Carl Roth
Bovine serum albumin (BSA)	Carl Roth
CaCl <sub>2</sub>	Carl Roth
Citric acid	Carl Roth
Complete EDTA-free Protase Inhibitor Cocktail	Roche
Ethanol (EtOH) ≥99.8 %, p.a.	Carl Roth
Ethylenediaminetetraacetic acid (EDTA) disodium salt	Carl Roth
Glycine	Carl Roth
Isopropanol ≥99.8 %, p.a.	Carl Roth
KOAc	Carl Roth
KCl <sub>2</sub>	Carl Roth
K <sub>2</sub> HPO <sub>4</sub>	Carl Roth
KH <sub>2</sub> PO <sub>4</sub>	Carl Roth
KOH solution 20 %	Carl Roth
Methanol (MeOH) ≥99.9 %, Blotting-Grade	Carl Roth
MgCl <sub>2</sub>	Carl Roth
MgSO <sub>4</sub>	Carl Roth
MnCl <sub>2</sub>	Carl Roth
N-2-Hydroxyethyl piperazine-N'-2-ethane sulphonic acid (HEPES)	Carl Roth
N,N-Bis-(2-hydroxyethyl)-2-aminoethane sulphonic acid (BES)	Carl Roth
NaCl <sub>2</sub>	Carl Roth
NaHCO <sub>3</sub>	Carl Roth
NaH <sub>2</sub> PO <sub>4</sub>	Carl Roth
NaOAc	Carl Roth
Phosphate-buffered saline (PBS) powder without Ca <sup>2+</sup> , Mg <sup>2+</sup>	Biochrome
Phenylmethylsulfonyl fluoride (PMSF)	Carl Roth
RbCl <sub>2</sub>	Carl Roth
Tris(hydroxymethyl)-aminomethane (Tris) ≥99.9 %, p.a.	Carl Roth

#### **Microbiology**

<b>Product</b>	<b>Vendor</b>
Agar-agar, Kobe I	Carl Roth
Ampicillin sodium salt	Carl Roth

*Continued on next page*

*Continued from previous page*

<b>Product</b>	<b>Vendor</b>
Biotin	Carl Roth
D-glucose	Carl Roth
D-Sorbitol	Carl Roth
Glycerol $\geq 98\%$ , Ph.Eur.,	Carl Roth
Kanamycin sulphate	Carl Roth
Tryptone/Peptone ex casein	Carl Roth
Yeast extract	Carl Roth
Yeast nitrogen base (YNB) with ammonium sulfate, without amino acids	Sigma-Aldrich
Zeocin	Invivogen

**Molecular biology**

<b>Product</b>	<b>Vendor</b>
Agarose Basic	AppliChem
Deoxynucleotide (dNTP) Set, 10 mM	Sigma-Aldrich
DNA-ladder (100 bp, 1 kb)	NEB
Gel loading dye 6x (blue/purple)	NEB
SYBR Safe DNA Gel stain	Thermo Fisher Scientific

**Protein biochemistry, fluorescence microscopy and flow cytometry**

<b>Product</b>	<b>Vendor</b>
2,2'-Azino-bis(3-ethylbenzothiazoline-6-sulfonic acid) (ABTS) diammonium salt	Sigma-Aldrich
4-Nitrophenyl phosphate disodium salt hexahydrate	Sigma-Aldrich
4,6-diamidino-2-phenylindole (DAPI)	Sigma-Aldrich
Acrylamide/bisacrylamide (37.5:1), 30%	Carl Roth
Ammonium persulfate (APS)	Carl Roth
Collagen R	Serva
Color Prestained Protein Standard, Broad Range (11 kDa–245 kDa)	NEB
ECL Western blotting substrate	Pierce
Fluoromount Aqueous Mounting Medium	Sigma-Aldrich
Imidazole $\geq 99\%$	Carl Roth

*Continued on next page*

Continued from previous page

<b>Product</b>	<b>Vendor</b>
Mouse IFN- $\gamma$ /IL-2/IL-6/IL-12/TNF- $\alpha$ , recombinant ELISA standard	eBioscience
N,N,N',N'-Tetramethylethylenediamine (TEMED)	Carl Roth
NeutrAvidin Protein horseradish peroxidase (HRP) conjugate	Pierce
Ovalbumin	Serva
Paraformaldehyde (PFA)	Carl Roth
Protein G chromatography cartridge (1 mL)	Pierce
Protino nickel-nitrilo-triacetic acid (Ni-NTA) agarose	Macherey-Nagel
Polyoxyethylene-20-sorbitan monolaurate (Tween 20)	Carl Roth
Polyethylene glycol alkylphenyl ether (Triton X-100)	Carl Roth
Powdered milk, blotting grade, low fat	Carl Roth
Roti-Blue	Carl-Roth
Roti-Quant	Carl Roth
Sephacryl S200 HR	Sigma-Aldrich
Sodium dodecyl sulfate (SDS), 20%	Carl Roth

### 3.1.6 Kits

<b>Kit</b>	<b>Vendor</b>	<b>Application</b>
EasySelect Pichia Expression Kit	Thermo Fisher Scientific	<i>P. pastoris</i> strains and protocols
NuceloBond Xtra Midi	Macherey-Nagel	Mid-scale DNA preparation
NucleoSpin Gel and PCR Clean-up	Macherey-Nagel	DNA extraction from agarose gels, general DNA clean up
Pierce BCA Protein Assay Kit	Thermo Fisher Scientific	Protein concentration determination by bicinchoninic acid (BCA) assay

### 3.1.7 Buffers and solutions

If not otherwise declared, all buffers and solutions were prepared with autoclaved Milli-Q Type 1 ultrapure water and solutions were sterilized by autoclaving for 20 min at 121 °C or filtration through 0.2  $\mu$ m cellulose acetate or polyvinylidene fluoride filters and stored at room temperature (RT).



---

**General stock solutions**


---

<b>Solution</b>	<b>Composition</b>
EDTA 0.5 M	500 mM EDTA in H <sub>2</sub> O, pH 7.6, filter sterilized
EDTA 2 M	EDTA 0.5 M diluted in sterile PBS, stored at 4 °C
Phosphate buffered saline (PBS)	8000 mg/L NaCl, 200 mg/L KCl, 1150 mg/L Na <sub>2</sub> HPO <sub>4</sub> , 200 mg/L KH <sub>2</sub> PO <sub>4</sub> , pH 7.4

---

**Microbiology**


---

<b>Solution</b>	<b>Composition</b>
Biotin 500x (0.02 %)	20 mg biotin in 100 mL H <sub>2</sub> O, filter sterilized, stored at 4 °C
Breaking buffer	50 mM sodium phosphate, pH 7.4, 1 mM PMSF, 1 mM EDTA, 5 % glycerol
Dextrose 10x (20 %)	200 g D-glucose in 1 L H <sub>2</sub> O
Glycerol 10x (10 %)	10 % (v/v) glycerol in H <sub>2</sub> O
TFBI	10 mM CaCl <sub>2</sub> , 15 % (v/v) glycerol, 30 mM KOAc pH 5.8, 100 mM RbCl <sub>2</sub> , 50 mM MnCl <sub>2</sub>
TFBII	10 mM MOPS pH 7.0, 10 mM RbCl <sub>2</sub> , 75 mM CaCl <sub>2</sub> , 15 % (v/v) glycerol
Potassium phosphate buffer 1 M	132 mL of 1 M K <sub>2</sub> HPO <sub>4</sub> , 868 mL of 1 M KH <sub>2</sub> PO <sub>4</sub> , pH 6.0 ± 0.1 adjusted with KOH
YNB 10x	134 g/L YNB in H <sub>2</sub> O, filter sterilized

---

**Molecular biology**


---

<b>Solution</b>	<b>Composition</b>
Mini-prep buffer I	Tris/HCl pH 8, 50 mM EDTA 10 mM, 100 µg/mL RNaseA, stored at 4 °C
Mini-prep buffer II	200 mM NaOH, 1 % (v/v) SDS
Mini-prep buffer III	3 M KOAc, pH 5.5
Tris-acetate-EDTA (TAE) 50x	2 M Tris, 1 M acetic acid, 0.05 M EDTA , pH 8,3

---

**Protein biochemistry**

<b>Solution</b>	<b>Composition</b>
ABTS buffer	0.1 M Citric acid, pH 4.35, stored at 4 °C.
AP substrate buffer	100 mM Tris-HCl, 100 mM NaCl, 1 mM MgCl <sub>2</sub> , pH 9.5, stored at 4 °C
DNP	50 mM NaH <sub>2</sub> PO <sub>4</sub> , 300 mM NaCl, 8 M urea pH 8
DNPI-10/20/250	50 mM NaH <sub>2</sub> PO <sub>4</sub> , 300 mM NaCl, 8 M urea, supplemented with 10, 20 or 250 mM imidazole, pH 8
ELISA blocking buffer	1 % (w/v) BSA in PBS
ELISA coating buffer	0.1 M NaHCO <sub>3</sub> in H <sub>2</sub> O, pH 8.2, stored at 4 °C
ELISA washing buffer	0.05 % Tween 20 in PBS
Fc-chimeric coating buffer	154 mM NaCl in H <sub>2</sub> O
Laemmli buffer 4x	250 mM Tris-HCl (pH = 6,8), 8 % (v/v) SDS, 40 % (v/v) glycerol, 0.08 % (w/v) Bromphenol blue, 10 % 2-Mercaptoethanol
NP	50 mM NaH <sub>2</sub> PO <sub>4</sub> , 300 mM NaCl pH 8
NPI-10/20/250	50 mM NaH <sub>2</sub> PO <sub>4</sub> , 300 mM NaCl supplemented with 10, 20 or 250 mM imidazole, pH 8
PBST	PBS, 0.05 % Tween 20
Protein G binding buffer	50 mM NaOAc, pH 5
Protein G elution buffer	0.1 M Glycine in H <sub>2</sub> O, pH 2.88
Protein G neutralization buffer	1 M Tris, pH 8.5
SDS running buffer 10x	250 mM Tris, 1.92 M glycine, 1 % (v/v) SDS
Tris buffered saline (TBS) 10x	500 mM Tris, 1.5 M NaCl, pH 7.5
TBST	TBS, 0.05 % Tween 20
TBSTC	TBST, 10 mM CaCl <sub>2</sub>
Towbin buffer	25 mM Tris, 192 mM glycine, pH 8.3

**Flow cytometry/Fluorescence microscopy**

<b>Solution</b>	<b>Composition</b>
FACS buffer	0.1 % (w/v) BSA, 0.1 % (w/v) NaN <sub>3</sub> in PBS, stored at 4 °C
Fixation buffer	4 % (w/v) PFA in PBS
Intracellular staining buffer	0.1 % Triton X-100, 5 % appropriate serum (mouse, rabbit or goat) in PBS
MACS buffer	FACS buffer, 2 mM EDTA

### 3.1.8 Media

#### Cell culture media

Medium	Composition
Bone marrow-derived dendritic cell (BM-DC) culture medium	IMDM, 10 % heat inactivated FCS clone, 100 U/mL penicillin and 0.1 mg/mL streptomycin, 50 mM 2-Mercaptoethanol
BM-DC uptake medium	IMDM, 10 % heat inactivated FCS clone, 100 U/mL penicillin and 0.1 mg/mL streptomycin, 50 $\mu$ M 2-Mercaptoethanol, 2.5 % J558L conditioned medium
Human embryonic kidney (HEK) cell medium	DMEM, 10 % heat inactivated FCS standard, 1 mM sodium pyruvate
J558L medium	RPMI 1640, 10 % heat inactivated FCS clone, 100 U/mL penicillin and 0.1 mg/mL streptomycin
T cell medium	RPMI 1640, 10 % heat inactivated FCS clone, 50 $\mu$ M 2-Mercaptoethanol, 100 U/mL penicillin and 0.1 mg/mL streptomycin, 1 mM sodium pyruvate

#### Microbiology media

If not otherwise declared, all microbiology media were prepared with autoclaved Milli-Q Type 1 ultrapure water.

Medium	Composition
BMGY	10 g/L yeast extract, 20 g/L tryptone/peptone, 100 mM potassium phosphate buffer pH 6.0, 1.34 % YNB, $4 \times 10^{-5}$ % biotin, 1 % glycerol, filter sterilized
BMMY	10 g/L yeast extract, 20 g/L tryptone/peptone, 100 mM potassium phosphate buffer pH 6.0, 1.34 % YNB, $4 \times 10^{-5}$ % biotin, 0.5 % MeOH, filter sterilized
LB medium	5 g/L NaCl, 5 g/L yeast extract, 10 g/L tryptone/peptone, autoclaved 20 min at 121 °C and stored at 4 °C
YB medium 2x	5 g/L NaCl, 10 g/L yeast extract, 16 g/L tryptone/peptone, pH 7.5, autoclaved 20 min at 121 °C and stored at 4 °C
YT medium	98 % YT-Media, 10 mM KCl, 20 mM MgSO <sub>4</sub> autoclaved 20 min at 121 °C and stored at 4 °C
YPD	10 g/L yeast extract, 20 g/L tryptone/peptone, 2 % dextrose

*Continued on next page*

Continued from previous page

Medium	Composition
YPDS-Agar	10 g/L yeast extract, 20 g/L tryptone/peptone, 1 M sorbitol, 2% dextrose, 2% (w/v) agar
YPM-Agar	10 g/L yeast extract, 20 g/L tryptone/peptone, 2% (w/v) agar, 0.5% MeOH

### 3.1.9 Bacteria and yeast strains, cell lines and mice strains

#### Yeast strains

Genus	Strain	Genotype	Description
<i>Pichia pastoris</i>	KM71H	aox1::ARG4, arg4	Mut <sup>S</sup> phenotype

#### Bacteria

Genus	Strain	Genotype
<i>Escherichia coli</i>	DH5 $\alpha$	F- $\Phi$ lacZ $\Delta$ M15 $\Delta$ (lacZYA-argF) U169 <i>recA1 endA1 hsdR17</i> (rK-, mK+) <i>phoA supE44</i> $\lambda$ - <i>thi-1 gyrA96 relA1</i>
<i>Escherichia coli</i>	XL1-Blue	<i>recA1 endA1 gyrA96 thi-1 hsdR17 supE44 relA1 lac</i> [F' <i>proAB lacI<sup>q</sup>Z</i> $\Delta$ M15 Tn10 (Tet <sup>r</sup> )]

#### Cell lines

Cell line	Description
HEK293T	HEK cells constitutively expressing the SV40 large T antigen
HEK-MR	HEK293T cells transfected with MR-internal ribosome entry site (IRES)-GFP [125]
HEK-IG	HEK293T cells transfected with IRES-GFP [125]
J558L-GM-CSF	Transgenic myeloma cell line received from BALB/c mice, constitutively secretes mouse granulocyte-macrophage colony-stimulating factor (GM-CSF), G418 selectable

Mice		
Mouse strain	Description	Background
C57BL/6J	Wild-type strain	C57BL/6J
DesTCR	Express a Kb-specific T cell receptor (KB5.C20 TCR) on CD8 <sup>+</sup> thymocytes [126]	B10.BR
OT-I	Bear CD8 <sup>+</sup> T cells, which have a TCR specific for the ovalbumin peptide OVA <sub>257-264</sub> in the context of Kb [127, 128]	Rag2 <sup>-/-</sup>
OT-II	Bear CD4 <sup>+</sup> T cells recognizing the ovalbumin peptide OVA <sub>323-339</sub> on I-Ab MHC-II molecules [129]	C57BL/6J
MR <sup>-/-</sup>	Bears a stop codon inserted at the Mannose receptor start codon of Exon 1, which abolishes the expression of MR [88]	C57BL/6J

### 3.1.10 Primers and plasmids

#### Primers

All primers were ordered from Thermo Fisher Scientific (formally Life Technologies) under the brand of Invitrogen™ custom DNA oligos.

Name	Sequence
oCK1	GACAGTGGATCCTTATGGCTCGCGATGATCCC
oCK2	TACGTACTGCAGACATGGCCTGCCCGTTA
oCK3	CCAAGCTCGAAATTAACCCTCAC
oCK9	TAGCGGATCCAGATGAGTCTTGGAGGTGTTTC
oCK16	CAGTGTCGACGTGATTACGATCGCGCTGCA
oCK26	GATCCCATGGATTACAAGGATGACGACG
oCK27	GCTCAGATCTCAATGATGATGATGATGATGG
oCK41	CAGCATCGATGGGTAATTCTACTATGGGTACCTGCAGTCGACTTCTA GACTCGAGTAGC
oCK42	GCTACTCGAGTCTAGAAGTCGACTGCAGGTACCCATAGTAGAATTAC CCATCGATGCTG
oCK45	CATAGGTACCATGGTGAGCAAGGGC
oCK46	CAGTTCTAGACTTGTACAGCTCGTCC
oCK47	CAGCATCGATGGGTC AATCTACTATGGGTACCTGCAGTCGACTTCTA GACTCGAGTAGC

*Continued on next page*

Continued from previous page

Name	Sequence
oCK48	GCTACTCGAGTCTAGAAAGTCGACTGCAGGTACCCATAGTAGATTGAC CCATCGATGCTG
oCK49	GCGCGAATTCGGGCGGAGGTAATTCTACTATGGGTACC
oCK50	GCGCGAATTCGGGCGGAGGTCAATCTACTATGGGTACC
oCK51	CGATGCTAGCTCAATGATGATGATGATGATGG
oCK56	CAGTTCTAGAGGCTGACATATGCTTGTACAGCTCGTCCATGC
oCK57	TATGTCAGGCCTTGAGCAGCTTGAGAGTATAATCAACTTTGAAAAAC TGACTGAATGGACCAGTTCTT
oCK58	CTAGAAGAAGTGGTCCATTCAGTCAGTTTTTCAAAGTTGATTATACTC TCAAGCTGCTCAAGGCCTGACA

### Plasmids

Maps of all plasmids which were generated during this work are provided in the appendix.

Name	Resistance	Description	Origin
pIgplus-MR-CTLD	Ampicillin	Secreted expression of MR-CTLD by HEK293T cells	Luisa Martinez-Pomares
pIgplus-MR-Nterm	Ampicillin	Secreted expression of MR-Nterm by HEK293T cells	Luisa Martinez-Pomares
pFUSE-hIgG1-Fc2	Zeocin	Secreted expression of Fc-control by HEK293T cells	Invivogen
pBS-IRES-NLS-lacZ	Kanamycin	Source of <i>Escherichia coli</i> ( <i>E. coli</i> ) <i>lacZ</i>	Dr. Christina Ginkel, DZNE, Bonn
pCMV-Tag2B	Kanamycin	Cloning intermediate for addition of FLAG-tag	Clontech
pCMV-Tag2B-EGFP	Kanamycin	Source of EGFP	AG Burgdorf, LIMES, University of Bonn
pQE60	Ampicillin	<i>E. coli</i> expression plasmid	Quiagen
pPICZ $\alpha$ C	Zeocin	<i>P. pastoris</i> expression plasmid for secreted expression	Invitrogen
pPICZ $\alpha$ -NST	Zeocin	<i>P. pastoris</i> expression plasmid for secreted NST-tagged expression	created during this work
pPICZ $\alpha$ -QST	Zeocin	<i>P. pastoris</i> expression plasmid for secreted QST-tagged expression	created during this work

Continued on next page

Continued from previous page

Name	Resistance	Description	Origin
pCK1	Kanamycin	Cloning intermediate, source of FLAG-tagged <i>lacZ</i>	created during this work
pCK15	Zeocin	Secreted expression of truncated $\beta$ -galactosidase ( $\beta$ -gal)(V10-H451) by <i>P. pastoris</i>	created during this work
pCK27	Zeocin	Secreted expression of truncated $\beta$ -gal(V10-L731) by <i>P. pastoris</i>	created during this work
pCK44	Zeocin	Expression of truncated $\beta$ -gal(V10-L731) by <i>E. coli</i>	created during this work
pCK45	Zeocin	Secreted expression of NST-tagged GFP by <i>P. pastoris</i>	created during this work
pCK50	Zeocin	Secreted expression of QST-tagged GFP by <i>P. pastoris</i>	created during this work
pCK51	Zeocin	Secreted expression of NST-tagged GFP by HEK293T cells	created during this work
pCK52	Zeocin	Secreted expression of QST-tagged GFP by HEK293T cells	created during this work
pCK57	Zeocin	Secreted expression of NST-tagged GFP with C-terminal SIINFEKL by <i>P. pastoris</i>	created during this work

### 3.1.11 Software

Software	Distributor	Application
Ascent Software	Thermo Scientific	Computer assisted control and data acquisition with Multiskan plate reader
AxioVision	ZEISS	Fluorescence microscopy data acquisition and image processing
BD FACSDiva	BD Bioscience	Flow cytometry data acquisition
CloneManager 5	Sci-Ed	<i>In silico</i> cloning and vector visualization
Excel	Microsoft	Data analysis
FlowJo v8.8.4	FlowJo, LLC	Flow cytometry data analysis and visualization

Continued on next page

*Continued from previous page*

<b>Software</b>	<b>Distributor</b>	<b>Application</b>
FluorEssence	Horiba	Computer assisted control and data acquisition with FluoroMaxx-4 spectrofluorometer
i-control	Tecan	Data acquisition Tecan microplate reader
Illustrator CS4	Adobe	Data visualization
Image Lab	Bio-Rad	Computer-assisted control and data acquisition with ChemiDoc MP System
ImageJ64	Open source under the GNU General Public License.	Image processing and visualization
NanoDrop 2000 / 2000c Software	Thermo Scientific	Computer-assisted control and data acquisition with NanoDrop 2000
Prism 4	GraphPad	Data analysis and visualization
PyMol	Schrödinger	Visualization of PDB files
R Studio	R Studio, Inc	R based statistical analysis

This thesis was typeset using the LaTeX typesetting system originally developed by Leslie Lamport, based on TeX created by Donald Knuth.



## 3.2 Methods

### 3.2.1 Molecular biology

#### 3.2.1.1 Polymerase chain reaction (PCR)

Amplification of nucleic acids from plasmid DNA was performed by standard PCR using the high fidelity polymerase Phusion according to the manufacturer’s manual. In short, a 50  $\mu$ L reaction was set up on ice as indicated in Table 3.1.

**Table 3.1: Cycling conditions**

Component	50 $\mu$ L reaction
H <sub>2</sub> O	added to 50 $\mu$ L
5x Phusion HF Buffer	10 $\mu$ L
10 mM dNTPs	1 $\mu$ L
Primer A	0.5 $\mu$ M
Primer B	0.5 $\mu$ M
Template	10 ng
DNA Polymerase	0.5 $\mu$ L

Primer melting temperatures ( $T_m$ ) were calculated using NEB’s  $T_m$ -calculator v1.8.1 (online at <http://tmcalculator.neb.com/#!/>) and according to the temperatures a 2- or 3-step protocol as indicated in Table 3.2 was run on a thermocycler.

**Table 3.2: Reaction setup**

Cycle step	2-step protocol		3-step protocol		Cycles
	Temperature	Time	Temperature	Time	
Initial denaturation	98 °C	30 s	98 °C	30 s	1
Denaturation	98 °C	10 s	98 °C	10 s	35
Annealing	—	—	calculated $T_m$	20 s	35
Extension	72 °C	15–30 s/kb	72 °C	15–30 s/kb	35
Final extension	72 °C	600 s	72 °C	600 s	1
	4 °C	hold	4 °C	hold	

### 3.2.1.2 Restriction digestion

Restriction reactions were generally set up according to the manufacturer's manual. Differing from standard protocols, analytical restriction digestions were performed with 100–300 ng DNA and 0.1–0.3 U restriction enzyme in the corresponding buffer system, incubated for 1–2 h at the indicated temperature and analyzed directly by gel electrophoresis without enzyme inactivation. Preparative restriction digestions were typically performed with 1–2 µg DNA template and 10-fold overdigestion by increasing the incubation time to 16 h if possible or increasing enzyme concentration to 10–20 U if prolonged incubation goes along with star activity.

### 3.2.1.3 Gel electrophoresis

Separation of nucleic acids was done by agarose gel electrophoresis. Briefly, agarose gels were prepared by solving 1% (w/v) low melting agarose in 1x TAE buffer. For low molecular weight DNA < 1 kb gels were prepared with 2% (w/v) agarose. For better resolution of high molecular weight DNA > 4 kb gels were prepared with 0.8% (w/v) agarose. After boiling the gel solution in a microwave oven to homogeneity, the gels were cooled below 50 °C and supplemented with 1:20,000 dilution (v/v) of SYBR Safe. Gels were poured at sizes and with a number of lanes as needed for the particular experiment. After polymerization, gels were mounted in a Bio-Rad horizontal Mini-Sub Cell GT system and covered with 1x TAE. DNA samples were supplemented with 1x gel loading dye prior loading and 6 µL of a 1 kb or 100 bp ladder were applied as size indicators. Electrophoresis was performed at 7 V/cm. Gels were investigated on a 470 nm light table. If needed, DNA was cut out for further processing and gels were photographed for documentation.

### 3.2.1.4 DNA purification

DNA purification from solutions (PCR or restriction digestion reactions) or agarose gels was performed by NucleoSpin Gel & PCR Clean Up Kit (Macherey-Nagel) according to the manufacturer's manual. Differing from the manual, samples were eluted in 16 µL ultrapure H<sub>2</sub>O. If Vector DNA was cut within the multiple cloning site (MCS) and the fragment to be removed was smaller than 100 nucleotides in length, digested vector DNA was not separated by gel electrophoresis first but directly purified with the kit. In

this case the loading buffer was adjusted as recommended in the manual with ultrapure H<sub>2</sub>O to exclude binding of small fragments.

#### 3.2.1.5 DNA quantification

DNA concentration was determined by absorption at 260 nm with a NanoDrop 2000 spectrophotometer against ultrapure H<sub>2</sub>O as a blank. Purity was determined by A260/A280 to monitor protein contamination.

#### 3.2.1.6 DNA ligation

Ligation was performed with NEB's T4 DNA Ligase according to the manufacturer's protocol for cohesive ends. Briefly, 250 fmol insert were mixed with 50 fmol vector backbone, 1x T4 DNA ligase reaction buffer and 1 µL T4 DNA Ligase (400 U) and the reaction was filled up with ultrapure H<sub>2</sub>O to 20 µL. Ligation was carried out for 10–15 min at RT, and the enzyme was inactivated for 10 min at 65 °C.

#### 3.2.1.7 Generation of transformation competent *Escherichia coli* strains

Generation of chemically competent *Escherichia coli* (*E. coli*) was performed according to the rubidium chloride method introduced by Hanahan 1983 [130]. In short, a 3 mL LB-culture was inoculated with a single DH5α or XL1-Blue *E. coli* clone and incubated overnight at 37 °C. This starter culture was used to inoculate 100 mL YB medium, which was grown at 37 °C up to an OD600 of 0.4–0.6. Bacteria were harvested by centrifugation (10 min, 3,220 x g, 4 °C), resuspended in 20 mL TFB I and incubated on ice for 10 min. Bacteria were harvested again by centrifugation (10 min, 3,220 x g, 4 °C) and resuspended in 4 mL TFB II. 200 µL aliquots were frozen in liquid nitrogen and stored until use at –80 °C.

#### 3.2.1.8 Transformation

50 µL chemical competent DH5α or XL1-Blue *E. coli* were used for each transformation. Cells were thawed on ice and incubated with 2–8 µL of a 20 µL ligation reaction for 30 min on ice, before a heat-shock was performed for 90 sec at 42 °C. Afterwards, cells were resuspended in 1 mL LB-media without antibiotics and incubated for 1 h at 37 °C and 600 rpm in a shaking heat block. The cells were harvested by centrifugation (1 min,

21,000 x g), resuspended in 50–100  $\mu$ L LB-medium and spread on 10 cm LB-agarose plates, including the appropriate antibiotics for positive selection. Ampicillin was used at 100  $\mu$ g/mL, kanamycin at 50  $\mu$ g/mL and zeocin at 25  $\mu$ g/mL for selection. Transformants were incubated at 37 °C overnight.

#### **3.2.1.9 Mini-preparation of plasmid DNA**

Single clones on LB-agar plates were used to inoculate 3 mL LB-medium supplemented with the respective antibiotics in a 15 mL conical tube. After incubation at 37 °C and 180 rpm overnight, 1.5 mL of each culture was transferred to an 1.5 mL reaction tube, and cells were collected by centrifugation (21,000 x g, 5 min). Supernatant was discarded and pellets were resuspended in 100  $\mu$ L Mini-prep buffer I. Alkaline cell lysis was started by adding 200  $\mu$ L Mini-prep buffer II. Samples were mixed 3 times by inverting and incubating for 5 min at RT. Cell lysis was stopped and proteins were precipitated by adding 200  $\mu$ L Mini-prep buffer III followed by inverting 3 times. Precipitated protein was collected by centrifugation (21,000 x g, 5 min). The supernatants were carefully transferred to a fresh tube and 1 mL ice-cold 100 % EtOH was added to precipitate DNA. Precipitation and collection of the DNA precipitate was carried out by centrifugation (21,000 x g, 30 min) at 4 °C. Supernatants were removed, and DNA-pellets were washed once with 1 mL ice-cold 70 % EtOH (v/v) in ultrapure H<sub>2</sub>O. Pellets were harvested again by centrifugation (21,000 x g, 10 min), and supernatants were fully removed by pipetting. Pellets were dried at RT and subsequently resuspended in 50  $\mu$ L ultrapure H<sub>2</sub>O.

#### **3.2.1.10 Midi-preparation of plasmid DNA**

For mid-scale preparation of plasmid DNA (Midi-preparation), 3 mL LB-medium supplemented with the appropriate selection antibiotics were inoculated with a single clone in a 15 mL conical tube and incubated overnight at 37 °C and 180 rpm. 1 mL of this starter culture was used to inoculate 100–200 mL LB-medium supplemented with the selection antibiotics and this culture was incubated overnight at 37 °C and 180 rpm in a 500–1000 mL flask. Bacteria pellets were harvested by centrifugation (3,220 x g, 20 min, 4 °C), and DNA preparation was performed using the NucleoBond Xtra Midi kit (Macherey-Nagel) according to the manufacturer's manual.

### 3.2.1.11 Sequencing

All sequencing reactions were performed by GATC biotech (Konstanz, Germany) with self-designed primers or standard primers provided by GATC biotech. Analysis of FASTA sequencing data was performed with Clone Manager 5 software (Scie-Ed), and evaluation of primary peak data was performed with 4Peaks software (nucleobytes).

### 3.2.1.12 Cloning strategies for expression plasmids

Quality of all generated plasmids was controlled by restriction digestion and sequencing. Plasmid maps are provided in the appendix.

#### **pCK27 — pPICZ $\alpha$ -FLAG:: $\beta$ -gal(V10–L731)**

The wildtype *lacZ* gene from *E. coli* was amplified via PCR with oCK1 and oCK2 from the template plasmid pBS-IRES-NLS-*lacZ* (gift from Christina Ginkel, DZNE, Bonn). The PCR product was digested with BamHI and PstI and ligated into the FLAG-tag containing plasmid pCMV-Tag2C to yield the intermediate plasmid pCK1. Another PCR was performed with pCK1 as a template with primers oCK3 and oCK9, which amplified a truncated version of *lacZ* starting with the FLAG-tag and comprising the  $\beta$ -galactosidase residues V10–L731. The PCR product was cloned via the SalI and NotI restriction sites into the pPICZ $\alpha$  C expression plasmid.

#### **pCK44 — pQE60-FLAG:: $\beta$ -gal(V10–L731)**

The truncated *lacZ* gene from pCK27 was amplified with primers oCK26 and oCK27 via PCR and cloned into pQE60 via NcoI and BglII restriction sites.

#### **pPICZ $\alpha$ -NST and pPICZ $\alpha$ -QST**

2  $\mu$ g of the oligos oCK41 and oCK42 (for pPICZ $\alpha$ -NST) or oCK47 and oCK48 (for pPICZ $\alpha$ -QST) were mixed in 50  $\mu$ L ultrapure H<sub>2</sub>O and heated for 5 min at 95 °C. The mixture was then slowly cooled ( $\sim$ 45 min) to room temperature for annealing. The annealed DNA-oligos were digested with ClaI and XhoI and then ligated into pPICZ $\alpha$  C, which was digested with ClaI and SalI, thereby destroying the original SalI site in pPICZ $\alpha$  C.

**pCK45 — pPICZ $\alpha$ -NST-EGFP and****pCK50 — pPICZ $\alpha$ -QST-EGFP**

EGFP was amplified from pCMV-Tag2B-EGFP (gift from Matthias Zehner, University of Bonn) with primers oCK45 and oCK46. The PCR product was digested with KpnI and XbaI and ligated into pPICZ $\alpha$ -NST (pCK45) or pPICZ $\alpha$ -QST (pCK50) in order to generate NST-tagged or QST-tagged EGFP (NST-GFP, QST-GFP).

**pCK51 — pFUSE-hIgG1-NST::EGFP::6xHis and****pCK52 — pFUSE-hIgG1-QST::EGFP::6xHis**

NST-tagged or QST-tagged EGFP was amplified with oCK49 and oCK51 or oCK50 and oCK51, respectively via PCR from pCK45. The PCR products were ligated into pFUSE-hIgG1-Fc2 via EcoRI and NheI by which the hIgG1 part was removed. NST-tagged EGFP is encoded by pCK51, QST-tagged EGFP by pCK52.

**pCK57 — pPICZ $\alpha$ -NST-EGFP-S8L**

EGFP was amplified from pCMV-Tag2B-EGFP (gift from Matthias Zehner, University of Bonn) with primers oCK45 and oCK56. The PCR product was digested with KpnI and NdeI and ligated into pPICZ $\alpha$ -NST (pCK45). Complementary oligos oCK57 and oCK58 were used to introduce the OVA epitope SIINFEKL (S8L) into the resulting plasmid via NdeI and XbaI.

**pCK15 — pPICZ $\alpha$ -FLAG:: $\beta$ -gal(V10-H451)**

A truncated  $\beta$ -gal(V10-H451) was amplified via PCR with primers oCK3 and oCK16 from pCK1 as a template. The product was cloned into pPICZ $\alpha$  C via SalI and NotI restriction sites.

### 3.2.2 Cell culture

All cell culture handling and experiments were performed under sterile working conditions and under mycoplasma-free conditions, as documented by frequent testing with a mycoplasma detection kit (PAA/GE Healthcare). If not otherwise declared, cell lines and primary cells were incubated in separate incubators at 37 °C and 90 % humidity with 5 % CO<sub>2</sub> saturation, and all media and solutions were pre-warmed to 37 °C before use.

### 3.2.2.1 Cultivation HEK293T cells

All types of HEK cells (HEK293T, HEK293T-IG and HEK293T-MR) were cultured in 15 mL HEK cell medium on 10 cm tissue culture treated plates (Sarstedt) and either freshly thawed and expanded once or kept at low passages (< 15) for the experiments. Passaging was performed every 2–3 days, when cells reached 60–70 % confluence by incubation for 1 min at 37 °C in 0.05 % Trypsin/0.02 % EDTA solution (PAA). Cells were detached from the plate by pipetting with additional 9 mL HEK cell medium and collected by centrifugation (300 x g, 5 min, RT). Cells were then resuspended in 10 mL and distributed on fresh plates with fresh HEK Medium.

### 3.2.2.2 J558L conditioned medium

J558L-GM-CSF cells were freshly thawed for the generation of conditioned medium.  $1 \times 10^6$  cells were plated in 30 mL J558L-medium per 15 cm plate and incubated for 8–10 days. Supernatants were collected and filtered through 0.2 µm cellulose acetate filters. GM-CSF content was determined by ELISA, and aliquots of 50 mL were frozen at –20 °C.

### 3.2.2.3 *In vitro* generation and cultivation of bone marrow-derived dendritic cells (BM-DCs)

BM-DCs were in principle generated as previously described [131, 132]. In short, mice were first anesthetized with isofluran and then euthanized by cervical dislocation. The hind limbs of the mice were isolated, and bones were rinsed with PBS to collect the bone marrow. Bone marrow was disaggregated rigorously by pipetting to get a single cell suspension. Cells were collected by centrifugation (300 x g, 5 min, RT) and resuspended in 45 mL BM-DC culture medium, which contains J558L conditioned medium as a GM-CSF source. Cells were spread on 3 untreated petri dishes and incubated for 3 days. Thereafter, supernatants containing swimming cells were collected, and adherent cells were detached with 2 mM EDTA in PBS. All cells were combined, harvested by centrifugation (300 x g, 5 min, RT), resuspended in 90 mL BM-DC culture medium and spread on 6 untreated petri dishes. Cells were incubated until their use on day 7–8 post isolation.

### **3.2.2.4 *In vitro* culture of human DCs and macrophages from human peripheral blood mononuclear cells (PBMCs)**

*In vitro* generation was performed by Susanne V. Schmidt and Lan Do (AG Schultze, LIMES, University of Bonn) as previously described [133]. Briefly, PBMCs were isolated by Ficoll (1.077 g/mL) gradient centrifugation from buffy coats. CD14<sup>+</sup> human monocytes were further purified from PBMCs by magnetic-activated cell sorting (MACS) (Miltenyi biotec) following the manufacturer's manual. Macrophages were differentiated from these monocytes by incubation in RPMI 1640, supplemented with 10 % FCS and 1 % PenStrep solution in the presence of 50 IU/mL macrophage colony-stimulating factor (M-CSF) for 72 h. PreDCs were generated by incubation with 500 IU/mL recombinant human GM-CSF and 800 IU/mL recombinant human interleukin-4 (IL-4) in RPMI 1640 supplemented with 10 % FCS and 1 % PenStrep solution for 72 h.

### **3.2.3 Protein expression in bacteria, yeasts and mammalian cells**

#### **3.2.3.1 Protein expression in *E. coli***

Chemically competent *E. coli* cells were transformed with pCK44, as described under section 3.2.1.8. A single clone was used to inoculate 20 mL LB-medium supplemented with 100 µg/mL ampicillin in a 50 mL conical tube, which was incubated overnight at 37 °C and 180 rpm. This starter culture was used to inoculate 2 L LB-medium supplemented with 100 µg/mL ampicillin. The culture was incubated at 37 °C and 160 rpm until an OD<sub>600</sub> of 0.5–0.7 was reached. Induction was then started by adding 1 mM IPTG. After incubating 4 h at 37 °C and 160 rpm, the culture was harvested by centrifugation (6,000 x g, 20 min, 4 °C). The pellet was washed once with NP-buffer, frozen in dry ice-ethanol and stored at -20 °C until used for protein purification.

#### **3.2.3.2 Electroporation of *P. pastoris***

Electroporation-competent *P. pastoris* KM71H cells were prepared according to the guidelines of the EasySelect Pichia Expression Kit manual (Invitrogen, ThermoFisher Scientific). 80 µL of the prepared competent cells were mixed with 10 µg PmeI-linearized plasmid DNA in 10 µL sterile water and incubated in a 0.2 µm electroporation cuvette on ice for 5 min. Cells were pulsed with the Bio-Rad Gene Pulser Xcell electroporation device with 1500 V, 25 µF and 200 Ω and resuspended in 1 mL of ice-cold 1 M sorbitol. This



solution was transferred to a 15 mL conical tube and incubated at 30 °C without shaking for 1 h before spreading on YPDS agar plates containing 100 µg/µL zeocin. Plates were incubated for 3–10 days at 30 °C until colonies became visible. Single colonies were then transferred to a fresh YPD-agar plate supplemented with 100 µg/µL zeocin and numbered for screening purposes.

### 3.2.3.3 Screening of $\beta$ -galactosidase secreting *P. pastoris* clones

Screening plates were transferred with a replicator stamp onto a methanol-containing YP-agar plate (YPM). Induction was carried out for 3 days at 30 °C and maintained by the addition of a few drops 100% MeOH every 24 h to the plate lid to account for evaporating MeOH. Secreting clones were then identified by yeast colony western blot as described previously [134]. 2–6 clones that showed strong western blot signal were then used to inoculate 2 mL BMGY in a 15 mL conical tube and were incubated overnight at 30 °C and 180 rpm to generate biomass. The culture was harvested by centrifugation (3,220 x g, 10 min, RT) and induced in 1 mL BMMY. Cultures were incubated for 96 h at 30 °C and 180 rpm. Induction was maintained by adding 1% (v/v) MeOH every 24 h. Pellets and supernatants were separated by centrifugation (13,000 x g, 5 min). Proteins from pellets were extracted with glass beads as described in the EasySelect Pichia Expression Kit manual, and pellet extracts and supernatants were analyzed for protein expression by SDS-gel electrophoresis and western blot to verify the yeast colony western blot. Positive  $\beta$ -galactosidase secreting clones were streaked out on fresh YPD plates, supplemented with 100 µg/mL zeocin as a source of single clones for protein expression.

### 3.2.3.4 Screening of GFP-derivatives secreting *P. pastoris* clones

Clones from a screening plate were directly used to inoculate 200 µL BMMY supplemented with 100 µg/mL ampicillin in a 96-well transparent round bottom plate. Plates were covered and incubated at 30 °C, 140 rpm overnight. Cells were harvested by centrifugation (3,220 x g, 10 min, RT) and resuspended in 100 µL NP-buffer supplemented with 2% (v/v) MeOH. Plates were incubated for additional 3 days at 30 °C and 140 rpm and re-induced every 24 h by adding 2% (v/v) MeOH. Supernatants were harvested by centrifugation (3,220 x g, 10 min, RT), and supernatants were transferred to a black FLUOTRAC plate. Plates were illuminated with a blue LED on the Bio-Rad Chemi-

Doc system, using the Alexa 488 filter for optical detection. Additionally, emission at 525/20 nm was detected after excitation at 485/25 nm. The presence of recombinant GFP-proteins in the supernatant was additionally validated by western blot against the His-tag. As for  $\beta$ -galactosidase clones, positive GFP secreting clones were streaked out on fresh YPD plates supplemented with 100  $\mu$ g/mL zeocin.

#### **3.2.3.5 Large-scale protein expression in *P. pastoris***

A single clone of the desired *P. pastoris* transformant was used to inoculate 20 mL YPD-medium supplemented with 100  $\mu$ g/mL ampicillin. After incubation overnight at 30 °C and 180 rpm this starter culture was used to inoculate 4 L BMGY that were separated on four 5 L baffled flasks. The biomass culture was supplemented with 100  $\mu$ g/mL ampicillin and 10  $\mu$ L antifoam and incubated overnight at 30 °C and 120 rpm until OD600 reached 5–6. Cells were harvested by centrifugation (3,000 x g, 8 min, RT) and resuspended in 400 mL NP-buffer supplemented with 100  $\mu$ g/mL ampicillin and 10  $\mu$ L antifoam. This suspension was split on two 2 L flasks (200 mL each), and 2% (v/v) MeOH were added for induction. Cultures were incubated for 48–72 h in the case of GFP variants, or for 72–96 h in the case of  $\beta$ -galactosidase at 30 °C and 140 rpm. 1% (v/v) MeOH was added every 24 h to re-induce the culture. Finally, supernatants were harvested by centrifugation (20,000 x g, 15 min, 4 °C) and filtered through a 0.2  $\mu$ m cellulose acetate filter. From here on solutions were kept on ice and directly processed for purification.

#### **3.2.3.6 Calcium phosphate transfection of HEK293T cells**

$3 \times 10^6$  HEK293T cells were plated in 10 mL HEK medium in a T75 flask and incubated overnight. Medium was aspirated and cells were washed once with PBS before 10 mL fresh HEK cell medium were added. Cells were incubated for at least 1 h. For the generation of DNA-precipitates, 10  $\mu$ g plasmid DNA were mixed with 1 M  $\text{CaCl}_2$  and ultrapure  $\text{H}_2\text{O}$  to adjust 0.25 M  $\text{CaCl}_2$  in 500  $\mu$ L. This solution was mixed with 500  $\mu$ L 2x BBS by vortexing and was incubated for 5–20 min at RT before adding to the HEK293T cells. Cells and precipitates were incubated overnight before the supernatant was aspirated, and cells were washed twice with 5 mL PBS. For protein production, cells were incubated for another 72 h in 20 mL OptiMem. Before proceeding with protein purification, supernatants were harvested by centrifugation (10 min, 3,220 x g, 4 °C) and filtered through a 0.2  $\mu$ m cellulose acetate filter.

### 3.2.4 Protein purification

#### 3.2.4.1 Purification of recombinant His-tagged $\beta$ -galactosidase from *P. pastoris* supernatants

The 400 mL filtered supernatants from large-scale expression cultures were concentrated by tangential filtration through a 30 kDa cut-off Hydrosart membrane to roughly 20–40 mL, and the concentrate was washed twice with fresh NP-buffer. The solution was further concentrated by ultrafiltration with a 15 mL Amicon centrifuge device (30 kDa cut-off) to a volume of 4 mL. The concentrate was adjusted with NPI-20 and 1 % Triton X-100 in NP-buffer to 10 mM imidazole and 0.1 % (v/v) Triton X-100. This solution was batch-purified on 2 mL settled Ni-NTA agarose (Macherey-Nagel) mainly as described in the section for native purification in the manufacturer’s manual. Briefly, 2 mL bed volume Ni-NTA beads were washed 5 times in a 15 mL conical tube with 10 mL NPI-10. Afterwards, the protein-containing solution was loaded on the beads, and beads were incubated for 60 min at RT with overhead rotation. Beads were harvested by centrifugation (5 min, 500 x g) and washed three times with 10 mL NPI-10 and once with 10 mL NPI-20 for 10 min each. Protein was eluted in 5 elution steps with 5 mL NPI-250 each. Fractions were pooled, concentrated over a 30 kDa cut-off Amicon ultrafiltration device and buffer was exchanged on that same device by washing four times with PBS.

#### 3.2.4.2 Purification of recombinant His-tagged GFP variants from *P. pastoris* supernatants

For GFP proteins, filtered supernatants were concentrated with 10 kDa cut-off Amicon ultrafiltration devices and washed within one device 3 times with NP buffer. Batch purification with Ni-NTA beads was then carried out as described for  $\beta$ -galactosidase in the previous paragraph, except that pooled elution fractions were concentrated to 2 mL with a 10 kDa cut-off Amicon ultrafiltration device and no buffer exchange was performed. Instead, the 2 mL were loaded at 2 mL/min onto a PBS-equilibrated size exclusion column packed with Sephacryl S200 HR with a Bio-Rad Biologic LP system. 2 mL fractions were collected and GFP containing fractions (determined by A280 and optically by the greenish-yellowish GFP color) were pooled, concentrated and washed 3 times with PBS, using a 10 kDa cut-off Amicon ultrafiltration device.

#### **3.2.4.3 Purification of recombinant His-tagged GFP variants from HEK293T cell supernatants**

GFP containing OptiMem-supernatants from transfected HEK293T cells was purified via Ni-NTA agarose like the recombinant GFPs from *P. pastoris*, except that elution fractions were pooled and directly concentrated and washed three times with PBS, using a 10 kDa cut-off Amicon ultrafiltration device without additional size exclusion chromatography.

#### **3.2.4.4 Purification of MR-Fc chimeric proteins from HEK293T cell supernatants**

Supernatants from HEK cells transfected with MR-Fc chimeras were purified by affinity chromatography over pre-packed 1 mL Protein G columns according to the manufacturer's manual. In short, the column was attached to the Bio-Rad BioLogicLP device, and a flow of 1 mL/min was used in all steps. The column was equilibrated with Protein G binding buffer until A280 and conductivity baselines were constant. Supernatants were diluted in double the volume Protein G binding buffer before loading. After loading, the column was washed with Protein G binding buffer until baselines were constant. Proteins were eluted with Protein G elution buffer. 970  $\mu$ L fractions were collected in 1.5  $\mu$ L reaction tubes, pre-filled with 30  $\mu$ L Protein G neutralization buffer. Tubes were directly inverted for mixing when fractions were collected. Fractions containing the main protein according to A280 were pooled and transferred to a 50 kDa cut-off Amicon ultrafiltration unit. Samples were concentrated and washed 4 times with PBS to get rid of contaminating salts.

#### **3.2.4.5 Purification of recombinant His-tagged $\beta$ -galactosidase from *E. coli* pellets**

Protein purification was mainly done according to the guidelines for denatured protein from the Protino Ni-NTA Agarose manual (Macherey-Nagel) with some modifications. The weight of the pellets was determined, and pellets were resuspended thoroughly in 2 mL/g DNPI-10 supplemented with protease inhibitors without EDTA and 1 mM PMSF. Pellets were lysed on ice by sonication (1 min constant pulse with 40% amplitude, followed by 10 min 3x pulse with 40% amplitude), and lysates were cleared by centrifugation (20,000 x g, 30 min, 4°C). Lysates were filtered through a 0.45  $\mu$ m cellulose acetate filter, and batch purification was performed with Ni-NTA agarose as

described for *P. pastoris*-derived proteins, except that all NP-buffers were exchanged by DNP-buffers containing 8 M urea as a denaturing agent. Elution fractions were pooled, and a 30 kDa cut-off Amicon ultrafiltration unit was used to concentrate and wash the protein five times with PBS to dilute the urea to submillimolar concentrations.

## 3.2.5 Protein modification

### 3.2.5.1 Enzymatic deglycosylation with Endo H or PNGase F

Proteins were enzymatically deglycosylated by treatment with Endo H or PNGase F. Endo H treatment was exclusively performed under native conditions. 1–5 mg of target protein were typically supplemented with 100 U enzyme per mg protein in 1x GlycoBuffer 3 (NEB) and incubated for 18 h at 37 °C. PNGase F treatment of OVA-647 intended for uptake experiments was also performed under native conditions with 5 U Enzyme per 20 µg Protein in 1x GlycoBuffer 2 (NEB) for 6 days at 37 °C. The PNGase F treatment of proteins intended for western blot analysis or ELISA-like binding assays was performed under denaturing conditions according to the manufacturer’s manual.

### 3.2.5.2 Labeling of $\beta$ -galactosidase with Alexa Fluor 647

The labeling of 100 µg  $\beta$ -galactosidase was performed with the Molecular Probes Alexa Fluor Antibody Labeling Kit according to the manufacturer’s manual. Labeling efficiency was calculated as described in the manual and suggested 1–2 mol of dye per mol protein. As an estimate, the molar extinction coefficient of unglycosylated  $\beta$ -galactosidase was determined with the ProtParam online tool at the ExPASy Bioinformatics Resource Portal ([web.expasy.org/protparam/](http://web.expasy.org/protparam/))[135] for this calculation.

### 3.2.5.3 Labeling of NST-GFP with DyLight 650

250 µg NST-GFP were labeled with the DyLight 650 NHS-ester labeling Kit (Thermo Fisher Scientific) according to the manufacturer’s manual. The degree of labeling was calculated according to the manual and suggested 4 mol dye per mol NST-GFP.

## 3.2.6 Protein analysis

### 3.2.6.1 Determination of protein concentrations

Protein concentrations of purified proteins were determined by A280 absorbance, using a Nanodrop 2000 UV/Vis spectrometer. In cases of complex solutions like cell lysates, a Bradford protein assay (Roti Quant, Carl Roth) or a bicinchoninic acid (BCA) assay (Pierce BCA Protein Assay Kit, Thermo Fisher Scientific) was performed, as described in the manufacturers' manuals. Tests were chosen according to the best compatibility with putative contaminants in the complex mixture, as recommended by Thermo Fisher Scientific.

### 3.2.6.2 Sodium dodecyl sulfate polyacrylamide gel electrophoresis (SDS-PAGE)

The separation of proteins according to their size was performed by discontinuous gel electrophoresis as described by Laemmli [136] with a vertical mini gel electrophoresis system from Bio-Rad. Stacking gels were prepared according to Table 3.3.

**Table 3.3: Composition of stacking gels — recipe for 2 mL**

Reagent	Volume of components (mL)
Ultrapure H <sub>2</sub> O	1.4
30 % acryl-bisacrylamide mix	0.33
1.5 M Tris (pH 6.8)	0.25
10 % (w/v) SDS	0.02
10 % (w/v) ammonium persulfate	0.02
TEMED	0.002

Polyacrylamide concentrations from 8–12% were used according to the molecular weight range at which separation was needed. Resolving gels were prepared according to Table 3.4.

**Table 3.4: Composition of resolving gels — recipe for 10 mL**

Reagent	Volume of components mL		
	for 8 %	for 10 %	for 12 %
Ultrapure H <sub>2</sub> O	4.6	4.0	3.3
30 % acryl-bisacrylamide mix	2.7	3.3	4.0
1.5 M Tris (pH 8.8)	2.5	2.5	2.5
10 % (w/v) SDS	0.1	0.1	0.1
10 % (w/v) ammonium persulfate	0.1	0.1	0.1
TEMED	0.006	0.004	0.004

Samples were denatured by supplementing them with 1x Laemmli buffer and boiling for 5 min at 95 °C. Typically, 1 µg purified protein or 100–300 µg total protein from cell lysates were loaded per lane. For comparative analysis during protein purification, volumes of loaded aliquots were chosen to represent equal proportions of each fraction, e.g. if 10 µL of a 10 mL input fraction were loaded, a 5 mL elution fraction would be potentially 2x concentrated and hence only 5 µL were loaded. Electrophoresis was carried out in 1x SDS buffer with 20 mA per gel.

### 3.2.6.3 Coomassie staining

For coomassie staining, SDS-gels were rinsed once in ultrapure H<sub>2</sub>O after gel electrophoresis and then incubated on a rocker at RT for 2–18 h in Roti-Blue, diluted in ultrapure H<sub>2</sub>O and supplemented with 20 % (v/v) MeOH. Afterwards, gels were destained by incubation in ultrapure H<sub>2</sub>O for 2–18 h.

### 3.2.6.4 Western blot/far-western blot analysis

All western and far-western blot analyses were performed according to the semi-dry method on nitrocellulose membranes. Briefly, gels, blotting paper, and nitrocellulose membranes were incubated for 5 min in Towbin buffer and then assembled on the Bio-Rad Trans-Blot SD Semi-Dry Transfer Cell according to the manufacturer’s manual. Blotting was carried out at 25 V and 200 mA per mini gel for 45 min. Blots were blocked in TBST + 5 % milk powder for 30 min at RT. Standard western blots were then incubated with primary antibodies, diluted 1/1000 in TBST for 1 h at RT. Blots were washed three times with TBST for 10 min and then incubated with the corresponding

horseradish peroxidase (HRP)-conjugated secondary antibody diluted 1/5000 in TBST for 1 h at RT. Finally, blots were washed again three times with TBST for 10 min. Far-western blots were incubated with 50 µg/mL MR-CTLD in TBSTC for 18 h at 4 °C and then washed three times with TBSTC for 10 min. Far-western blots were then incubated with 1/5000 HRP-conjugated anti-human IgG secondary antibody in TBSTC for 1 h at RT and finally washed three times with TBSTC for 10 min. Blots were developed by adding ECL substrate, and chemiluminescence was detected with the Bio-Rad ChemiDoc MP system.

#### **3.2.6.5 Enzyme-linked immunosorbent assay (ELISA)**

Transparent 96-well ELISA plates were coated with 0.5 µg/mL capture antibody in 50 µL ELISA coating buffer for 1 h at 37 °C and then washed three times with 150 µL ELISA washing buffer. Wells were then blocked with 100 µL ELISA blocking buffer for 30 min at RT and afterwards washed again three times. 50 µL samples and the appropriate standard serial dilution were added, and plates were incubated for 1 h at 37 °C, followed by three washing steps. Captured proteins were detected by incubation with 0.5 µg/mL biotinylated capture antibody in 50 µL ELISA blocking buffer for 1 h at 37 °C and then washed three times. Wells were then incubated with 10 µg/mL HRP-conjugated neutravidin in PBS for 30 min at RT and afterwards washed again three times. HRP activity was monitored by adding 50 µL 2,2'-Azino-bis(3-ethylbenzothiazoline-6-sulfonic acid) (ABTS) solution (1 mg/mL ABTS in ABTS buffer, supplemented with 15 µL H<sub>2</sub>O<sub>2</sub> per 10 mL solution) and measuring the absorbance at 405 nm.

#### **3.2.6.6 Fc-chimeric ELISA-like binding assay**

Assays were carried out as described previously [66], except that TBS was used instead of PBS to prevent precipitation of insoluble calcium phosphate. In short, 96-well plates were coated with 0.1 mg/mL of the protein substrate in Fc-chimeric coating buffer for 1 h at 37 °C. Plates were washed three times with 150 µL TBST and blocked for 1 h with TBST + 0.3 % BSA at RT. For assays including the MR-Nterm Fc-chimera, Fc-chimeric proteins (10 µg/mL) were pre-incubated for 1 h at RT with anti-human alkaline phosphatase (AP)-conjugate (1:100) in TBSTC + 0.3 % BSA. Plates were then incubated with these immune complexes for 1 h at RT. After three washing steps with 150 µL TBSTC, plates were incubated with 1 mg/mL 4-Nitrophenyl phosphate in AP substrate



buffer, and absorbance was monitored at 405 nm. For all downstream analyses without MR-Nterm, the MR-CTLD Fc-chimeric protein and Fc control were not complexed as described above. Instead, after 1 h incubation with uncomplexed Fc-chimeras (10  $\mu\text{g}/\text{mL}$ ) in TBSTC, plates were washed three times with TBSTC and incubated with anti-human AP (1:1000) for 1 h at RT. After another three washes with TBSTC, detection was performed with the substrate as described above.

### **3.2.6.7 Fluorescence spectroscopy**

For emission and excitation spectra, proteins were adjusted to 0.1 mg/mL in PBS, and 500  $\mu\text{L}$  were placed in a 1 mL quartz cuvette. Spectra were collected with a FluoroMax-4 spectrofluorometer. Excitation spectra were collected from 340–520 nm with a bandwidth of 10 nm, and fluorescence was detected at 540 nm with a bandwidth of 1 nm. Emission spectra were detected from 500–750 nm with a bandwidth of 1 nm by constant excitation at 488 nm with 5 nm bandwidth.

## **3.2.7 Cellular assays**

### **3.2.7.1 Antigen uptake by BM-DCs**

BM-DCs were harvested with 2 mM EDTA in PBS on day 7 or 8.  $2 \times 10^5$  BM-DCs were seeded per well in a 24-well cell culture plate. Cells were incubated at 37 °C and 5% CO<sub>2</sub> for at least 45 min to allow the cells to attach to the plate bottom. If not otherwise declared, cells were pulsed for 20 min with 250 ng/mL Alexa Fluor 647-labeled ovalbumin (OVA-647), 500 ng/mL Alexa Fluor 647-labeled  $\beta$ -gal or 1  $\mu\text{g}/\text{mL}$  GFP in uptake medium at 37 °C and 5% CO<sub>2</sub>. The blocking of the uptake was performed by co-incubation with 3 mg/mL yeast mannan, 3 mg/mL unlabeled ovalbumin or by adding 2.5 mM EDTA. Cells were harvested by scraping, transferred to FACS tubes and washed once with 3 mL PBS. Finally, cells were resuspended in 250  $\mu\text{L}$  FACS buffer and analyzed by flow cytometry with either a guava easyCyte (Millipore) or an LSR II (BD Biosciences).

### **3.2.7.2 Subcellular localization of antigens and colocalization in BM-DCs**

BM-DCs were harvested with 2 mM EDTA in PBS on day 7.  $2 \times 10^5$  BM-DCs were seeded on glass coverslips that were placed in a 24-well cell culture plate. Cells were al-

lowed to adhere for 30–60 min at 37 °C and 5 % CO<sub>2</sub> and were then pulsed with 1 µg/mL Alexa Fluor 647-labeled β-gal alone or in combination with 500 ng/mL Alexa Fluor 488-labeled OVA or transferrin (Trf) for 20 min. In order to study NST-GFP localization, cells were incubated with 500 ng/mL NST-GFP and 250 ng/mL OVA-647. Cells were washed three times with PBS and fixed with fixation buffer for 15 min. Samples intended for intracellular staining were then permeabilized and blocked in intracellular staining buffer + 5 % BSA for 1 h and then stained with 1/200 anti-EEA1, 1/500 anti-LAMP-1 or 1/100 Alexa Fluor 488-conjugated anti-MR primary antibodies in staining buffer for 1 h. After washing three times with PBS, EEA1 and LAMP-1 stained cells were incubated with 1/1000 Alexa Fluor 568-labeled anti-rabbit or anti-rat secondary antibodies, respectively, in staining buffer for 30 min and washed again three times with PBS. All samples were then stained with 1 µg/mL DAPI in PBS for 10 min. Afterwards, samples were washed 4 times with PBS and once with ultrapure H<sub>2</sub>O and finally mounted in Fluoromount onto microscope slides. Fluorescence microscopy was performed on an AxioObserver inverse microscope with a ZEISS ApoTome system.

#### **3.2.7.3 Antigen uptake by HEK293T cells expressing the MR**

HEK293T cells expressing the MR (HEK-MR) or control cells (HEK) were harvested the day before the experiment with Trypsin/EDTA solution, and  $2 \times 10^5$  cells were seeded per well in a 24-well plate. 10 min before the experiment, 4 °C samples and Alexa Fluor 647-labeled β-gal solutions were put on ice in the fridge. 37 °C cells were then pulsed with 500 µg/mL pre-warmed Alexa Fluor 647-labeled β-gal in HEK cell medium for 15 or 30 min at 37 °C. 4 °C cells were treated likewise with the pre-cooled antigen at 4 °C on ice in the fridge. Cells were washed once with 1 mL ice-cold PBS. Supernatants were aspirated, and cells were harvested in 250 µL ice-cold fluorescence-activated cell sorting (FACS) buffer and analyzed by flow cytometry on an LSR II.

#### **3.2.7.4 Antigen uptake by PBMC-derived DCs and macrophages**

$4 \times 10^5$  PBMC-derived DCs or macrophages were seeded per well in a 24-well plate. Cells were incubated for at least 1 h before 1 µg/mL of NST-GFP, QST-GFP or Endo H-treated NST-GFP were applied in the absence or presence of 3 mg/mL mannan for 20 min. Uptake was stopped by putting the cells on ice and adding 1 mL ice-cold PBS. Cells were harvested by scraping, transferred to FACS tubes and collected by centrifuga-

tion (300 x g, 5 min, 4 °C). Cells were washed once with FACS buffer, then resuspended in FACS buffer and analyzed on an LSR II flow cytometer.

### **3.2.7.5 MR-surface expression of PBMC-derived DCs and macrophages**

PBMC-derived DCs or macrophages were harvested in FACS buffer by scraping, and  $4 \times 10^5$  cells were transferred to FACS tubes and washed once with FACS buffer. Cells were incubated with 1/1000 biotinylated anti-human CD206 in FACS buffer supplemented with 1% (v/v) mouse serum for 20 min at 4 °C. Cells were harvested by centrifugation (300 x g, 5 min, 4 °C), washed twice with FACS buffer and then incubated with 1/1000 Alexa Fluor 647-conjugated streptavidin in FACS buffer for 20 min at 4 °C. Cells were washed again with FACS buffer, resuspended in FACS buffer and analyzed on an LSR II flow cytometer.

### **3.2.7.6 Acquisition of activation marker surface expression on BM-DCs after stimulation**

Day 3 BM-DCs were directly split on 3 cm dishes in order to minimize pre-activation of BM-DCs due to additional harvesting at day 7. On day 6, 4 µg/mL control-treated or Endo H-treated β-gal from *P. pastoris*, 4 µg/mL β-gal from *E. coli* or 1 µg/mL LPS were added and cells were incubated for another 18 h. The next day, cells were harvested by scraping, collected by centrifugation (300 x g, 5 min, 4 °C) and washed once with FACS buffer. Cells were then stained with 1/200 dilutions of fluorescently labeled anti-CD40, anti-CD80, anti-CD86 or anti-MHC I in FACS buffer, supplemented with 1% (v/v) mouse serum for 20 min at 4 °C. Cells were washed again with FACS buffer and analyzed on the guava easyCyte flow cytometer.

### **3.2.7.7 Detection of cytokine secretion by BM-DCs after stimulation**

Day 7 BM-DCs were harvested with 2 mM EDTA in PBS, and  $1 \times 10^5$  cells were seeded per well in a 96-well plate. Cells were stimulated with 100 µg/mL control-treated or Endo H-treated β-gal for 24 h. As controls, cells were incubated with 0.1 µg/mL LPS or without any further stimuli. Cells were centrifuged (300 x g, 5 min), and supernatants were carefully transferred and analyzed for the presence of IL-6, IL-12 and TNF-α by ELISA.

### 3.2.7.8 Proliferation and IL-2 secretion of OT-I, OT-II and DesTCR cells after stimulation

Day 7 BM-DCs were harvested with 2 mM EDTA in PBS, and  $1 \times 10^5$  cells were seeded per well in a 96-well plate. Cells were incubated for 30 min before adding 20  $\mu\text{g}/\text{mL}$  untreated  $\beta$ -gal, Endo H-treated  $\beta$ -gal, 1  $\mu\text{g}/\text{mL}$  LPS or medium only and incubating for 1 h. After three washing steps with PBS, BM-DCs intended for presentation to OT-I or OT-II cells were pulsed for 1 h with 125 nM OVA<sub>257-264</sub> or 800 nM OVA<sub>323-339</sub>, respectively. In the mean time splenocytes from OT-I, OT-II and DesTCR mice were isolated. Mice were first anesthetized with isofluran and then euthanized by cervical dislocation. Spleens were removed, passed through a metal cell strainer, and resuspended thoroughly in PBS by pipetting to get a single cell suspension. This suspension was further purified through a nylon sieve to remove rough debris. Cells were counted by adding acetic acid (0.5% (v/v)) and trypan blue to exclude erythrocytes and other dead cells.

For the assessment of IL-2 secretion, BM-DCs were washed again with PBS and then incubated with  $1 \times 10^5$  splenocytes for 18 h in T cell medium. Finally, cells were centrifuged and supernatants were analyzed by ELISA for the presence of IL-2.

To analyze T cell proliferation, splenocytes were stained with 1  $\mu\text{M}$  carboxyfluorescein succinimidyl ester (CFSE) in PBS for 20 min at 37 °C. Staining was stopped by adding ice-cold T cell medium, and cells were subsequently washed twice with PBS. The cell number was determined again as described above. BM-DCs were then washed with PBS, and  $1 \times 10^5$  cells were added in 100  $\mu\text{L}$ . After 24 h, 200  $\mu\text{L}$  fresh T cell medium was added, and cells were incubated for another 48 h. After a total of 3 days co-culture, T cells were harvested by centrifugation (500 x g, 7 min, 5 °C) and stained with 1/1000 PerCP/Cy5.5-conjugated anti-CD8 or anti-CD4 antibodies in 40  $\mu\text{L}$  FACS buffer for 20 min at 4 °C. Cells were washed with 200  $\mu\text{L}$  FACS buffer and resuspended on the 96-well plate in 50  $\mu\text{L}$  FACS buffer. Cells were analyzed by flow cytometry with a HTS plate reader system (BD Biosciences) on the LSR II. Analysis was performed by gating on single cells that were positive for the respective surface marker and then measuring the cell count of the individual CFSE dilution profile peaks. Expansion indices were then calculated as previously described [137].

### 3.2.8 *In vivo* experiments

Animal handling and immunizations were performed by Janina Küpper (AG Schumak, UK Bonn). C57BL/6J mice were immunized by subcutaneous injection into the left inguinal area at day -13 and day -6 with 50 µg glycosylated or deglycosylated β-gal or NST-GFP-S8L supplemented with 50 ng LPS per injection. Naïve mice received no treatment.

#### 3.2.8.1 *In vivo* cytotoxicity assay

On day -1 the assessment of *in vivo* cytotoxicity was mostly performed as previously described [138]. In brief, C57BL/6J splenocytes were isolated as described above. Target cells were pulsed with the β-gal<sub>497-504</sub>, β-gal<sub>96-103</sub> or OVA<sub>257-264</sub> peptide (2 µM) in PBS for 25 min at 37 °C, control cells were incubated in PBS only. Target cells were then stained with 1.5 µM CFSE, whereas control cells were stained with 0.15 µM CFSE for another 25 min at 37 °C. Staining was stopped by adding ice-cold T cell medium, and cells were washed twice with ice-cold PBS. Staining was controlled by flow cytometry on a BD FACSCanto™ II (BD Bioscience). Cells were then pelleted by centrifugation and adjusted to  $5 \times 10^7$  cells per mL in 0.9 % NaCl, and the three groups of mice (naïve, untreated glycoprotein, Endo H-treated glycoprotein) were injected intravenously with a mixture of  $5 \times 10^6$  control cells and  $5 \times 10^6$  target cells. After another 18 h (day 0), animals were anesthetized with isofluran and then euthanized by cervical dislocation. Inguinal lymph nodes were isolated, perfused with 0.05 % collagenase, cut in small pieces and incubated for 30 min at 37 °C. Cells were washed, resuspended in MACS buffer and filtered through a nylon sieve before being analyzed by flow cytometry on a BD FACSCanto™ II (BD Bioscience). Specific killing was calculated with the formula:

$$\% \text{ specific kill} = 100 - \frac{\left( \frac{\text{target cells}}{\text{control cells}} \right)_{\text{sample}}}{\left( \frac{\text{target cells}}{\text{control cells}} \right)_{\text{naïve group mean}}} \times 100$$

### **3.2.8.2 *Ex vivo* restimulation and IFN- $\gamma$ ELISA**

To determine the secretion of IFN- $\gamma$ , cells from draining lymph nodes isolated as described above were resuspended in T cell medium, and  $1 \times 10^6$  cells were seeded per well in a 96-well plate. Cells were re-stimulated with  $2 \mu\text{M}$  of  $\beta\text{-gal}_{497-504}$  peptide overnight at  $37^\circ\text{C}$ . The next day, cells were centrifuged, and IFN- $\gamma$  concentration in the supernatant was determined by ELISA.

### **3.2.8.3 *Ex vivo* determination of antigen-specific antibodies**

Before euthanasia, blood was taken from animals immunized as described above. The blood was allowed to clot and sera were collected by centrifugation ( $2000 \times g$ , 10 min). Control-treated or Endo H-treated  $\beta\text{-gal}$  ( $25 \mu\text{g}/\text{mL}$ ) were coated to an ELISA plate at  $4^\circ\text{C}$  for 18 h. Afterwards, plates were washed three times with PBST. Samples were then incubated with serum (diluted 1/64 in PBS) for 2 h and detected with 1/1000 HRP-conjugated whole mouse IgG-specific antibody in PBS by the standard ELISA procedure.

## 4 Results

### 4.1 The binding of ovalbumin to the mannose receptor is mediated by N-linked glycans

The C-type lectin-like domains (CTLDs) of the MR are essential for binding to OVA, which was demonstrated by several studies inhibiting its C-type lectin activity [139, 140]. These studies rely either on competitive inhibition with C-type lectin ligands such as yeast mannan, or on the absence or active removal of calcium ions, which are essential for the CTLDs to fulfill their sugar-binding activity [62, 141]. Though all these data indicate that the glycoprotein OVA has to bind via its glycan to the CTLDs of the MR, a direct proof is still missing.

To directly address the issue of glycan-dependency we used human IgG1 Fc-chimeric proteins of MR-subunits, which have been successfully applied to investigate the binding specificities of MR-subdomains to different ligands *in vitro* [66]. The chimeric proteins either comprise the N-terminal portion of the MR (MR-Nterm) consisting of the CR, the FNII domain and the first two carbohydrate recognition domains, or the C-type lectin activity-bearing C-terminal domain (MR-CTLD) comprising the CRDs 4–7 (Figure 2.4). As a control, the human Fc fragment was used to exclude binding artifacts of the fused IgG1 Fc region.

In an ELISA-like assay the MR-CTLD clearly bound to immobilized ovalbumin (Figure 4.1 A), whereas MR-Nterm bound to collagen as previously described [66]. BSA served as a negative control and was bound by neither of the detecting proteins. To investigate whether the binding of the MR-CTLD to OVA is really mediated by an N-glycan, OVA was treated with the glycosidase PNGase F. Indeed, binding of MR-CTLD was lost after the deglycosylation of OVA (Figure 4.1 A).

We also used the MR-CTLD protein in a far-western blot analysis of deglycosylated and control-treated OVA, thereby confirming the binding of the MR-CTLD to glycosylated OVA (Figure 4.1 B) and excluding binding artifacts to contaminating proteins, which occur in commercial OVA preparations [72].

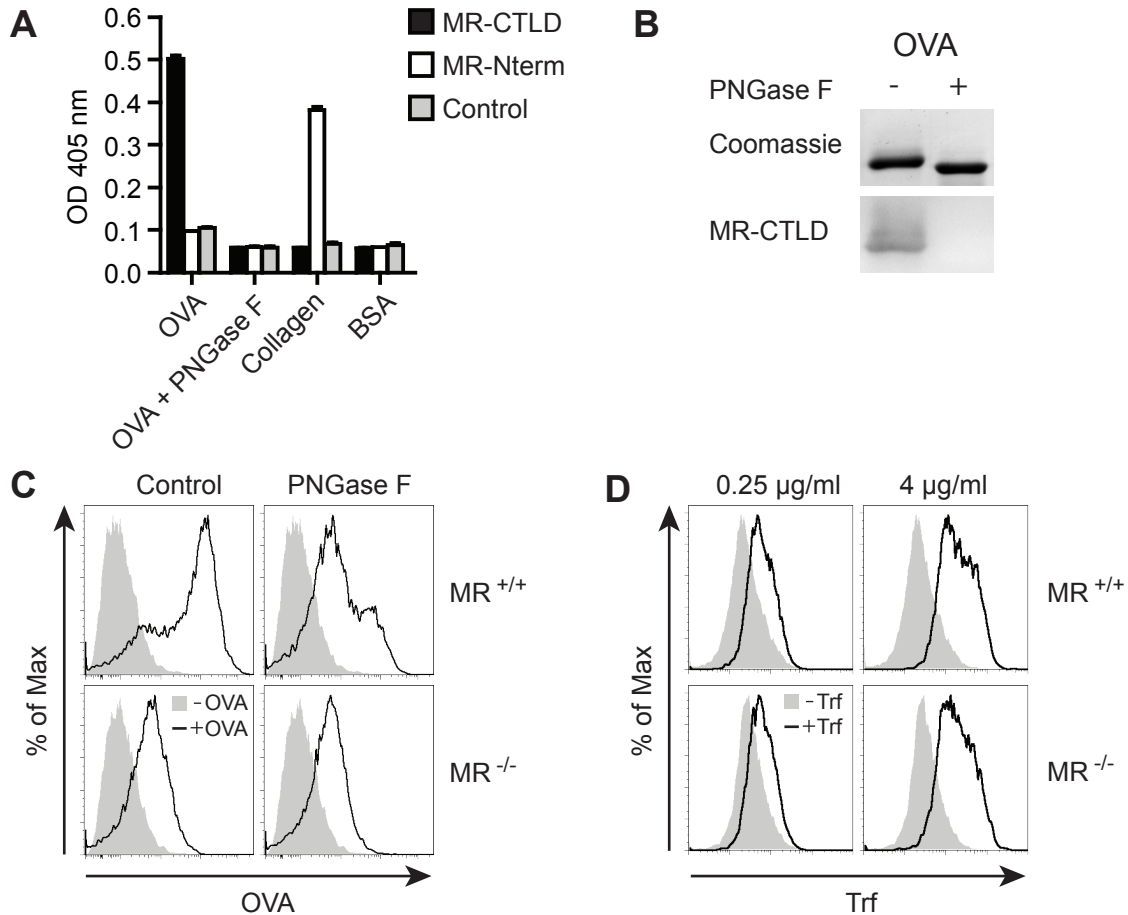


**Figure 4.1: Glycan-dependent binding and uptake of OVA by the mannose receptor**

(A) Binding of MR-CTLD, MR-Nterm Fc-chimeric proteins or isotype control to immobilized OVA, PNGase F-treated OVA, collagen or BSA was determined by ELISA. The graph depicts the mean of three replicates. Error bars indicate standard error of the mean (SEM). (B) OVA or PNGase F-treated OVA were separated by SDS-PAGE and detected by coomassie staining or far-western blot with MR-CTLD. (C) Wildtype or MR-deficient BM-DCs were pulsed for 15 min with Alexa Fluor 647 OVA conjugate, which was either control-treated or PNGase F-treated. Fluorescence intensity was monitored by flow-cytometry. (D) Wildtype or MR-deficient BM-DCs were pulsed for 15 min with low (0.25 µg/mL) or high (4 µg/mL) concentrations of Alexa 647-conjugated transferrin (Trf). All graphs show representative data of at least three independent experiments.



Finally, we pulsed bone marrow-derived dendritic cells (BM-DCs), generated either from wild-type (MR<sup>+/+</sup>) or mannose receptor-deficient mice (MR<sup>-/-</sup>), for 20 min with deglycosylated or control-treated OVA and monitored the uptake by flow cytometry. OVA uptake was markedly reduced after deglycosylation to a level comparable to MR<sup>-/-</sup> BM-DCs (Figure 4.1 C), which exhibit strongly impaired OVA-uptake, as previously described [51, 139]. Importantly, MR<sup>-/-</sup> BM-DCs are as competent in MR-independent endocytosis as wild-type cells, demonstrated by the uptake of fluorescently labeled transferrin (Trf) (Figure 4.1 D).

These experiments not only verify that the binding and internalization of OVA by the MR depends on the C-type lectin domains of the MR, but also show for the first time that it is indeed solely attributed to the N-glycans on OVA.

## **4.2 *Pichia pastoris* glycosylates N-glycosylation motifs incidentally present in non-glycoproteins and thereby generates mannose receptor ligands**

Lam et al. have previously expressed a part of ovalbumin (AA230–359) comprising the glycosylation sites N292 and N311 in *P. pastoris* [120]. In a follow-up study they showed that this recombinant protein was taken up by MR-expressing chinese hamster ovary (CHO) cells but uptake was strongly reduced if both asparagines were substituted by glutamines or upon blocking with yeast mannan [122]. Together with our data from the deglycosylation experiments of hen ovalbumin this strongly suggests that *P. pastoris* not only glycosylates the glycoprotein ovalbumin at its designated N-glycosylation sites, but also adds N-glycans which are similar to OVAs natural N-glycans and hence are ligands of the MR.

We followed up these findings and wanted to investigate whether we could use *P. pastoris*-derived N-glycosylation as a general MR-targeting strategy for proteins that are non-glycosylated in their native state (e.g. cytosolic proteins). To this end, we chose a portion (V10–L731) of the cytosolic *E. coli* protein  $\beta$ -galactosidase ( $\beta$ -gal) as a model antigen. Though not glycosylated in its native state in *E. coli*,  $\beta$ -gal incidentally comprises five N-X-S/T motifs which could act as potential N-glycosylation sites (Figure 4.2 A). Four of these motifs are present in  $\beta$ -gal(V10–L731) (Figure 4.2 B).

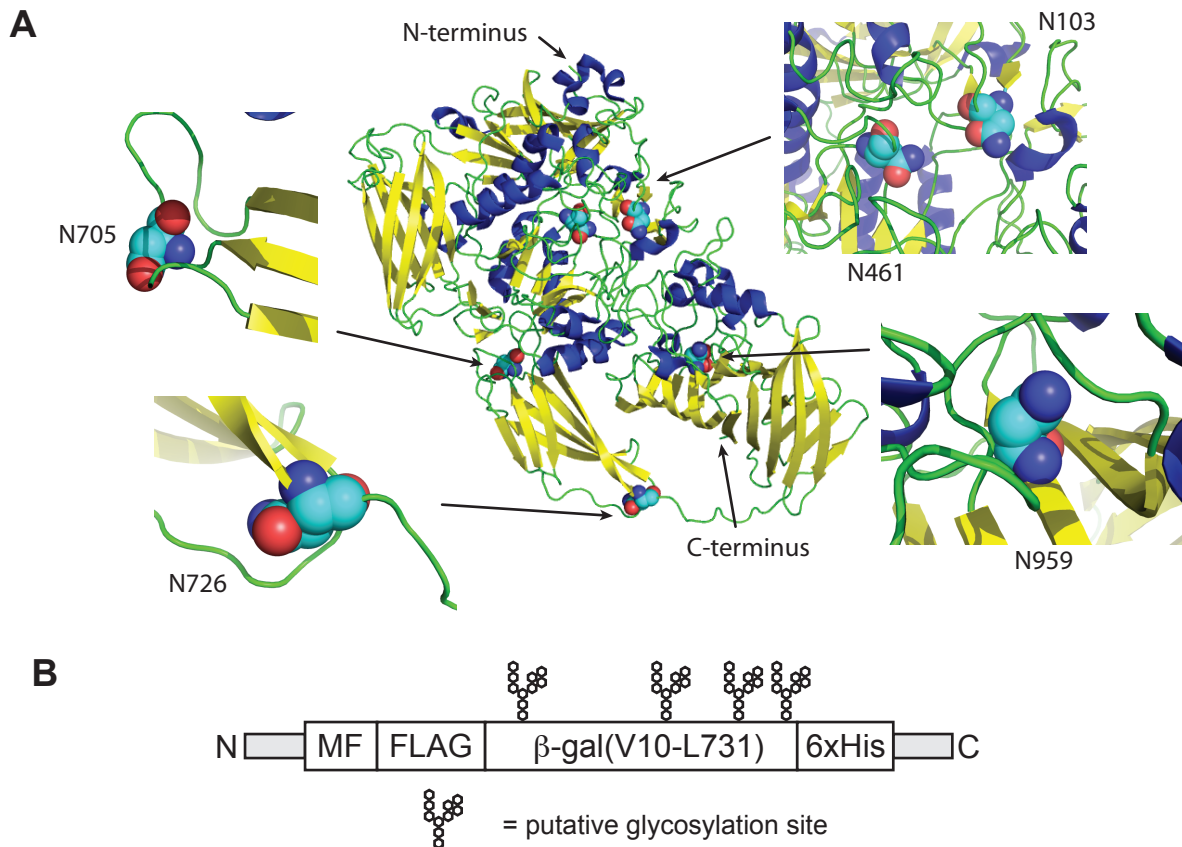


**Figure 4.2: The model antigen  $\beta$ -galactosidase with its putative N-glycosylation sites**

(A) 3D structure of whole  $\beta$ -gal (PDB 1JZ7 [142]) with secondary structures visualized as cartoons.  $\alpha$ -helices in blue,  $\beta$ -sheets in yellow, loops and undefined structures in green. The 5 asparagines within N-X-S/T motifs are visualized as spheres. (B) Schematic overview of recombinant  $\beta$ -gal(V10-L731) as expressed in *P. pastoris*. MF = mating factor alpha prepro leader sequence.

A protein has to enter the endoplasmic reticulum (ER) to get N-glycosylated [91]. Hence, N-terminal FLAG-tagged  $\beta$ -gal(V10-L731) was subcloned into the methanol inducible yeast expression vector pPICZ $\alpha$ , which contains the mating factor alpha prepro leader sequence for secretion and a C-terminal 6xHis-tag for purification by immobilized metal affinity chromatography (IMAC) (Figure 4.2 B). Assuming correct processing (i.e. cleavage of the proteases Kex2 and Ste3 at the corresponding cleavage sites after the leader sequence) the calculated molecular weight of the final protein without any post-translational modifications is 87.9 kDa.

*P. pastoris* KM71H cells were stably transformed with this expression plasmid, and protein expression was monitored during methanol induction for 120 h in yeast pellets

and supernatants by SDS-PAGE and subsequent coomassie staining or western blot analysis against the FLAG- and the 6xHis-tag. A roughly 90 kDa protein, which was positive for the FLAG- and the 6xHis-tag, was detected after 48 h in the supernatant of  $\beta$ -gal(V10-L731)-transformed but not control-transformed (pPICZ $\alpha$  backbone) yeast cells (Figure 4.3). Analysis of yeast pellets revealed that expression started after 24 h with protein species of a slightly higher apparent molecular weight (Figure 4.3). For subsequent large-scale productions, induction was carried out for 72–96 h to reduce the risk of the autolysis of yeast cells and proteolysis of the target protein after prolonged incubation in buffer only.

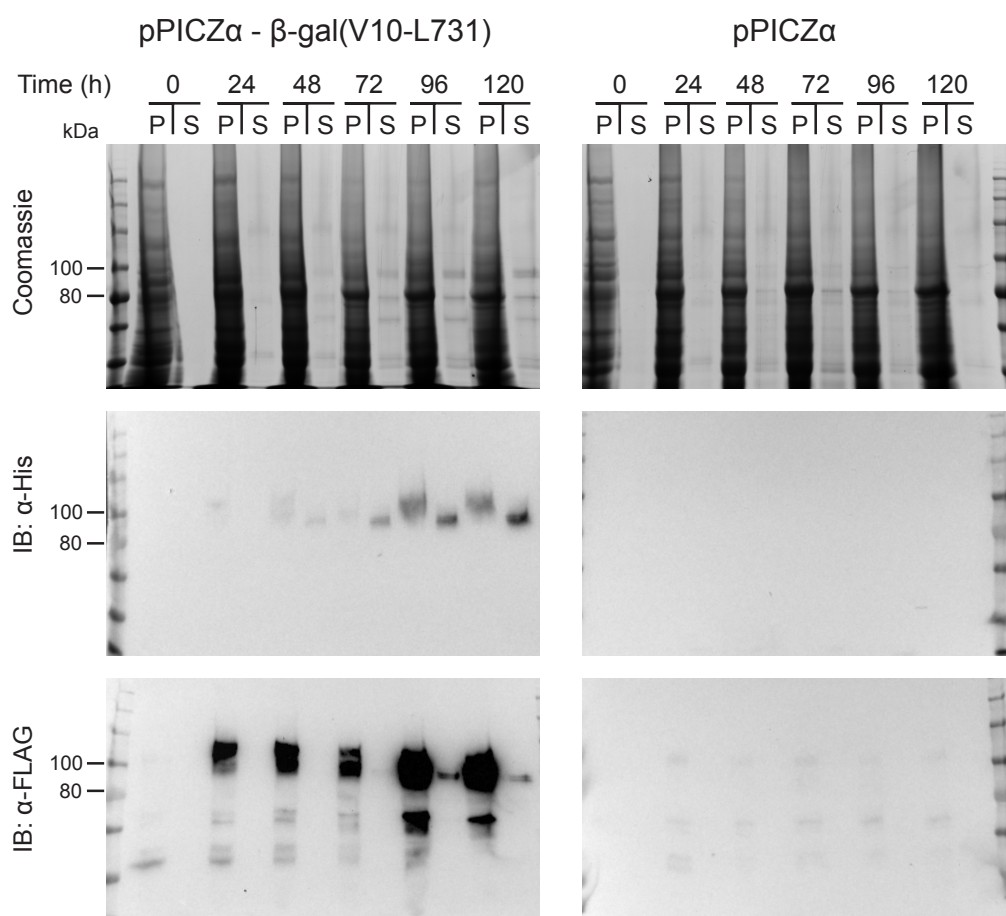


**Figure 4.3: Expression and secretion of recombinant  $\beta$ -gal(V10-L731) after stable transformation into *P. pastoris* KM71H**

*P. pastoris* KM71H was stably transformed with recombinant  $\beta$ -gal(V10-L731), as depicted in Figure 4.2 B. Protein expression in yeast pellets (P) and secretion in the supernatant (S) during MeOH induction was monitored every 24 h for 120 h and visualized by SDS-PAGE and subsequent coomassie staining or western blot against the 6xHis- and the FLAG-tag.

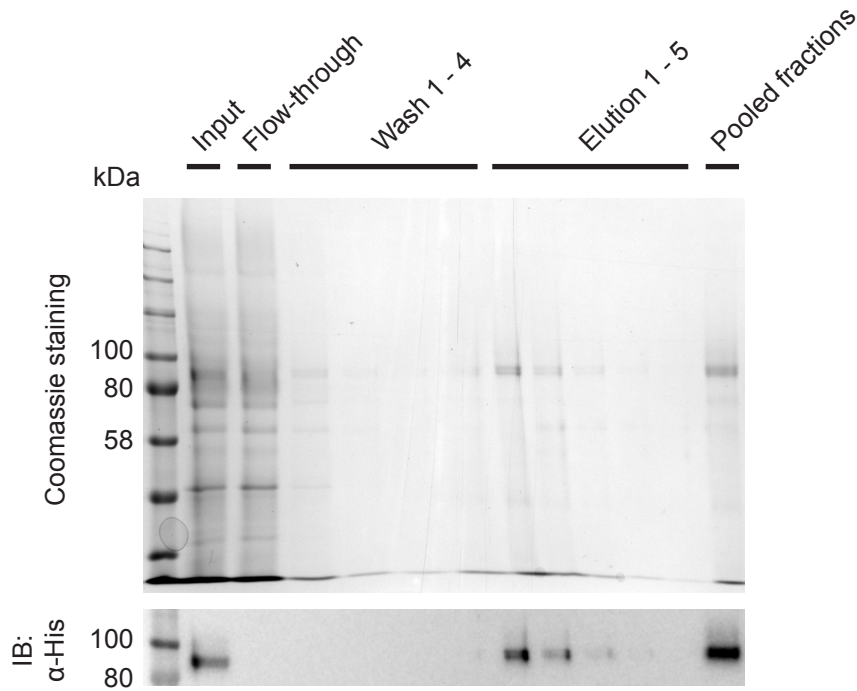


**Figure 4.4: Immobilized metal affinity chromatography of recombinant  $\beta$ -gal(V10-L731) via Ni-NTA resin**

Concentrated supernatants (Input) were loaded for 1 h on Ni-NTA resin. Flow-through was kept for analysis, and resin was extensively washed (wash 1–4). Bound protein was eluted in 5 steps, and eluted fractions were pooled. Aliquots of each fraction were separated by SDS-PAGE and visualized by coomassie staining or western blot against the His-tag.

Supernatants of large scale cultures were concentrated for purification by ultrafiltration, and buffer was exchanged before His-tagged proteins were further purified by IMAC. Visualization of the different fractions during IMAC by western blot revealed that nearly all His-tagged proteins bound to the resin (i.e. no signal was found in the flow-through fraction) and eluted readily within the first three elution steps (Figure 4.4). The elution fractions were pooled, and buffer was exchanged against PBS to get rid of the eluting reagent imidazole for further analysis.

We were then interested in finding out whether any domain of the MR could bind to this secreted  $\beta$ -gal(V10-L731), which for convenience will from now on be referred to as  $\beta$ -gal. To answer this question, the ELISA with MR-CTLTD and MR-Nterm Fc-chimeras was performed on immobilized purified protein. Binding could be detected for MR-CTLTD but not for MR-Nterm or the Fc control (Figure 4.5 A).

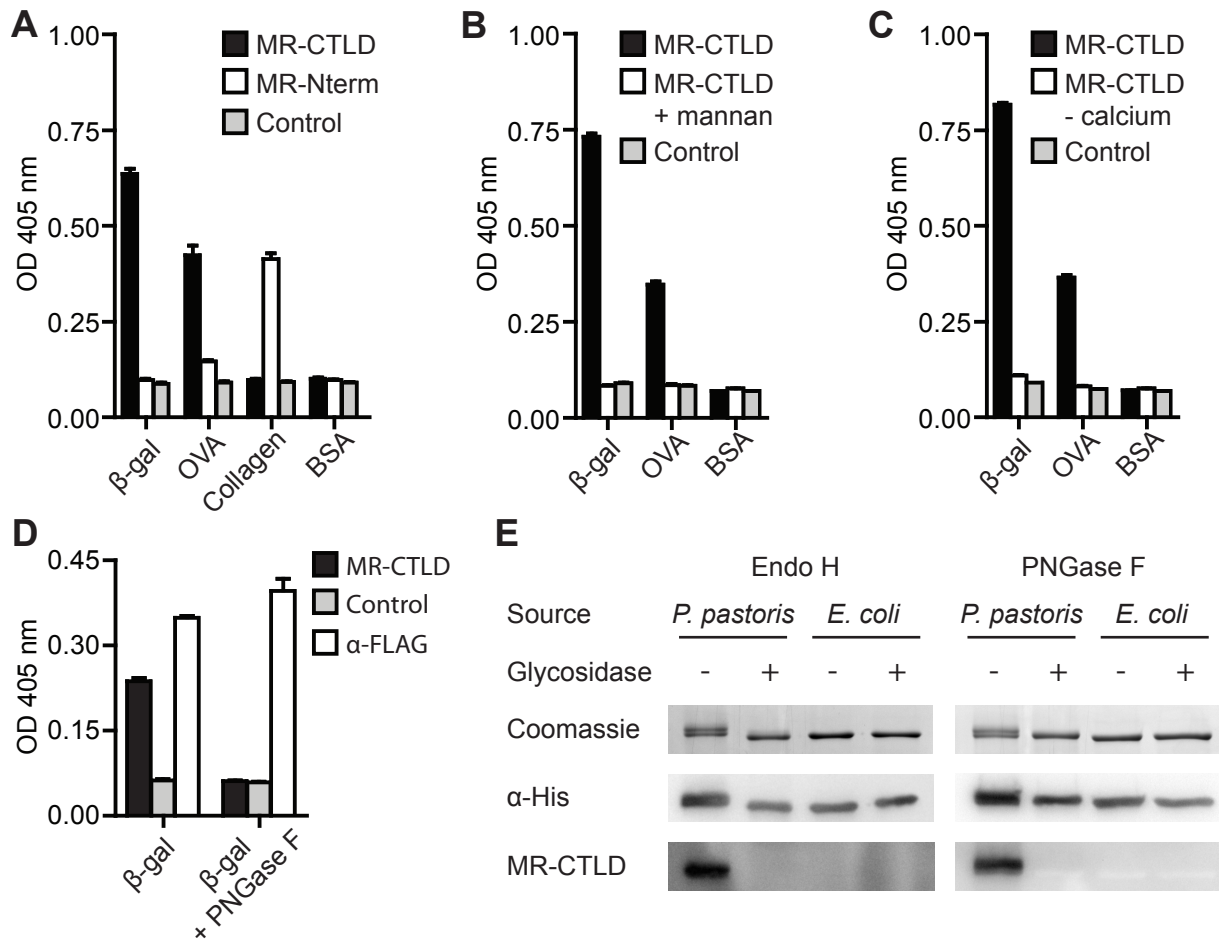


**Figure 4.5: MR-CTLD binds to recombinant  $\beta$ -gal from *P. pastoris* in a C-type-lectin- and glycan-dependent manner**

(A) The binding of MR-CTLD and MR-Nterm Fc-chimeric proteins or isotype control (Control) to immobilized recombinant  $\beta$ -gal, OVA, collagen or BSA determined by ELISA. (B) The binding of MR-CTLD to recombinant  $\beta$ -gal, OVA or BSA in the absence or presence of 3 mg/mL mannan determined by ELISA. Control = isotype control. (C) The binding of MR-CTLD to recombinant  $\beta$ -gal, OVA or BSA in the presence or absence of calcium ions determined by ELISA. Control = isotype control. (D) The binding of MR-CTLD, isotype control or FLAG-antibody to control- or PNGase F-treated  $\beta$ -gal, determined by ELISA. (E) Recombinant  $\beta$ -gal, purified from *P. pastoris* or *E. coli*, was treated with PNGase F, Endo H or control-treated. Samples were analyzed by SDS-PAGE and subsequent coomassie staining, western blot against the His-tag or far-western blot with MR-CTLD. All graphs depict the mean values of three replicates and are representative data of three independent experiments. Error bars indicate SEM.

Importantly, the binding of MR-CTLD to  $\beta$ -gal was inhibited by the competitive MR-CTLD inhibitor mannan or in the absence of calcium ions, just like the binding to ovalbumin (Figure 4.5 B, C). This points out that  $\beta$ -gal binding required the MR C-type lectin activity, which in turn suggests the presence of glycosylation on  $\beta$ -gal. Strikingly, the binding of MR-CTLD was abolished upon the deglycosylation of  $\beta$ -gal with PNGase F, whereas deglycosylation had no influence on the recognition of the FLAG-tag on that protein (Figure 4.5 D).

Next, purified  $\beta$ -gal, either secreted from *P. pastoris* or purified from *E. coli* lysates, was deglycosylated with either glycosidase, PNGase F or Endo H. Proteins were then separated by SDS-PAGE and analyzed by coomassie staining, western blot against the His-tag and far-western blot using MR-CTLD. MR-CTLD bound *P. pastoris*- but not *E. coli*-derived  $\beta$ -gal and, in accordance with the results from the ELISA-like binding assay, this binding was sensitive to glycosidase treatment with PNGase F or Endo H (Figure 4.5 E).

These data demonstrate that incidentally occurring N-X-S/T motifs in cytosolic proteins are N-glycosylated by *P. pastoris* and, importantly, that the attached glycans are ligands of the MR C-type-lectin part, the same domain that also accounts for the binding of OVA.

### **4.3 *Pichia pastoris*-derived $\beta$ -galactosidase is internalized by the mannose receptor**

Since the binding of OVA to the MR leads to receptor mediated endocytosis of OVA [51, 125], we investigated if the same holds true for *P. pastoris*-derived  $\beta$ -gal. For this purpose, HEK293T cells expressing the MR (HEK-MR) or HEK293T control cells (HEK) [125] were pulsed with fluorescently labeled  $\beta$ -gal (Figure 4.6). At 4 °C increased binding of  $\beta$ -gal to HEK-MR cells was already detected as indicated by an increase in the mean fluorescence intensity in comparison to HEK control cells. Upon incubation at 37 °C, HEK cells expressing the MR actively took up the fluorescently labeled  $\beta$ -gal, as indicated by increasing fluorescence over time, whereas HEK cells lacking the MR did not show such distinct uptake.

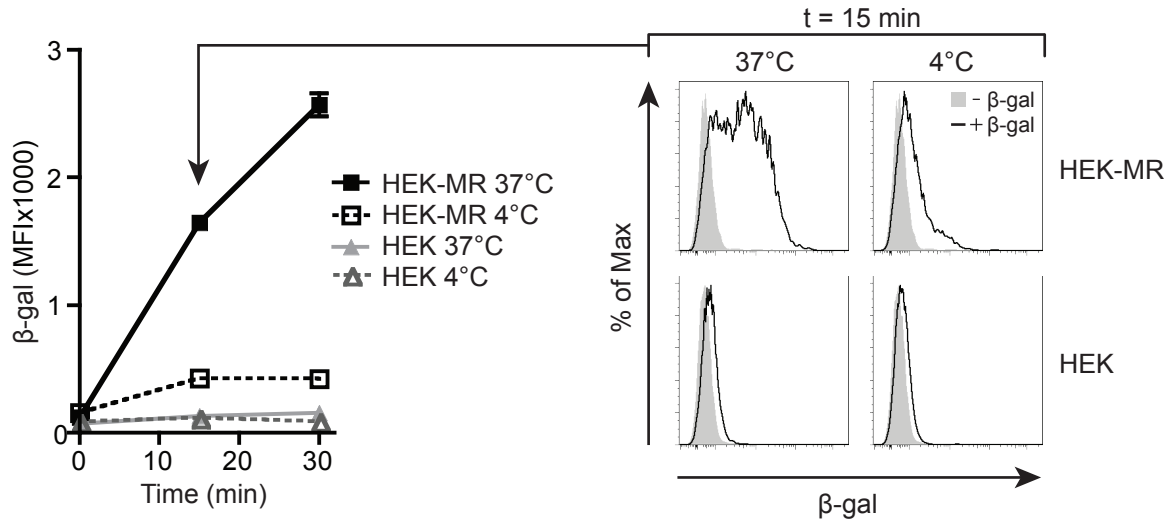


**Figure 4.6: Uptake of fluorescently labeled  $\beta$ -gal by MR-expressing HEK293T cells** MR-expressing HEK293T cells (HEK-MR) or control HEK293T cells (HEK) were pulsed with Alexa Fluor 647-conjugated  $\beta$ -gal at 37°C or 4°C for 15 or 30 min. Fluorescence intensities were measured by flow cytometry, and arithmetic mean fluorescence intensities (MFIs) were calculated. The graph shows the mean MFI of three replicates. Error bars indicate SEM. The graph is representative for three independent experiments. The histograms show one representative replicate of the 15 min samples depicted in the graph.

Next we investigated the uptake of *P. pastoris*-derived  $\beta$ -gal by wild-type (MR<sup>+/+</sup>) or MR-deficient BM-DCs (MR<sup>-/-</sup>). To this end, we first pulsed BM-DCs with increasing concentrations of fluorescently labeled  $\beta$ -gal for 20 min and monitored  $\beta$ -gal uptake by flow cytometry. MR-sufficient BM-DCs were superior in  $\beta$ -gal uptake to MR-deficient BM-DCs at all concentrations tested (Figure 4.7 A), indicating that the MR plays a dominant role in the uptake of glycosylated  $\beta$ -gal by BM-DCs. Pulsing BM-DCs with constant  $\beta$ -gal amounts for different lengths of time further revealed that  $\beta$ -gal accumulation by the MR even increased over time (Figure 4.7 B). This demonstrates the benefit of targeting a recycling receptor like the MR [74] to specifically accumulate proteins in target cells, even at low concentrations. The impact of MR-mediated  $\beta$ -gal uptake was also investigated by fluorescence microscopy, which not only confirmed that MR-sufficient cells accumulated more  $\beta$ -gal than their MR-deficient counterparts, but also showed that the fluorescence is located in punctual subcellular compartments (Figure 4.7 C).

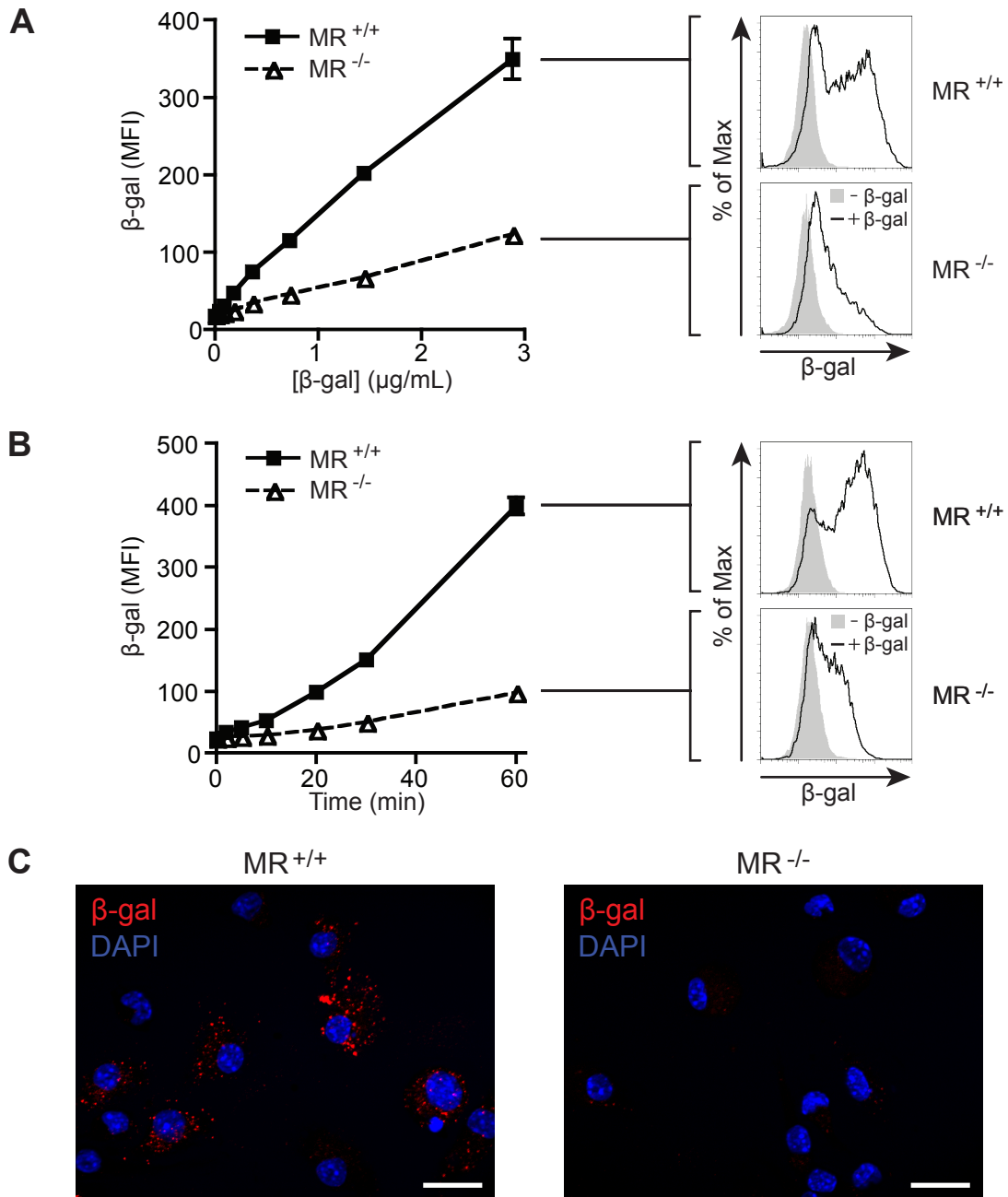


**Figure 4.7: Uptake of fluorescently labeled  $\beta$ -gal by BM-DCs**

(A, B) Wildtype (MR<sup>+/+</sup>) or MR-deficient BM-DCs (MR<sup>-/-</sup>) were pulsed with different concentrations of Alexa Fluor 647-conjugated  $\beta$ -gal for 20 min (A) or with 500 ng/mL Alexa Fluor 647-conjugated  $\beta$ -gal for different time period (B). Fluorescence intensities were measured by flow cytometry and arithmetic MFIs were calculated. Graphs show the mean  $\pm$  SEM MFI of three replicates and are representatives of three independent experiments. Histograms show one representative replicate of the last data points depicted in the graphs. (C) Wildtype or MR-deficient BM-DCs were pulsed with 1  $\mu$ g/mL Alexa Fluor 647-conjugated  $\beta$ -gal for 20 min. Nuclei were stained with DAPI and cells were analyzed by fluorescence microscopy. White bars indicate 20  $\mu$ m.



To investigate whether this MR-mediated  $\beta$ -gal uptake depended on the C-type lectin activity, we again pulsed BM-DCs with fluorescently labeled  $\beta$ -gal but this time co-administered excess amounts of established MR ligands (i.e. yeast mannan or unlabeled OVA) or the calcium chelating molecule EDTA and measured uptake by flow cytometry. In accordance with the findings on the isolated MR-CTLD, both the competitive inhibition and the withdrawal of calcium ions abolished MR-mediated  $\beta$ -gal uptake comparable to the knock-out level (Figure 4.8 A). Likewise, the uptake of deglycosylated  $\beta$ -gal was also reduced to knock-out level (Figure 4.8 B).

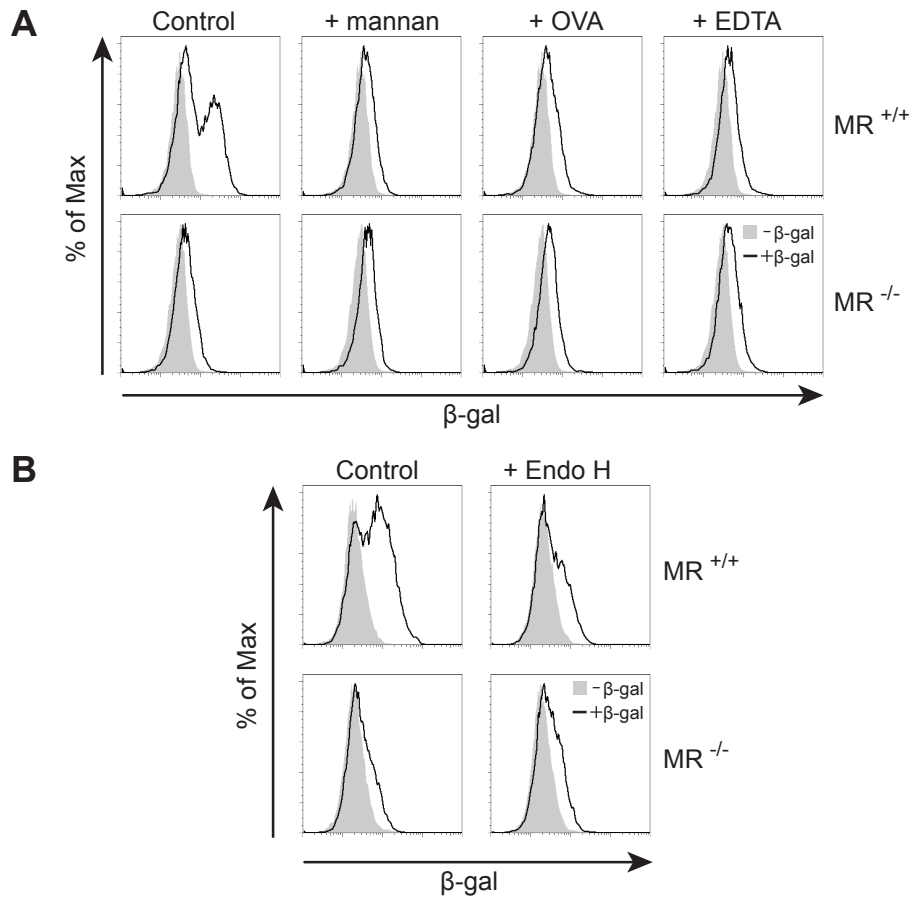


**Figure 4.8: The uptake of fluorescently labeled  $\beta$ -gal by BM-DCs depends on the C-type lectin activity of the MR and N-glycans on  $\beta$ -gal**

(A) Wildtype (MR<sup>+/+</sup>) or MR-deficient BM-DCs (MR<sup>-/-</sup>) were pulsed for 20 min with Alexa 647-conjugated  $\beta$ -gal either alone or in the presence of 3 mg/mL yeast mannan, 3 mg/mL OVA, or in the presence of the calcium chelator EDTA. The uptake of antigen was monitored by flow cytometry. (B) Cells as in (A) were pulsed with control- or Endo H-treated fluorescently labeled  $\beta$ -gal. Uptake was monitored by flow cytometry. Histograms show one representative replicate of at least three independent experiments.

These experiments prove that *P. pastoris*-derived  $\beta$ -gal is not only bound but also subsequently internalized by the cell-associated full-length MR. Binding to the MR is solely mediated by the interaction of its C-type lectin part with the *P. pastoris*-derived N-glycan, confirming our previous findings with isolated MR subdomain-Fc chimeras. Noteworthy, the attached N-glycans targeted the MR on BM-DCs very selectively, as demonstrated by the low uptake of MR<sup>-/-</sup> cells.

#### **4.4 *Pichia pastoris*-derived $\beta$ -galactosidase is delivered to early endosomal compartments**

Endocytosed proteins typically enter the endolysosomal pathway for degradation. In contrast to this, MR-endocytosed ovalbumin was shown to end up in an endosomal compartment positive for the MR, transferrin (Trf), the early endosome antigen-1 (EEA1) but not the lysosomal-associated membrane protein 1 (LAMP-1), from where it was processed for cross-presentation [51]. Hence, we were interested in the detailed subcellular localization of endocytosed  $\beta$ -gal. To investigate this, we pulsed BM-DCs with differently labeled  $\beta$ -gal and ovalbumin and analyzed the cells by fluorescence microscopy. Both proteins ended up in the same compartments and importantly,  $\beta$ -gal positive compartments were also positive for the MR, EEA1 and Trf, but not for the lysosomal marker LAMP-1 (Figure 4.9). This suggests that *P. pastoris*-derived  $\beta$ -gal indeed ended up in the same compartment that is related to cross-presentation of OVA.

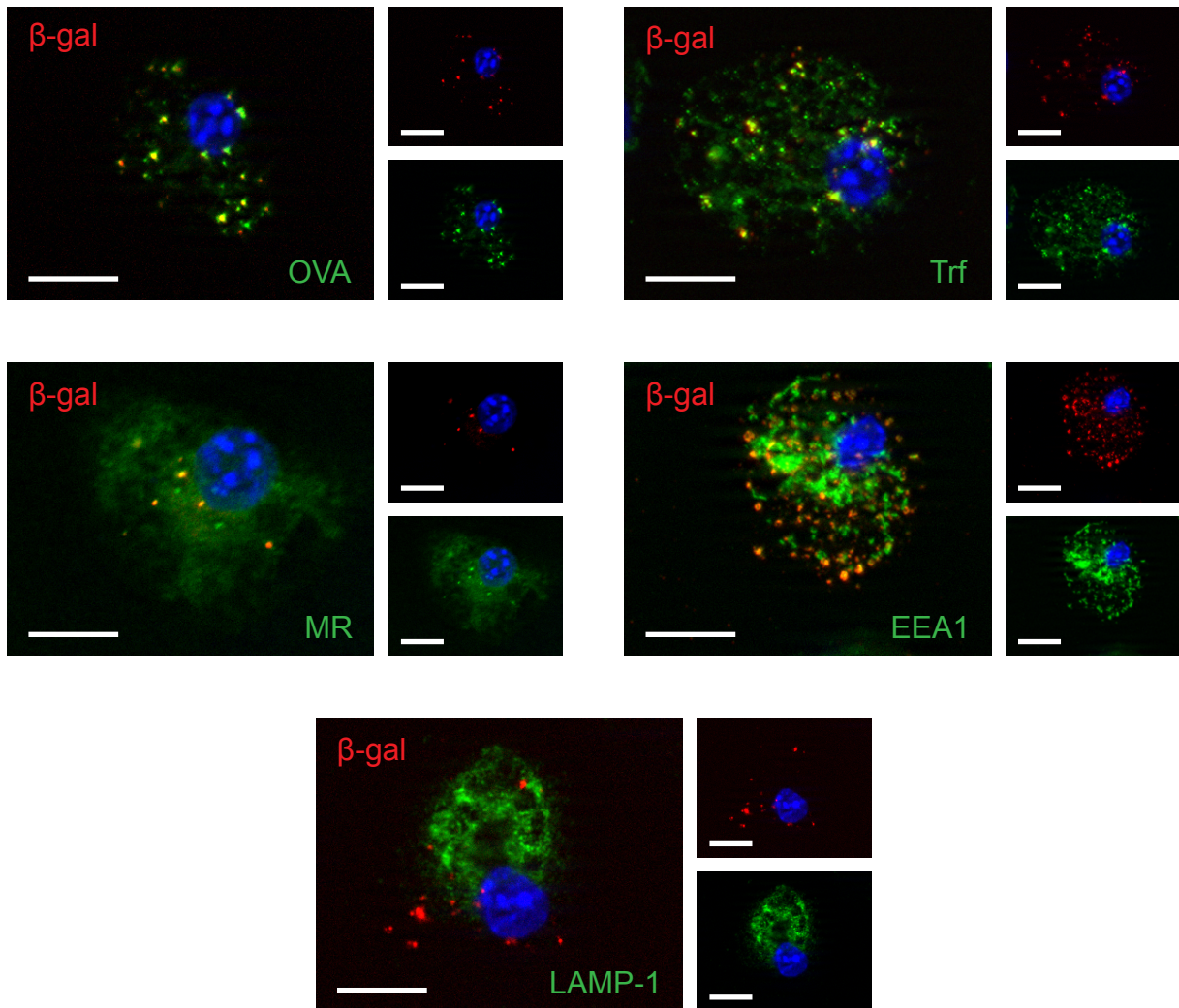


**Figure 4.9: Fluorescently labeled  $\beta$ -gal ends up in compartments related to cross-presentation after uptake by BM-DCs**

Wildtype ( $MR^{+/+}$ ) BM-DCs were pulsed for 20 min with 1  $\mu\text{g}/\text{mL}$  Alexa Fluor 647-conjugated  $\beta$ -gal and chased for another 20 min. Cells in the first panel were simultaneously pulsed with 500  $\text{ng}/\text{mL}$  Alexa Fluor 488-conjugated OVA or Trf. Cells in the lower panels were stained for MR, EEA1 and LAMP-1. White bars indicate 10  $\mu\text{m}$ .

## 4.5 *Pichia pastoris* glycosylates an artificial N-glycosylation site, which can be used as a mannose receptor-targeting strategy for proteins lacking intrinsic N-X-S/T motifs

Since not all proteins incidentally bear N-X-S/T motifs like  $\beta$ -gal, a system was needed to expand the MR-targeting strategy to all remaining non-glycoproteins. Hence, we designed a *P. pastoris* expression plasmid (pPICZ $\alpha$ -NST) which contains an N-terminal N-X-S/T motif right between the mating factor alpha prepro leader sequence (MF) for secretion and a multiple cloning site, followed by the His-tag for purification. We optimized the glycosylation motif to guarantee a high degree of N-glycosylation. To this end, the motif was initially placed N-terminally, because glycosylation site occupancy was found to decrease from N- to the C-terminus [143]. Next, we preferred N-X-T to N-X-S, as it has been shown that threonine is favored over serine at position 3 [143, 144], and we chose the amino acid serine at position 2 (denoted as X in N-X-S/T), which gave high N-glycosylation yield in a study investigating the X-position [145]. Finally, the tag was flanked by glycine and methionine, which are structurally and chemically inert and should thereby improve the sequon's accessibility by the oligosaccharyltransferase [146].

To test this vector on a model protein, we chose enhanced green fluorescent protein (GFP) [147–149]. Besides lacking intrinsic N-glycosylation motifs and having a free accessible N-terminus (Figure 4.10 A), this protein has already been successfully secreted by *P. pastoris* [150] and is easily detectable in downstream assays by its intrinsic fluorescence. The resulting modified GFP will henceforth be named NST-GFP (Figure 4.10 B). After transformation into *P. pastoris* KM71H, we made use of the intrinsic GFP fluorescence to develop a simple 96-well format semi-high throughput screen (see methods section 3.2.3.4 for more details) to identify clones that show high secretion of NST-GFP (Figure 4.10 C). Additionally, induced yeast pellets were also checked for remaining GFP fluorescence and revealed that high secretion correlated with low residual fluorescence in pellets (data not shown). This demonstrates the power of our screening method to easily select clones with proper protein folding and secretion kinetics.

A high secreting clone was selected for large scale purification and NST-GFP was readily detected during and after IMAC purification from *P. pastoris* supernatants by its yellow color and green fluorescence (Figure 4.10 C).

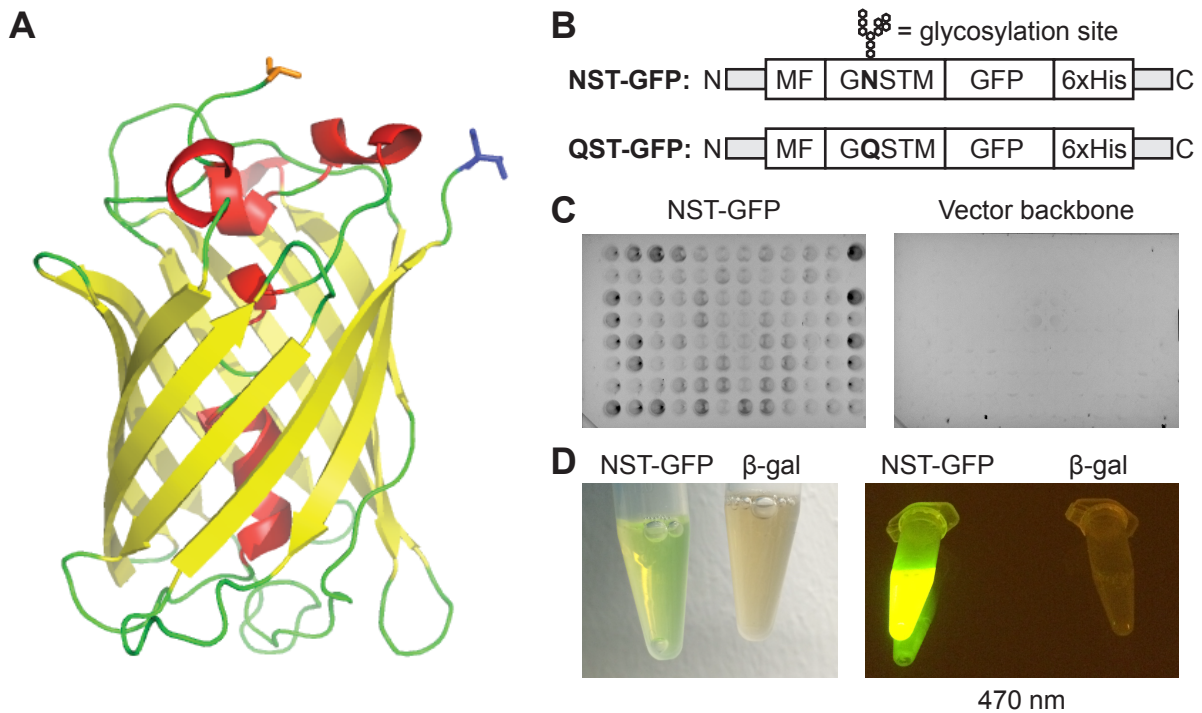


**Figure 4.10: GFP as a model for proteins lacking intrinsic N-X-S/T motifs and its purification from *P. pastoris***

(A) 3D structure of GFP (PDB 1GFL [151]) with secondary structures visualized as cartoons.  $\alpha$ -helices in red,  $\beta$ -sheets in yellow, loops and undefined structures in green. N- and C-termini are illustrated in orange and blue, respectively. (B) Scheme of GFP with the N-terminal glycosylation site (NST-GFP) or control sequence (QST-GFP). MF = mating factor alpha prepro leader sequence. (C) Supernatants of n=96 NST-GFP or vector backbone transformed *P. pastoris* clones were transferred to a 96-well plate after 48 h induction and GFP fluorescence was detected. (D) Purified NST-GFP and  $\beta$ -gal at daylight and after illumination with 470 nm.

Using the Fc-chimeric MR-proteins in an ELISA we first investigated if any part of the MR bound to immobilized, purified NST-GFP. Indeed, MR-CTLTD again recognized the recombinant protein from *P. pastoris*, whereas MR-Nterm did not (Figure 4.11 A). Furthermore, MR-CTLTD binding to NST-GFP was inhibited by mannan (Figure 4.11 B) or the absence of calcium ions (Figure 4.11 C) just like MR-CTLTD binding to OVA or *P. pastoris*-derived  $\beta$ -gal. Concurrently, this binding was strongly reduced after deglycosylation with Endo H (Figure 4.11 D), suggesting that GFP was truly N-glycosylated and MR-CTLTD again recognized the *P. pastoris*-derived N-glycan.

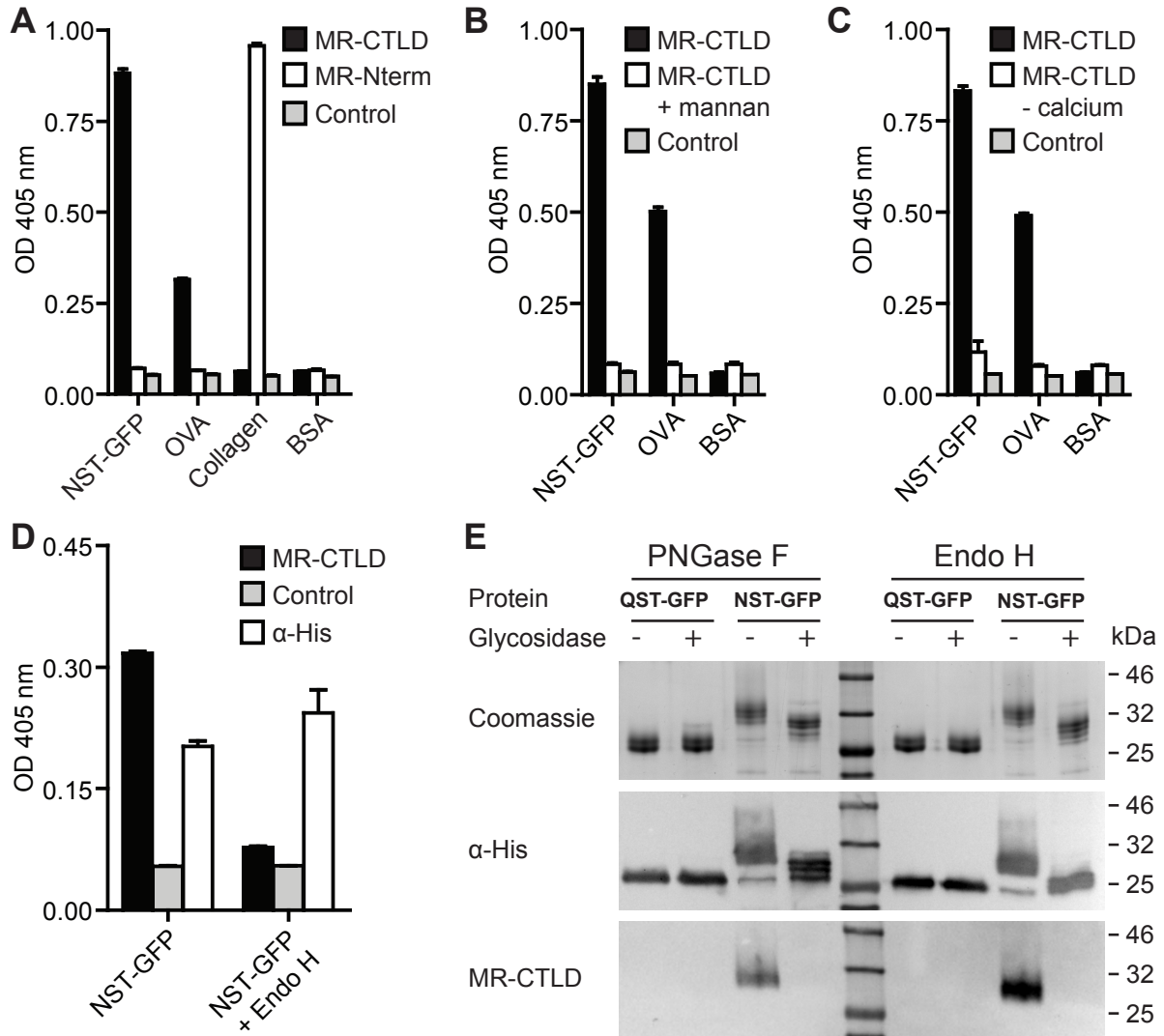


**Figure 4.11: *P. pastoris* glycosylates the artificial N-X-S/T motif in NST-GFP resulting in a C-type lectin- and glycan-dependent recognition by the MR**

(A) Binding of MR-CTLD, MR-Nterm or isotype control (Control) to immobilized NST-GFP, OVA, collagen or BSA, determined by ELISA. (B) Binding of MR-CTLD to NST-GFP, OVA or BSA in the absence or presence of 3 mg/mL mannan, determined by ELISA. Control = isotype control. (C) As (B) but in the presence or absence of calcium ions. (D) Binding of MR-CTLD, isotype control or His-tag antibody to control- or Endo H-treated NST-GFP, determined by ELISA. (E) NST-GFP or QST-GFP purified from *P. pastoris* were PNGase F-, Endo H- or control-treated. Samples were analyzed by SDS-PAGE and subsequent coomassie staining, western blot against the His-tag or far-western blot with MR-CTLD. All graphs depict the mean values of three replicates. Error bars indicate SEM. The graphs are representative data of at least three independent experiments.

To verify that this N-glycosylation is due to the optimized N-X-S/T motif, we purified a control protein expressed by *P. pastoris*, where the asparagine in the motif was exchanged by a glutamine (QST-GFP, Figure 4.10 B). SDS-PAGE of both proteins not only revealed that QST-GFP has a lower apparent molecular weight, but also proved that only NST-GFP is sensitive to deglycosylation by PNGase F or Endo H, whereas QST-GFP is not (Figure 4.11 E). Concordantly, MR-CTL D only bound to NST-GFP but not QST-GFP in a far-western blot analysis, and binding was lost after deglycosylation of NST-GFP, confirming that MR-CTL D recognizes an N-glycan attached to the artificial glycosylation site in NST-GFP.

Next, we investigated the uptake of NST-GFP by BM-DCs. To this end we pulsed wild-type or MR-deficient BM-DCs with the antigen and monitored the GFP fluorescence by flow cytometry. Wild-type BM-DCs clearly took up more NST-GFP than MR-deficient BM-DCs over a wide range of concentrations and incubation times (Figure 4.12 A). MR-mediated uptake could be blocked by yeast mannan and was strongly reduced after deglycosylation of NST-GFP to the knock-out level (Figure 4.12 B). Additionally, QST-GFP did not show such pronounced MR-dependent uptake (Figure 4.12 B), all together pointing to the necessity of the glycan-lectin interaction between NST-GFP and the MR for the increased uptake of NST-GFP by wild-type BM-DCs. Equally to  $\beta$ -gal, NST-GFP ended up in the same compartment as ovalbumin (Figure 4.12 C), suggesting that the presented targeting strategy not only robustly targets the MR, but also directs antigens reliably to compartments related to cross-presentation [51].

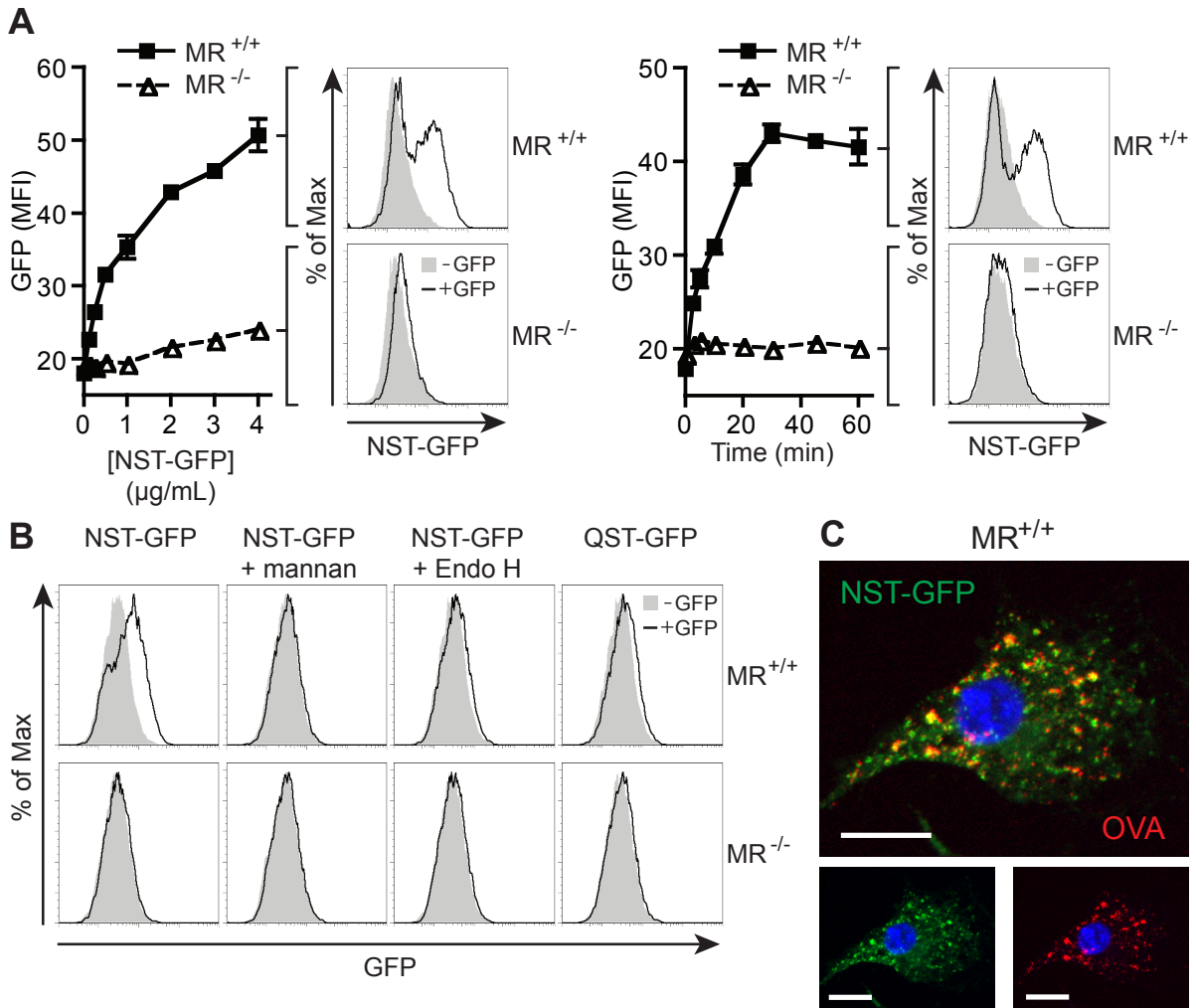


**Figure 4.12: BM-DCs take up NST-GFP by the MR in a C-type lectin- and glycan-dependent manner**

(A) Wild-type or MR-deficient BM-DCs were pulsed for 20 min with different concentrations of NST-GFP, or with 1  $\mu\text{g/mL}$  NST-GFP for different period. Protein uptake indicated by increase in GFP fluorescence was monitored by flow cytometry. The graphs show the mean MFI  $\pm$  SEM of three replicates and are representatives of three independent experiments. The histograms show one representative replicate of the last data points depicted in the graphs. (B) Wild-type or MR-deficient BM-DCs were pulsed for 20 min with 1  $\mu\text{g/mL}$  NST-GFP, 1  $\mu\text{g/mL}$  NST-GFP + 3 mg/mL mannan, 1  $\mu\text{g/mL}$  Endo H-treated NST-GFP or 1  $\mu\text{g/mL}$  QST-GFP. Protein uptake was monitored by flow cytometry. Representative histograms of three independent experiments are shown. (C) Wild-type BM-DCs were pulsed for 20 min with NST-GFP and Alexa 647-conjugated OVA. The uptake of both proteins was visualized after 20 min chase by fluorescence microscopy. White bars indicate 10  $\mu\text{m}$ .



Although previous work on MR ligands [70] and the glycan composition of *P. pastoris* (reviewed in [97]) strongly argues for a direct link between the attached glycan and the MR-binding, we wondered whether *P. pastoris*-derived high-mannose glycosylation is responsible for the success of our targeting strategy, or if any N-glycosylation is sufficient for generating a MR ligand. HEK-derived N-glycans have been shown to contain terminal fucose and to some extent GlcNAc and mannose [152], all of which can act as MR ligands [68]. Hence, to answer our question, we expressed secreted NST-GFP and QST-GFP variants in HEK293T cells (hNST-GFP and hQST-GFP, respectively).

The separation of HEK-derived hNST- and hQST-GFP by SDS-PAGE revealed that hNST-GFP contained a protein species with higher apparent molecular weight compared to hQST-GFP as visualized by coomassie staining and immunoblot (Figure 4.13 A). In contrast to hQST-GFP, hNST-GFP was also sensitive to PNGase F treatment (Figure 4.13 A), strongly suggesting that hNST-GFP was truly N-glycosylated by HEK cells. Nonetheless, MR-CTLD only bound to *P. pastoris*-derived and not to HEK-derived NST-GFP in a far-western blot (Figure 4.13 A). Consistently, increased MR-dependent uptake of NST-GFP by BM-DCs was only detected for the *P. pastoris*- but not the HEK-derived protein (Figure 4.13 B).

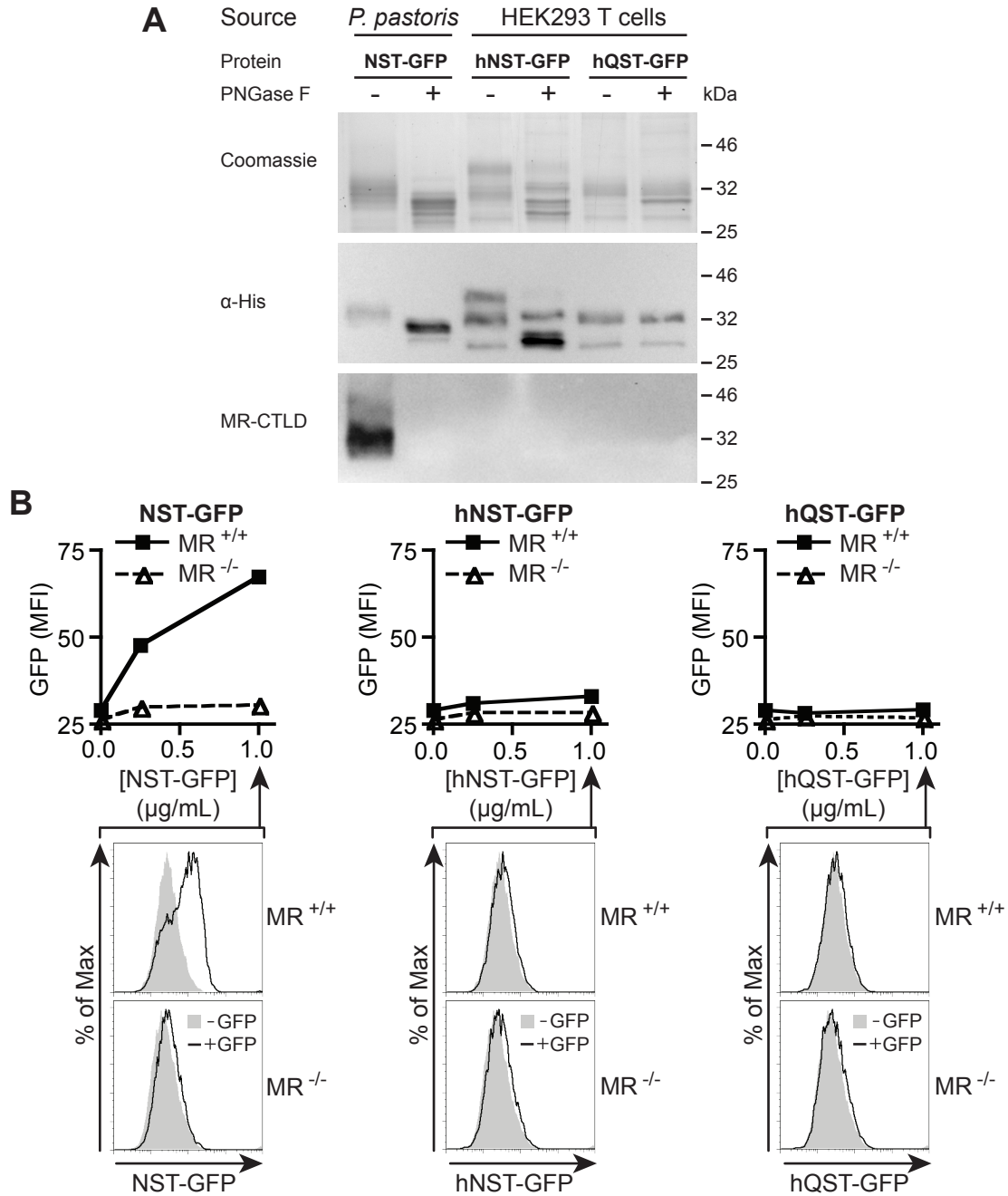


**Figure 4.13: The MR-mediated binding and uptake of NST-GFP depend on the attached N-glycans**

(A) GFP variants were expressed in HEK293T cells (hNST-GFP, hQST-GFP). *P. pastoris*-derived NST-GFP and HEK proteins were treated with PNGase F and separated by SDS-PAGE. Proteins were visualized by coomassie staining or western blot against the His-tag, and binding to MR-CTLD was determined by far-western blot. (B) BM-DCs were pulsed for 20 min with different concentrations of *P. pastoris*-derived NST-GFP or HEK-derived hNST-GFP and hQST-GFP. The uptake of the proteins was determined by monitoring the GFP-fluorescence with a flow cytometer. The graphs depict the mean MFIs of three replicates. Histograms show one representative replicate from each 1  $\mu$ g/mL samples.

To investigate whether differences in mean fluorescence intensities detected by flow cytometry are really due to different uptake and not to altered fluorescence properties, excitation and emission spectra of all GFP variants were collected. Neither the source of the protein (*P. pastoris* vs. HEK cells) nor the presence or absence of the N-glycans had any influence on the wavelengths of excitation and emission maxima (Figure 4.14 A). Importantly, deglycosylation did not decrease the fluorescence intensity at 540 nm after excitation at 488 nm (Figure 4.14 B), which would also explain lower fluorescence signals during flow cytometry analysis.

In addition, one could argue, that GFP fluorescence is strongly pH dependent [153]. If MR-deficient BM-DCs shuttled GFP to a more acidic compartment than wild-type BM-DCs, one could not distinguish whether the protein is less taken up, or whether fluorescence simply vanishes directly after the uptake by MR-deficient BM-DCs. To test this hypothesis, we pulsed wild-type or MR-deficient BM-DCs with NST-GFP conjugated to DyLight 650 fluorophors, which are stable over a broad pH range (pH 4–9), and monitored DyLight instead of GFP fluorescence. The uptake of DyLight-conjugated NST-GFP by BM-DCs showed the same MR-dependency as observed for the GFP-fluorescence (Figure 4.14 C), ruling out any effects of altered GFP fluorescence to account for our observations.

Taken together, these data show that the optimized N-X-S/T motif can be used to artificially glycosylate proteins which lack an intrinsic N-glycosylation site. The expression of such a protein in *P. pastoris* generated a MR ligand that behaved like the model antigen OVA in both the binding and the uptake by the MR.

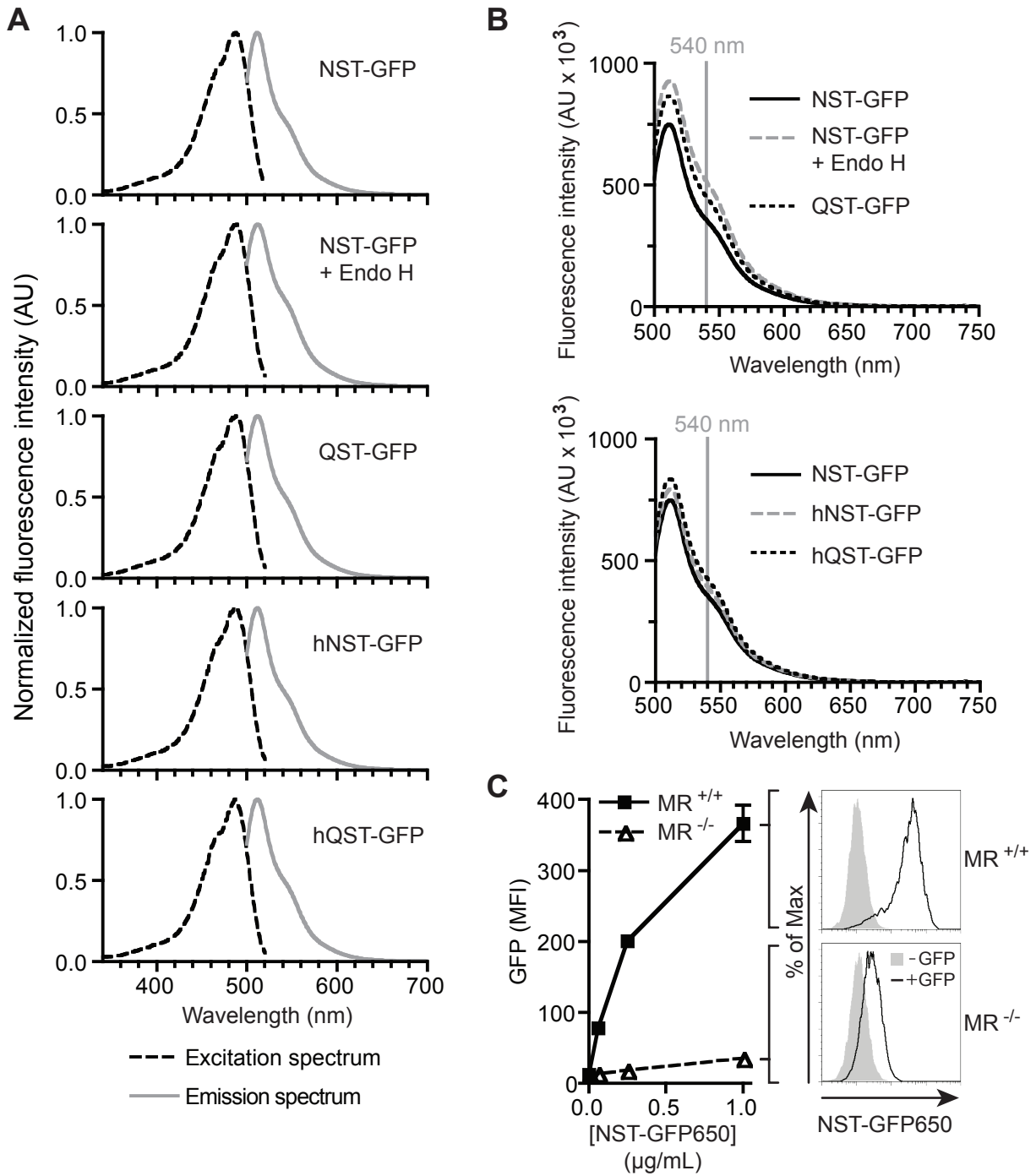


**Figure 4.14: Differences in uptake are not explained by altered fluorescence properties of GFP variants**

(A) Normalized excitation and emission spectra of *P. pastoris*-derived (NST-GFP, NST-GFP + Endo H, QST-GFP) or HEK-derived GFP variants (hNST-GFP, hQST-GFP). Excitation spectra were monitored by emission at 540 nm. Emission spectra were collected for excitation at 488 nm. (B) Emissionspectra as in (A) without normalization. (C) Wild-type or MR-deficient BM-DCs were pulsed for 20 min with DyLight 650-conjugated NST-GFP. Protein uptake was monitored by flow cytometry. The graph shows mean DyLight 650 MFIs of three replicates.

Finally, we wanted to know if our targeting system might also be transferred to human antigen presenting cells. To answer this question, we differentiated human PBMCs with GM-CSF and IL-4 into dendritic cells (DCs) or with M-CSF into macrophages (MΦs). We then pulsed these cells with NST-GFP or QST-GFP and investigated antigen uptake by flow cytometry. Similar to the results with murine BM-DCs (Figure 4.12 B), there was a strong increase in the uptake of NST-GFP in comparison to QST-GFP in human DCs and a moderate increase in uptake by MΦs (Figure 4.15 A, left and right panel respectively).

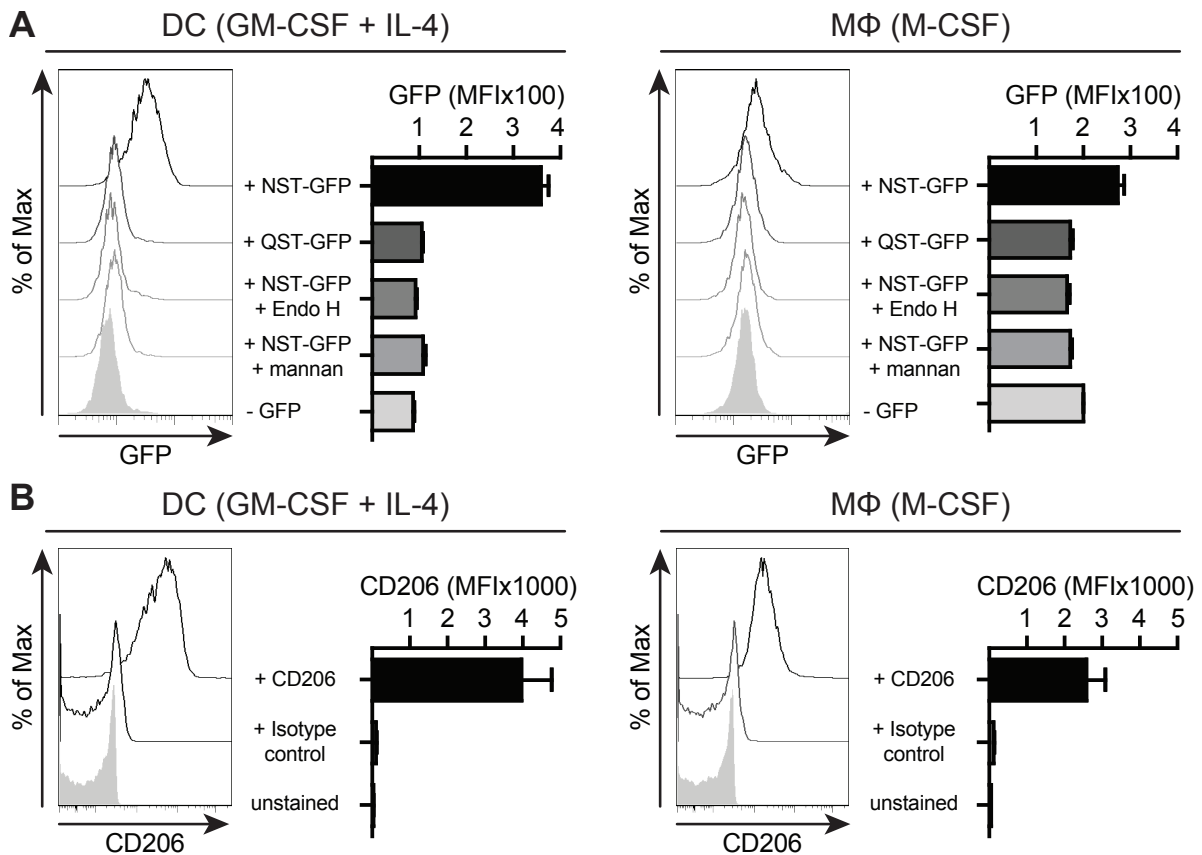


**Figure 4.15: *P. pastoris*-derived glycans target human peripheral blood mononuclear cell-derived DCs and MΦs**

(A) Human PBMCs were differentiated with GM-CSF and IL-4 into DCs or with M-CSF into MΦs. Cells were pulsed with NST-GFP, QST-GFP or Endo H-treated NST-GFP in the absence or presence of mannan, and uptake was monitored by flow cytometry. (B) Cells differentiated as in (A) were stained with CD206 antibody, isotype control or left unstained. Staining was monitored by flow cytometry. The graphs show the mean values of three biological replicates. Error bars indicate SEM. The histograms show one representative sample of each triplicate.

NST-GFP uptake was reduced to QST-GFP uptake-level upon deglycosylation or by addition of yeast mannan, suggesting a role of mannose-specific receptors in the enhanced uptake of N-glycosylated NST-GFP (Figure 4.15 A). To check whether the MR (CD206) could be one candidate for the lectin-dependent uptake of NST-GFP, we stained both cell types for this receptor (Figure 4.15 B). Both cell types are positive for the MR, and surface expression of the MR seems to correlate with the uptake of NST-GFP since DCs not only take up more NST-GFP than MΦs, but are also more positive for the MR (Figure 4.15 A, B).

This data clearly shows that enforced N-glycosylation by *P. pastoris* can serve as a targeting strategy for human antigen presenting cells and suggests that the MR is one possible target on these cells.

## **4.6 Enforced N-glycosylated proteins from *Pichia pastoris* do not exhibit immunostimulatory effects *in vitro***

Foreign glycosylation patterns can trigger signalling via pattern recognition receptors [154, 155]. Hence, the question arises whether the artificial N-glycosylation has an immunostimulatory effect on dendritic cells. To answer this question, we pulsed BM-DCs with N-glycosylated or deglycosylated  $\beta$ -gal and monitored the secretion of cytokines. Whereas the TLR-4 ligand lipopolysaccharide (LPS) stimulated secretion of IL-6, IL-12 and TNF- $\alpha$ , none of these cytokines was released after 24 h upon treatment with either glycosylated or deglycosylated  $\beta$ -gal (Figure 4.16 A). Similarly, treatment of BM-DCs with LPS strongly increased the surface expression of the activation markers CD40, CD80, CD86 and MHC class I molecules, whereas *P. pastoris*-derived  $\beta$ -gal did hardly affect surface expression in either its glycosylated or its deglycosylated form (Figure 4.16 B). Noteworthy, *E. coli*-derived  $\beta$ -gal enhanced surface expression similar to pure LPS (Figure 4.16 B).

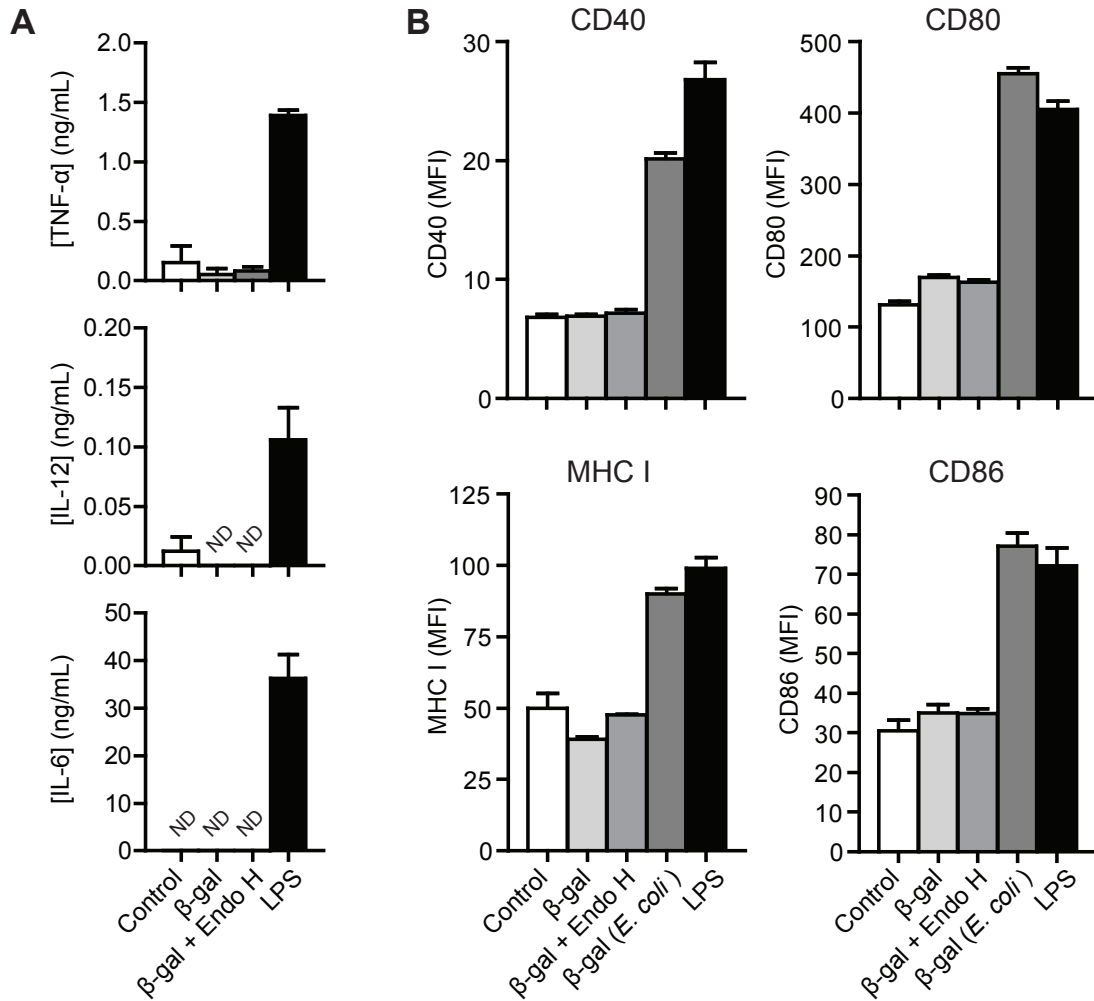


**Figure 4.16: *P. pastoris*-derived N-glycans do not activate BM-DCs**

(A) BM-DCs were pulsed with medium (control),  $\beta$ -gal, Endo H-treated  $\beta$ -gal or LPS. Cytokine secretion after 18 h was analyzed by ELISA. ND = not detectable. (B) BM-DCs were pulsed with medium (control),  $\beta$ -gal, Endo H-treated  $\beta$ -gal, *E. coli*-derived  $\beta$ -gal or LPS. After 18 h, surface expression of the indicated activation markers was analyzed by flow cytometry, and MFIs were calculated. All graphs show the mean values of three replicates. Error bars depict SEM.

To fully assess the immunostimulatory impact of *P. pastoris* derived N-glycosylation in the context of antigen presentation, we pre-treated BM-DCs with glycosylated or de-glycosylated  $\beta$ -gal and investigated their capacity to present the OVA-derived epitopes OVA<sub>257-264</sub> or OVA<sub>323-339</sub> to OVA-specific CD8<sup>+</sup> (OT-I) or CD4<sup>+</sup> (OT-II) T cells, respectively (Figure 4.17 A, B). Concordantly detected by IL-2 secretion and lymphoproliferation, CD8<sup>+</sup> and CD4<sup>+</sup> T cell activation was both increased after BM-DC stimulation with LPS but not  $\beta$ -gal, irrespective of the proteins glycosylation state.

We also investigated the presentation of endogenous peptides by BM-DCs to DesTCR T cells. These are transgenic T cells with a H-2K<sup>k</sup> haplotype that recognize three endogenous peptides on H-2K<sup>b</sup> expressed by C57BL/6J BM-DCs in an alloreaction [126, 156, 157]. Similar to the presentation of exogenous antigens on MHC I to OT-I cells, the presentation of endogenous peptides to DesTCR T cells was not altered by pre-stimulation with *P. pastoris*-derived  $\beta$ -gal (Figure 4.17 C).

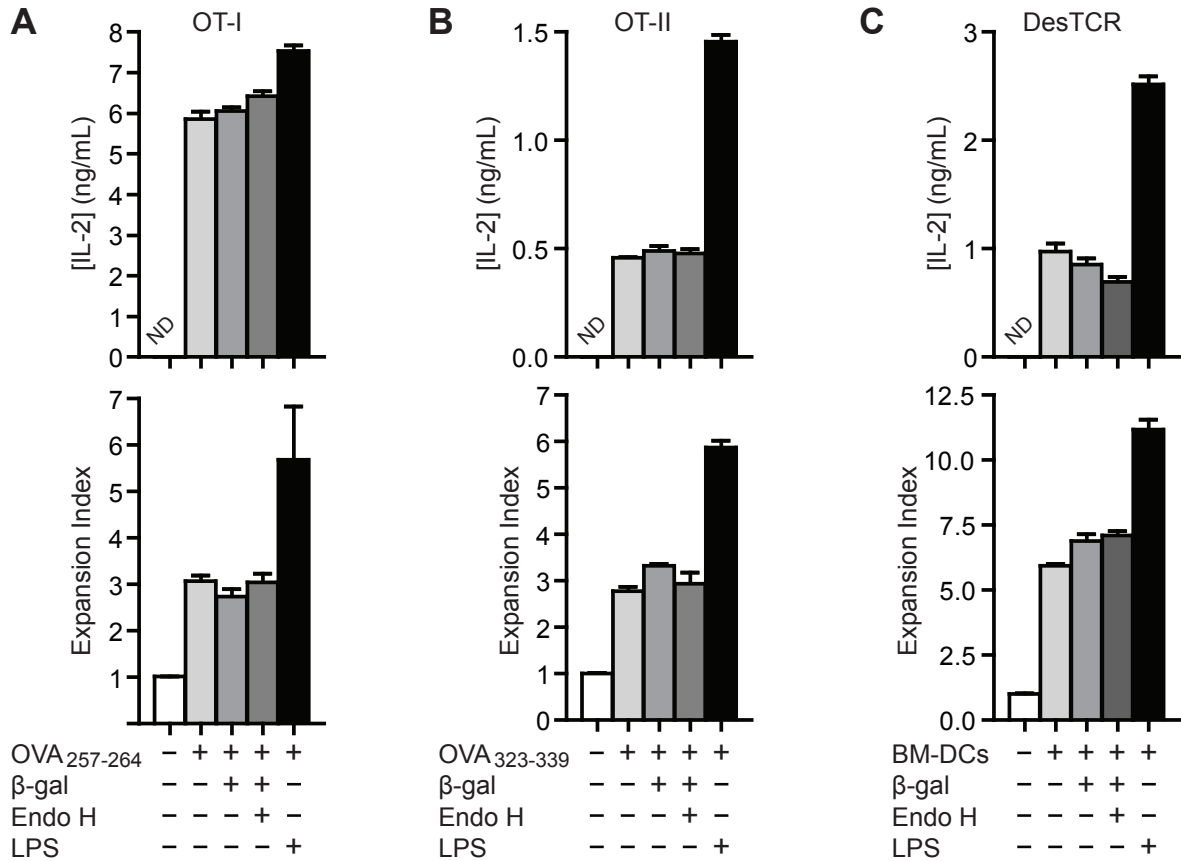


**Figure 4.17: The mere presence of *P. pastoris*-derived N-glycans has no effect on antigen presentation**

(A) BM-DCs were pre-stimulated with  $\beta$ -gal, Endo H-treated  $\beta$ -gal or LPS and pulsed with the MHC I-restricted OVA-peptide OVA<sub>257-264</sub>. Cells were either co-cultured with OVA-specific CD8<sup>+</sup> T cells (OT-I) and IL-2 secretion after 18 h was determined by ELISA (upper panel), or cells were co-cultured with fluorescently labeled OT-I T cells, and proliferation was determined after 3 days by flow cytometry (lower panel). (B) Experimental procedure as in (A), except that BM-DCs were pulsed with the MHC II-restricted peptide OVA<sub>323-339</sub> and co-cultured with OVA-specific CD4<sup>+</sup> T cells (OT-II). (C) Experimental procedure as in (A) except that no exogenous peptide was pulsed, negative control was without BM-DCs and co-culturing was done with DesTCR T cells. ND = not detectable. All graphs show the mean values of three replicates and are representative for three independent experiments. Error bars depict SEM.



The presented data strongly suggest that *P. pastoris*-derived N-glycosylation has no impact on DC maturation and subsequent T cell activation *per se*.

#### **4.7 *Pichia pastoris*-derived N-glycans evoke converse cytotoxic activities for different antigens and are not beneficial for a humoral response *in vivo***

As described in the introduction, *P. pastoris* was already used in different *in vivo* experiments as an expression system for glycoproteins in vaccination approaches. However, these studies neither used enforced N-glycosylation on non-glycoproteins, nor did they compare the immunogenicity of glycosylated vs. glycosidase-treated proteins. Hence, the effects of *P. pastoris*-derived N-glycans *in vivo* remained elusive.

We addressed this open question by performing *in vivo* immunization trials with glycosylated or Endo H-treated  $\beta$ -gal (Figure 4.18 A). Each protein was injected subcutaneously into recipient mice as depicted in Figure 4.18 B. To investigate the influence of such a vaccination strategy on cytotoxic CD8<sup>+</sup> T cell activity, we intravenously injected a 1:1 mixture of differentially labeled splenocytes, either pulsed with the  $\beta$ -gal specific epitope ICPMYARV (target cells) or medium only (non-target cells), into the tail vein of the recipients. After 18 h, draining lymph nodes were isolated and analyzed for the presence of target and non-target cells by flow cytometry. Analysis revealed a specific elimination of target cells after immunization with glycosylated  $\beta$ -gal, which was markedly — though not significantly — reduced in the group vaccinated with deglycosylated  $\beta$ -gal (Figure 4.18 C). Concordantly, re-stimulated lymph node cells from mice immunized with glycosylated  $\beta$ -gal showed robust IFN- $\gamma$  secretion after 24 h, which was decreased in the group immunized with deglycosylated  $\beta$ -gal (Figure 4.18 D).

To investigate whether this increase in cytotoxicity is a general feature of *P. pastoris*-derived N-glycans, we fused the OVA epitope SIINFEKL (S8L) to NST-GFP (NST-GFP-S8L) and immunized mice with glycosylated or Endo H-treated NST-GFP-S8L, as depicted in Figure 4.18 B. To our surprise, cytotoxicity against NST-GFP-S8L was significantly increased after deglycosylation (Figure 4.18 E), which is contrary to the effect of N-glycans on  $\beta$ -gal. Since both proteins showed a similar N-glycan-dependent capacity to ligate the C-type lectin domain of the MR, it was anticipated that N-glycans will have similar effects on the *in vivo* cytotoxicity of both proteins.

Instead, this result suggests that the effect of *P. pastoris*-derived N-glycans on a cytotoxic response *in vivo* depends on the nature of the antigen.

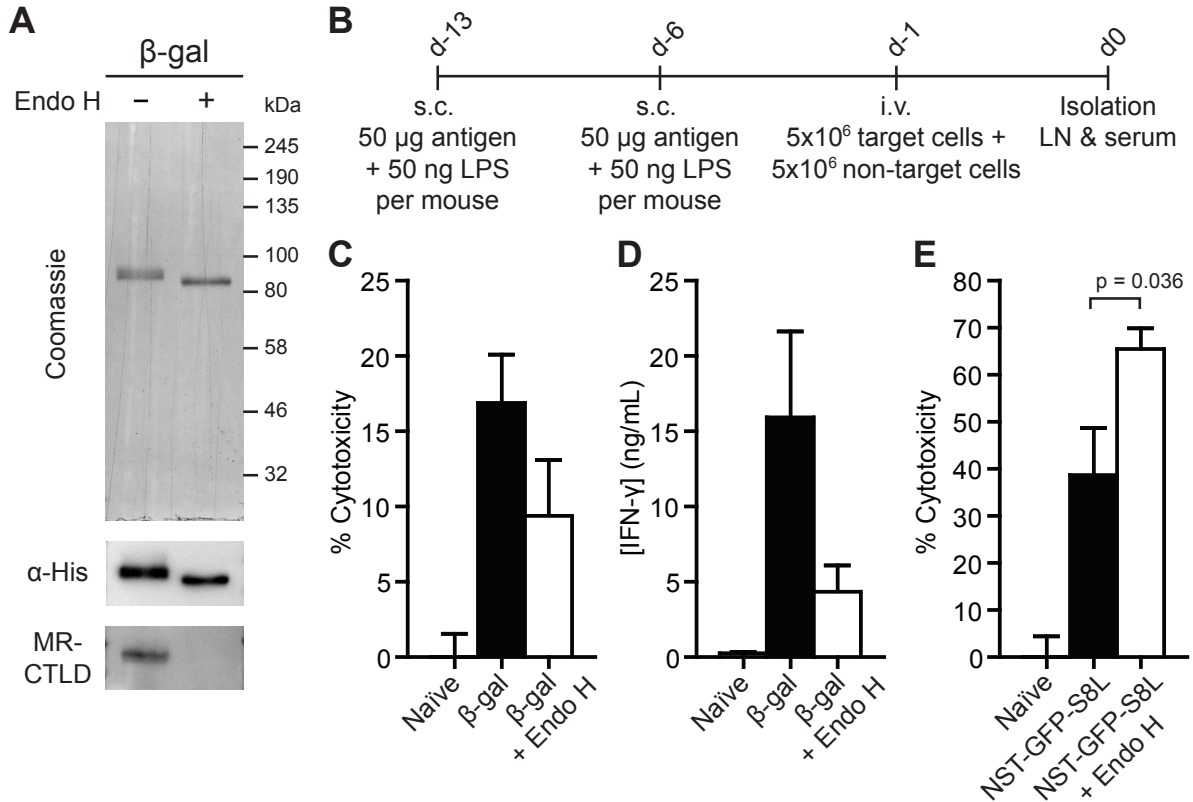


**Figure 4.18: Converse *in vivo* cytotoxicity after deglycosylation of  $\beta$ -gal and NST-GFP-S8L**

(A)  $\beta$ -gal was purified as before, Endo H- or control-treated and further purified by ultrafiltration. Proteins were separated by SDS-PAGE and analyzed by coomassie staining, western blot against the His-tag or far-western blot with MR-CTLD. (B) Immunization scheme. s.c. = subcutaneous, i.v. = intravenous, LN = lymph node. (C) Recipient mice (n = 28) were immunized according to the scheme in (B) with Endo H- or control-treated  $\beta$ -gal depicted in (A). Draining lymph nodes were isolated, and  $\beta$ -gal-related cytotoxicity was determined by measuring the specific elimination of  $\beta$ -gal<sub>497-504</sub> (ICPMYARV)-pulsed target cells by flow cytometry. (D) Isolated lymph node cells from n = 12 mice treated as in (B) were re-stimulated with  $\beta$ -gal<sub>497-504</sub> (ICPMYARV), and IFN- $\gamma$  was detected after 18 h by ELISA. (E) Recipient mice (n = 6) were immunized according to the scheme in (B) with Endo H- or control-treated NST-GFP-S8L. Draining lymph nodes were isolated, and cytotoxicity was determined by measuring the specific elimination of OVA<sub>257-264</sub> (SIINFEKL, S8L)-pulsed target cells by flow cytometry. Error bars depict SEM. P-values were calculated by ANOVA and Tukey HSD post hoc analysis.

Next, we were interested in the question how enforced N-glycosylation would effect CD4<sup>+</sup> T cell activity. To this end, we measured the humoral response in the sera of the same mice as in Figure 4.18 C and E by detecting whole IgG specific for glycosylated or deglycosylated  $\beta$ -gal or NST-GFP-S8L (Figure 4.19 A, B).

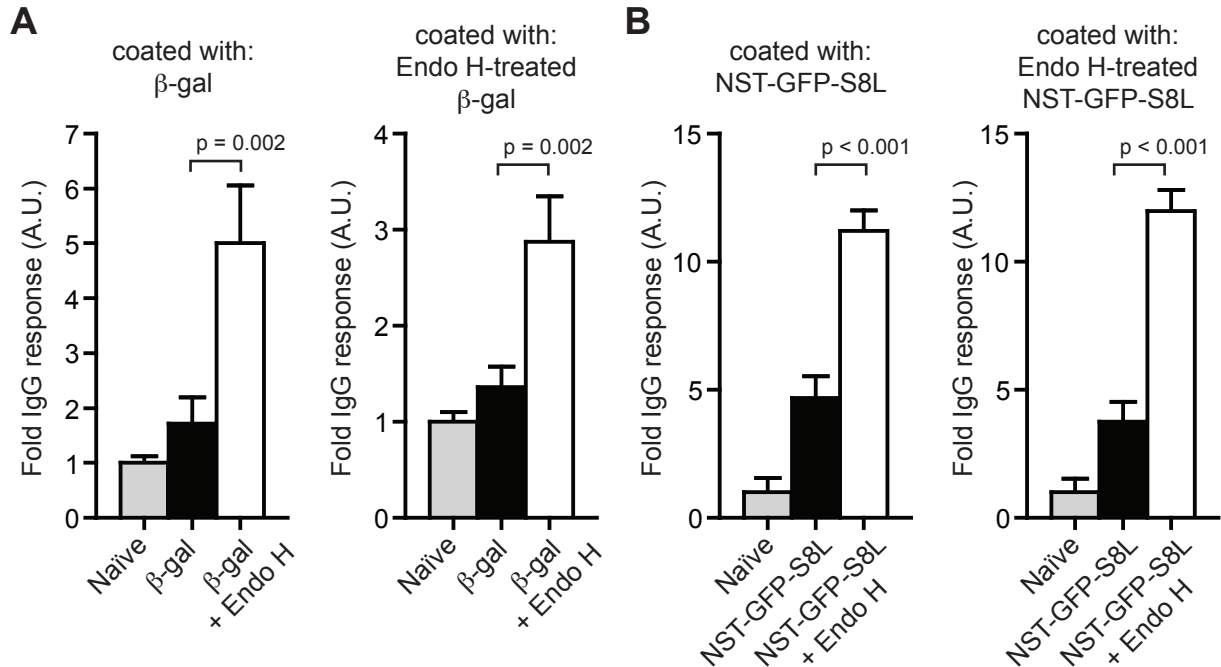


**Figure 4.19: Increased humoral immune response after the removal of *P. pastoris*-derived N-glycans**

(A) Serum from recipient mice ( $n = 28$ ) depicted in Figure 4.18 C was analyzed for the presence of IgG antibodies specific for  $\beta$ -gal (left panel) or Endo H-treated  $\beta$ -gal (right panel) by ELISA. Vaccination groups are indicated on the x-axis: Naïve group = grey bars,  $\beta$ -gal group = black bars, Endo H-treated  $\beta$ -gal group = white bars. (B) Serum of NST-GFP-S8L immunized mice ( $n = 6$ ) depicted in Figure 4.18 E was collected and analyzed for the presence of IgG antibodies specific for NST-GFP-S8L (left panel) or Endo H-treated NST-GFP-S8L (right panel) by ELISA. Vaccination groups are indicated on the x-axis: Naïve group = grey bars, NST-GFP-S8L group = black bars, Endo H-treated NST-GFP-S8L group = white bars. Whole IgG was determined as fold response of naïve control group. All graphs show mean values and error bars indicate SEM. P-values were determined by one-way ANOVA and post-hoc Tukey HSD analysis. The experiments depicted in (B) were performed by Matthias Zehner.

Despite their converse cytotoxic responses, both tested antigens showed similar humoral responses. Surprisingly, a strong increase in IgG was detected in mice immunized with the deglycosylated proteins, whereas IgG levels were only slightly elevated after the

injection of untreated proteins. Noteworthy, all antibodies detected both the glycosylated and deglycosylated isoform, implying that the fungal N-glycans do not contribute to epitopes recognized by these antibodies. Both findings suggest that *P. pastoris*-derived N-glycans do not improve MHC II-restricted presentation to CD4<sup>+</sup> T cells.

Taken together, these *in vivo* data challenge the common conception that yeast-derived N-glycans generally increase immunogenicity. The findings rather suggest that beneficial effects on the cytotoxic response are antigen-dependent, and that fungal N-glycans even bear the potential to decrease both cytotoxic and humoral responses *in vivo*.

## 4.8 Enforced N-glycosylation of non-glycoproteins can affect MHC class I-restricted epitopes

One of the most important steps during T cell activation is the recognition of the MHC-peptide complex on antigen presenting cells by the specific T cell receptor (TCR). The binding of a peptide to the MHC binding groove is mainly mediated by MHC-specific anchor residues [158, 159], and for MHC class I molecules critically depends on the interaction of the peptide C-terminus with the F-pocket in the binding groove [159]. Glycans linked to anchor residues or any other residue facing towards the binding groove can prevent the binding of peptides to MHC molecules [160, 161]. In addition, TCRs are highly specific for their cognate MHC-peptide complex, and glycans on a certain epitope can destroy the interaction that would normally occur between the TCR and the unglycosylated epitope [160]. Since enforced N-glycosylation thereby holds the potential to destroy MHC I-restricted epitopes, we finally wanted to elucidate whether N-glycosylation of  $\beta$ -gal within a putative MHC I epitope is able to prevent cross-presentation. To this end we investigated the cytotoxic response to  $\beta$ -gal<sub>96-103</sub> (DAPIYTNV), another H-2K<sup>b</sup>-restricted  $\beta$ -gal epitope which can induce potent CD8<sup>+</sup> T cell responses [162, 163]. It is important to note that the asparagine in this epitope is one of the putative N-glycosylation sites in  $\beta$ -gal (N103, see Figure 4.2). Since N103 is the first N-glycan acceptors in  $\beta$ -gal (Figure 4.2), and N-glycosylation preferentially occurs towards the N-terminus [143], it is very likely that N103 is glycosylated after expression by *P. pastoris*. We repeated the immunization experiment as depicted in Figure 4.18 B and investigated the *in vivo* cytotoxicity against peptide-pulsed target cells after the immunization of mice with the *P. pastoris*-derived  $\beta$ -gal as before. This time, however, we pulsed target cells with the (unglycosylated)  $\beta$ -gal<sub>96-103</sub> peptide (DAPIYTNV). In contrast to the

response to ICPMYARV, we did not observe any cytotoxicity against target cells that were pulsed with the DAPIYTNV peptide (Figure 4.20 A). This result indicates that CD8<sup>+</sup> T cells in these mice were not primed against the (unglycosylated)  $\beta$ -gal<sub>96-103</sub> peptide (DAPIYTNV) after vaccination with the *P. pastoris*-derived  $\beta$ -gal. This, in turn, could be explained by an N-glycan present on N103 in  $\beta$ -gal.

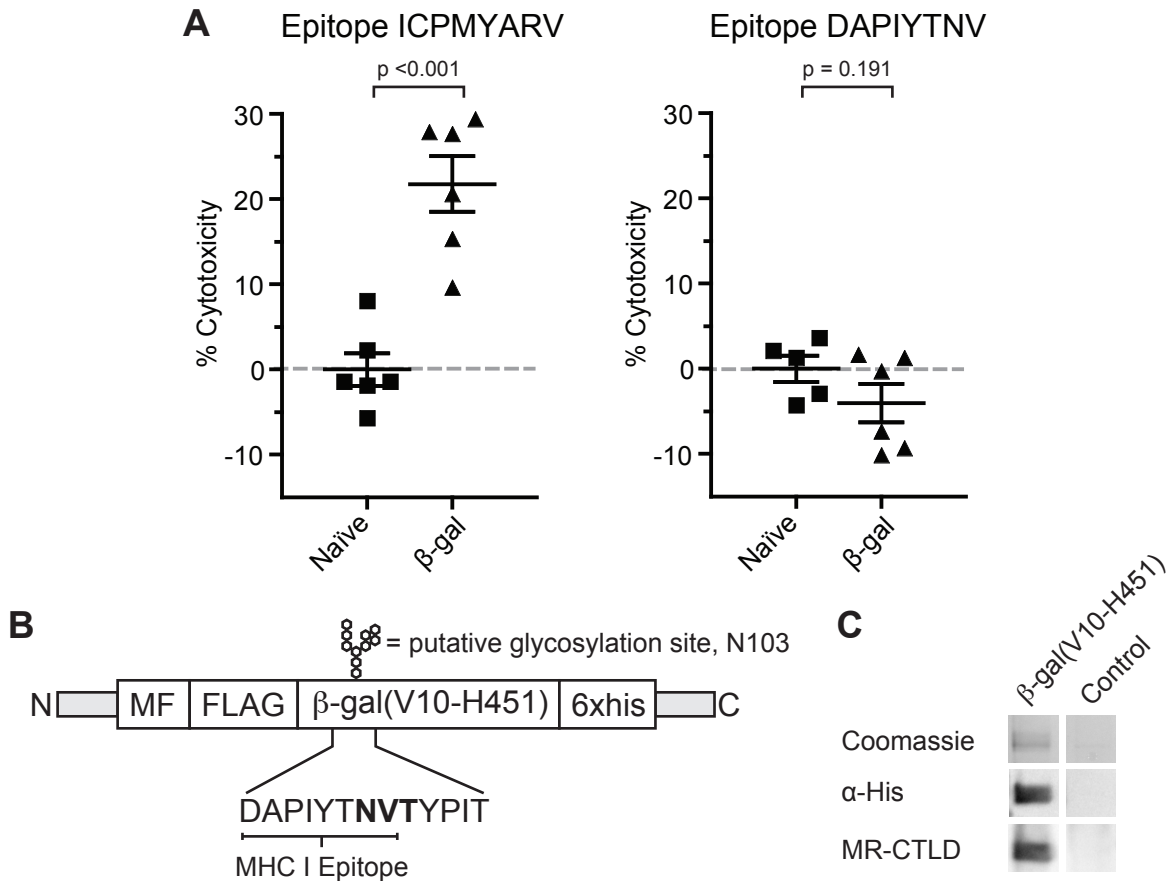


**Figure 4.20: Epitope-specific *in vivo* cytotoxicity of *P. pastoris*-derived  $\beta$ -gal**

(A) Recipient mice ( $n \geq 5$ ) were vaccinated with  $\beta$ -gal (triangles) or left untreated (squares) as depicted in Figure 4.18 B. Injected target cells were either pulsed with  $\beta$ -gal<sub>497-504</sub> (ICPMYARV, left panel) or  $\beta$ -gal<sub>96-103</sub> (DAPIYTNV, right panel). The specific elimination of target cells was determined by flow cytometry and % cytotoxicity was calculated. Bars show mean values, error bars indicate SEM. P-values were determined by one-way ANOVA and post-hoc Tukey HSD analysis. (B) Scheme of truncated  $\beta$ -gal(V10-H451). (C) His-tagged proteins were purified by affinity chromatography from *P. pastoris* transformed with  $\beta$ -gal(V10-H451) or vector backbone only (control). Pooled eluate fractions were separated by SDS-PAGE and analyzed by coomassie staining, western blot against the His-tag and far-western blot with MR-CTLD.

To further investigate the glycosylation state of the asparagine N103, we transformed *P. pastoris* with the deletion-mutant  $\beta$ -gal(V10-H451). This protein comprises the  $\beta$ -gal<sub>96-103</sub> epitope DAPIYTNV with the putative glycosylation site N103 but lacks the remaining N-X-S/T motifs N461, N705 and N726 present in  $\beta$ -gal(V10-L731)(compare Figure 4.20 B and Figure 4.2 B). This highly truncated protein was not efficiently secreted anymore and was hence purified by a one-step IMAC from yeast pellets. As a purification control, yeast cells were transformed with vector backbone only. We were able to purify a His-tagged protein from  $\beta$ -gal(V10-H451)-transformed yeast cells, which was not present in control-transformed cells (Figure 4.20 C). Importantly, this purified  $\beta$ -gal(V10-H451) still reacted with the MR-CTLD in a far-western blot (Figure 4.20 C), just like  $\beta$ -gal(V10-L731) did before (Figure 4.5 E). Since N103 is the only N-glycan acceptor site in the truncated  $\beta$ -gal(V10-H451), this reactivity indicates the presence of a high-mannose glycan on N103, which in turn also argues for the glycosylation of N103 in the initially used  $\beta$ -gal(V10-L731).

Together, these results suggest that the N103 within the DAPIYTNV epitope is indeed glycosylated in *P. pastoris*-derived  $\beta$ -gal, which prevents the cytotoxic activity against (unglycosylated)  $\beta$ -gal<sub>96-103</sub> (DAPIYTNV)-pulsed target cells, or in other words, destroys the original DAPIYTNV epitope in  $\beta$ -gal.

## 5 Discussion

Due to their pivotal role in the initiation of an adaptive immune response, professional antigen presenting cells (APCs) like dendritic cells (DCs) have become important targets in vaccination approaches, and various strategies have been developed to deliver antigens specifically towards DCs [164]. Among these strategies, fungal glycosylation was shown to be a promising strategy to target C-type lectin receptors on DCs and increase the immunogenicity of certain antigens [120–123, 165]. Yet, success of this strategy has so far only been proved for proteins which are glycosylated in their native state, and the immunostimulatory impact of fungal N-glycans has remained elusive. In the thesis we have demonstrated that the yeast *Pichia pastoris* (*P. pastoris*) glycosylates proteins as soon as they are secreted, even if they are not glycosylated in their native state. We have established a method to transfer this strategy to proteins that lack intrinsic N-glycosylation sites by the introduction of an engineered glycosylation motif and have proved that the attached N-glycans are specifically recognized by the MR. However, our data do not indicate an immunostimulatory effect of yeast-derived N-glycans per se and suggest that the effect of such targeting strategies *in vivo* critically depend on the nature of the antigen and potential immunodominant epitopes.

### 5.1 Enforced N-glycosylation by *Pichia pastoris* as a tool to glycosylate non-glycoproteins

In comparison to the bacterial expression system *E. coli*, *P. pastoris* has been introduced relatively recently [111]. Yet, it quickly gained popularity and is now broadly used in industry and academia [108, 166–168]. One advantage that accounts for its increasing application in protein production is the ability for post-translational modifications such as disulfide bond formation and glycosylation [112]. These modifications contribute to proper protein folding considerably and are important for protein functionality [169].

N-glycosylation of characterized glycoproteins at their native glycosylation sites has been repeatedly reported in *P. pastoris* [170–172]. Additionally, putative glycoproteins that have been expressed for biochemical studies in *P. pastoris* show N-glycosylation at predicted N-glycosylation sites [173, 174], though it is not known whether these sites are also glycosylated in the native proteins. Taken together, this suggests that any N-X-S/T sequon will be readily glycosylated by *P. pastoris*, as long as the protein enters the secretory pathway.

Indeed, our data clearly show that recombinant  $\beta$ -gal(V10–L731), though not glycosylated in its native state in *E. coli*, is N-glycosylated when expressed in *P. pastoris*, as confirmed by glycosidase treatment and subsequent SDS-PAGE analysis in comparison to the *E. coli*-derived protein (Figure 4.5). These data are in line with the work of García et al., who showed that  $\alpha$ -amylase from *Bacillus licheniformis* gets N-glycosylated after expression by *P. pastoris* [175], but seem to contradict a study on the human prostaglandin H synthases 1 and 2 [176]. In the latter study, the two glycoproteins with 4 or 5 N-X-S/T sequons respectively have been expressed in *P. pastoris*. In each of the native proteins, one of these motifs is not glycosylated. Interestingly, Kukk et al. showed that the recombinant proteins from *P. pastoris* are glycosylated not at all potential but only at the same sequons that are also occupied in the native proteins. On the other hand, ovalbumin, which bears only one N-glycan attached to N292 in its native form [72], is consistently glycosylated at both possible N-X-S/T motifs (N292, N311) after recombinant expression in *P. pastoris* [120, 171]. Of note, during biosynthesis in the hen oviduct, native ovalbumin occurs in the di-glycosylated form, too. However, this di-glycosylated species exists only transitionally and is deglycosylated by a site-specific peptide:N-glycanase at position N311 before secretion [177]. This suggests that the mere presence of N-X-S/T might not automatically be sufficient for efficient glycosylation by *P. pastoris*. Instead, other factors like the presence of substrate-specific glycosidases or sequon accessibility during protein folding (i.e. sterical hinderance) might influence site occupancy and thereby the success of enforced N-glycosylation.

The recombinant  $\beta$ -gal(V10–L731) used in this thesis bears 4 putative N-glycosylation sites (N103, N461, N705 and N726, Figure 4.2). N103 and N461 are both located within less defined loop-like structures in the binding groove and play a role rather in substrate binding than in structure determination [178]. N103 is more exposed to the surface, whereas N461 is slightly buried within the protein’s core. N705 is located at a surface loop structure within a beta-barrel and N726 is positioned on a linker peptide between



two beta-barrel domains. It has been suggested that protein folding into secondary domains can progress too fast for the oligosaccharyltransferase to glycosylate a sequon, simply by reducing the sequon's spatial and temporal accessibility before it gets buried within the protein [179]. Additionally, surface exposed sequons might not be glycosylated when they engage in hydrogen bonds or are close to disulfide bridges [180]. Vice versa, protein glycosylation at unintended sites could interfere with protein folding. Taking this into account, it is likely that glycosylation of e.g. N461 favors misfolding and protein aggregation. Western blot analysis of yeast pellets and supernatants revealed that pellets include protein isoforms which show a roughly 10 kDa higher apparent molecular weight (Mw) (Figure 4.3). The uncleaved signal sequence has a calculated Mw of 9.3 kDa and could account for the molecular weight shift. Nonetheless, the pellet signal is also less sharp than the supernatant signal, suggesting that it might rather represent additional glycoforms with several glycosylated sites or a hypermannosylated glycan. These glycoforms are possibly not secreted due to protein misfolding or sterical issues when passing through the translocon.

Standard high-mannose glycans with 8–12 mannose residues have a Mw of roughly 1.7–2.4 kDa. As the deglycosylation of the purified  $\beta$ -gal(V10–L731) resulted in a very small electromobility shift (Figure 4.5 E), it seems plausible that only one or two asparagines are glycosylated in the secreted glycoform. The expression of the truncated  $\beta$ -gal(V10–H451) suggests that N103 is glycosylated, because  $\beta$ -gal(V10–H451) only bears this particular N-X-S/T motif but is still recognized by the MR (Figure 4.20 C). Further studies with the recombinant  $\beta$ -gal(V10–L731) such as mass-spec analysis could shed light on the site occupancy, thereby adding more information on the restrictions of enforced N-glycosylation on intrinsic N-X-S/T sites as a glycosylation strategy. Additionally, as protein folding rates are influenced by culture and induction conditions, the fine-tuning of these parameters might allow to adjust the ratio of distinct glycoforms to a more or less glycosylated variant, thereby generating the optimal glycosylation-degree needed for a certain purpose such as receptor targeting.

## 5.2 Translating enforced N-glycosylation to non-glycoproteins that lack intrinsic N-X-S/T motifs

Current subunit vaccines mainly focus on outer surface proteins of pathogens like viral envelope proteins [110, 181, 182]. These antigens are of particular interest in terms of humoral responses against extracellular pathogens. When it comes to intracellular pathogens, where a cytotoxic response is needed, inner pathogenic proteins like viral core proteins could represent additional targets. Unfortunately, many core proteins such as those of certain HBV genotypes [183, 184] do not bear any intrinsic glycosylation motif at all and would hence not be a substrate for the presented enforced glycosylation strategy. To solve this problem, we introduced an engineered glycosylation site upstream of the multiple cloning site in a yeast expression vector. Our proof of principle experiments with GFP clearly show that the elaborate engineering of a glycosylation motif yields a high percentage of glycosylated protein in *P. pastoris* (Figure 4.11). Interestingly, our glycosylation tag also worked for HEK293T cells, though in these cells roughly half of the protein was obtained in its unglycosylated form, which might be either a result of the yeast-optimized amino acid sequence or the applied cell culture conditions (Figure 4.13 A).

The GFP fluorophore forms after protein folding by covalent linkage involving the residues 65–67 [185]. Changes in GFP amino acid composition have led to the development of enhanced GFP with changed fluorescent properties [149], and the introduction of structural constraints like disulfide bonds even led to the discovery of redox sensitive GFPs [186], which show altered fluorescence properties in their oxidized and reduced states respectively. Hence, we would expect to detect different fluorescent properties if artificially introduced glycans would lead to misfolding or structural disturbance of GFP. However, the comparison of fluorescence properties among our yeast-derived and HEK-derived GFPs (Figure 4.14) shows identical properties throughout all GFP variants irrespective of their glycosylation state. This suggests that placing an N-X-S/T motif distant from structure determining residues could help to minimize the risk of glycan interference with protein folding. Besides being beneficial for protein secretion, proper folding might be an issue if enforced N-glycosylation is applied to proteins that should retain their native conformation, e.g. for an enzyme replacement therapy.

Engineered N-glycosylation sites have previously been applied by other groups in several expression systems for quite different purposes such as topology studies of membrane proteins [187], increasing the secretion of heterologous proteins [188], or rendering protein properties like their stability in terms of *in vivo* clearance [189]. We suggest that engineered glycosylation sites are additionally useful to tag unglycosylated proteins with certain glycans — determined by the expression host — in order to target receptors or other proteins that bind to these certain glycans.

In addition to N-glycosylation, it has to be considered that O-glycosylation might also occur during recombinant expression. Similar to the data on N-glycosylation, O-glycosylation by *P. pastoris* has been reported for serine and threonine residues that are not occupied in the native proteins [190, 191]. Additionally to a possible interference of such O-glycans with the folding and the function of recombinant proteins, they might also serve as additional ligands of certain lectins, and hence represent a targeting strategy themselves. Nevertheless, there is no clear consensus sequence for O-glycosylation, and attempts to introduce O-glycans accordingly rely on the fusion of larger protein subunits or whole proteins that are known to be O-glycosylated in their native state [120, 123]. Hence, enforced N-glycosylation should be favored especially for small proteins, where the fusion of large polypeptides can strongly influence the protein's physicochemical properties and functionality.

### **5.3 Targeting C-type lectin receptors by protein expression in *Pichia pastoris***

In the early days of protein biochemistry, receptors were mainly discovered by the purification of homogenous protein solutions from cells that are responsible for a certain binding or enzymatic activity. Following this forward approach, the mannose receptor was first purified by Philip D. Stahl and coworkers when they tried to isolate the receptor on macrophages that mediates the binding to and the uptake of mannosylated glycoproteins [192, 193]. Nowadays, modern genetic techniques prove that the simple picture of one receptor mediating one activity is outdated. Certain receptors are evolutionary or functionally related to each other and might show partially overlapping ligand specificities [61, 194]. Such receptors might simply be redundant and serve as backup systems. However, in the case of antigen presentation, the uptake of the same antigen

by different receptors even leads to different processing pathways [51]. Additionally, receptors like the MR bear multiple domains allowing the binding of not only one, but several quite different substrates, which enables the receptor to fulfill diverse functions [195]. Thus, modern targeting strategies have to handle different challenges regarding target specificity. They have to discriminate between structurally related but functionally different receptors and to target those structures on the receptors that lead to the desired downstream effects like certain signaling or trafficking events.

The uptake of *P. pastoris*-derived  $\beta$ -gal by HEK cells proved that the yeast-derived glycans on the recombinant protein are indeed ligands of the MR (see Figure 4.6). These findings are perfectly in line with the results of Lam et al., who demonstrated the uptake of *P. pastoris*-derived OVA by MR expressing CHO cells [122]. Together, this not only suggests that *P. pastoris* uses quite a restricted set of high-mannose glycans, regardless of whether the glycosylation site is occupied in the native protein or not, but also that the natural glycans of OVA and *P. pastoris*-derived glycans are structurally closely related. This idea is further supported by a ligand analysis of purified human mannose receptor performed by Kéry et al. in 1992 [70]. In this study, they show that the receptor has a strong preference for branched mannosides with  $\alpha$ -1,6- and  $\alpha$ -1,3-linkages. These linkages not only occur as free accessible branched trimannosides in the most prevalent N-glycans found on OVA [72], but are also a core structure of all high-mannose glycans in the  $\alpha$ -1,6 branch [196] and hence potentially present in *P. pastoris*-derived glycans.

In contrast to HEK cells, BM-DCs are well equipped to capture a broad variety of antigens by the expression of diverse endocytic receptors such as the MR [51], DEC205 [197, 198], Dectin-1 and Dectin-2 [199, 200], Fc receptors for IgG (Fc $\gamma$ R) II and III [201] or scavenger receptors [202] but also by constitutive macropinocytosis [203]. Hence, it should be highlighted that the vast majority of the *P. pastoris*-derived recombinant antigens are taken up by the MR on these cells, as shown by the decreased uptake in MR-deficient BM-DCs (see Figure 4.7). Beyond that, our data clearly show that yeast-derived  $\beta$ -gal and NST-GFP are solely recognized by the C-type lectin part of the MR but neither by its cysteine-rich domain nor the fibronectin II domain (see Figure 4.5 and Figure 4.11). Importantly, binding and uptake disappeared after deglycosylation with PNGase F or Endo H, thus proving that our model antigens bound exclusively via N-glycans to the MR. Since the MR was also shown to bind *P. pastoris*-derived O-glycans [122, 123], this further suggests that neither  $\beta$ -gal nor NST-GFP bear excessive O-glycans. Taken together, this implies that the interaction between *P. pastoris*-derived

N-glycosylated proteins and the MR closely resembles the interaction between the model antigen ovalbumin and the MR. Concordantly, both antigens,  $\beta$ -gal and NST-GFP, are internalized by BM-DCs into the same compartments as ovalbumin (see Figure 4.9 and Figure 4.12 C), which proves that the presented method shows a very accurate MR specificity for the *in vitro* targeting of BM-DCs. Noteworthy, glycan-dependent uptake could also be demonstrated for human peripheral blood mononuclear cell-derived DCs and macrophages (Figure 4.15), suggesting that targeting strategies based on N-glycosylation by *P. pastoris* might also be translated to humans.

Beside two recent studies that used novel plant lectin-based arrays to characterize glycans on recombinant proteins from *P. pastoris* [123, 204], only two other mammalian C-type lectins have been tested explicitly for the binding of *P. pastoris*-derived glycans, namely DC-SIGN [122, 123] and the mannose-binding lectin (MBL) [123]. The mouse genome encodes 8 different homologues of human DC-SIGN (SIGNR1-8), none of which is a clear ortholog [205]. Of these, only SIGNR3 shows the same substrate specificity as DC-SIGN for both high-mannose and fucose-terminated glycans [206]. SIGNR3 has been shown to be expressed by some subtypes of DCs and other myeloid cells *in vivo* but not by BM-DCs [200, 207]. MBL, on the other hand, is a soluble serum protein which is secreted by the liver [208]. Both proteins are hence possible binding partners of enforced N-glycosylated proteins in *in vivo* targeting strategies, or in the case of SIGNR3 also for *ex vivo* targeting strategies of isolated primary cells.

Other C-type lectins that were described to bind mannose comprise Endo180 (uP-ARAP) [209], langerin (CD207) [210], Dectin-2 [211], dendritic cell immunoreceptor (DCIR) [212, 213], dendritic cell lectin (DLEC or BDCA-2) [212, 214], macrophage C-type lectin (MCL) and macrophage-inducible C-type lectin (Mincle) [212] as well as the collectin surfactant protein D (SP-D) [215]. The latter is structurally related to the MBL but is mainly secreted by epithelia lining environment-exposed surfaces like the lung, where it participates in innate immunity against inhaled microorganisms [216]. Of the other C-type lectins Endo180 is structurally the closest relative of the MR and thus a member of the MR family [209]. It is also expressed on macrophages and fibroblasts [217]. Instead of antigen-uptake, however, the prominent function of this receptor seems to be the turnover of the extracellular matrix, as it binds collagen via its MR-homolog fibronectin II domain and directs it towards lysosomal degradation [218]. In this respect, Endo180 has gained interest for its role in cancer progression and has recently been identified as a target to treat bone cancer [219].

Up to now, there is no data available on the interactions between *P. pastoris*-derived glycans and C-type lectins other than the MR, DC-SIGN or MBL. Like the MR or DC-SIGN many of the other membrane bound C-type lectin receptors were described to play a role in antigen uptake and presentation [55, 58, 60, 220, 221]. Consistently, the targeting of mannose-specific lectins by *P. pastoris*-derived proteins is widely considered to be used as a vaccination strategy [116, 120–122, 222, 223]. However, some receptors like Endo180 also play important roles in diseases, for example cancer [224]. Hence, it will be interesting to identify interactions of *P. pastoris*-derived glycoproteins with other putative targets to reveal both unwanted side effects of therapeutics and potential new applications beyond antigen delivery.

## 5.4 Alternative targeting approaches for C-type lectins in comparison to enforced N-glycosylation

DEC205 (CD205) and phospholipase A2 receptor, the two remaining members of the MR family besides Endo180 and the MR, bear mutations in the CRD residues that coordinate calcium and have therefore no predicted calcium-dependent carbohydrate binding activity. Indeed, no C-type lectin activity has been documented for either DEC205 or phospholipase A2 receptor so far. Instead, DEC205 was described to participate in the uptake of ligands that are expressed during apoptosis and necrosis, thereby playing a role in peripheral tolerance [225]. Additionally, DEC205 was reported to mediate the binding and the uptake of class B CpG oligonucleotide, and it thus plays a key role in the adjuvants effect of CpG by delivering it to TLR9 positive endosomes [226]. The phospholipase A2 receptor on the other hand binds non-glycosylated ligands independently of  $\text{Ca}^{2+}$  by protein-protein interaction via its CTLD5 [227–229].

These two members of the MR-family illustrate how enforced glycosylation with specific glycans might complement classical targeting strategies in the case of lectins. Classical approaches typically rely on the generation of monoclonal antibodies against the target of interest, which are subsequently coupled to the cargo protein. A recent alternative to antibodies are aptamers — small RNA molecules with a defined structure that resulted from repeated selection cycles in a process termed systematic evolution of ligands by exponential enrichment (SELEX) [230]. Both techniques have, for instance, been used to target DEC205 [231–233]. However, aptamers require the generation and

purification of the selective targeting agent (i.e. the aptamer), the purification of the cargo protein and finally a coupling reaction to connect those two. Recombinant antibody technology allows at least to circumvent these additional steps by encoding the fusion protein directly in the DNA. Enforced glycosylation follows the same recombinant principle and combines all three steps in one purification, which might save costs and time when it comes to large-scale production for therapeutic purposes. Another possible pitfall of both antibody and aptamer approaches is inbuilt by the choice of the target molecule that is used to raise the antibody or aptamer. If, for example, an aptamer or antibody is raised against a CRD of a C-type lectin, it is likely that a positively selected molecule binds to one of the conserved regions that determine the overall CRD fold. There are only subtle changes in the amino acid composition that determine whether a CRD coordinates calcium or not [234]. Hence, such approaches require a very careful post-production negative selection, as the sole positive selection against the main target cannot exclude off-target binding to structurally related receptors with different ligand selectivity.

In approaches where the target is a substrate binding site within a broadly distributed protein motif like the CRD fold, attaching a natural ligand to the cargo-protein could help to decrease off-target binding, and hence be a valuable alternative. Indeed, such an approach has been performed recently by fusing the chemokine (C motif) ligand (XCL1) to a model antigen to target its receptor XCR1 [235]. However, the fusion of full-length proteins shares also a possible drawback with antibody fusion. As in the case of antibodies, larger protein ligands might critically change the physicochemical properties by the additional protein mass. Moreover, antigen-fusion with a natural ligand that is biologically active might introduce unwanted side-effects. In this respect, enforced glycosylation could help to break down the problem to the smallest unit that is needed to bind the target receptor. In the case of the MR, this is only a glycan with no need for any proteinaceous component (see Figure 4.1). Gain in total molecular weight after the enforced glycosylation of the cargo protein will be way smaller in comparison to a fused antibody, as demonstrated in the case of  $\beta$ -gal and NST-GFP where glycosylation added only about 5 kDa (see Figure 4.11 E and Figure 4.18 A).

In any case, all targeting strategies have advantages and disadvantages and should be considered as alternatives for each other to find the optimal strategy for the intended target.

## 5.5 The role of high-mannose glycans as pathogen-associated molecular patterns and their immunostimulatory capacity

Recombinant proteins are often associated with safety concerns due to possible immunogenic side-effects related to their atypical glycosylation patterns [236]. In particular, fungal proteins have repeatedly been associated with immunogenicity due to their potential to target mannose-specific C-type lectin receptors of the immune system by their high-mannose glycans [112, 117, 118]. However, though less abundant, high-mannose glycans are also found on human cells [237, 238] and mannose residues are not limited to high-mannose glycans but remain also present in mammalian hybrid glycans (see Figure 2.5). Furthermore, mannose-specific C-type lectins such as the MR or Endo180 have been related to homeostasis [124, 218]. Accordingly, Gazi and Martinez-Pomares have proposed that mannose is no classical 'danger signal' [80], which in turn suggests that mannosylated proteins are not immunogenic per se. Our data support the thesis of Gazi and Martinez-Pomares, as they show that the *P. pastoris*-derived glycans on  $\beta$ -gal did not lead to BM-DC maturation (see Figure 4.16). Moreover, BM-DC pre-incubation with the glycoprotein had neither an influence on the MHC class II-restricted presentation of OVA, nor on the cross-presentation of OVA, nor on the MHC class I-restricted presentation of endogenous peptides (see Figure 4.17). These findings are perfectly in line with the work of Luong et al., who did not measure any IL-12 or TNF- $\alpha$  release by BM-DCs upon incubation with *P. pastoris*-derived OVA [165].

Interestingly, the comparison of the relationship between C-type lectins across humans and rodents revealed that lectins binding to endogenous ligands are more often conserved than lectins involved in pathogen recognition [61]. Drickamer and Taylor suggested that this could be explained from an evolutionary point of view, as each species encounters unique pathogens, and hence pressure is much higher on the diversification of pathogen recognition [61]. One example of such diversification is DC-SIGN with its 8 homolog SIGN proteins encoded by mice genomes mentioned above [205]. Conversely, the MR is highly conserved among both species, further supporting the idea that its basic role might rather be homeostasis, and pathogen recognition would require additional 'danger signals'. In line with this, the MR lacks any known signaling motif and seems to acquire signaling capacity only by the interaction with other signaling competent receptors [80].



This could also provide an explanation, why some studies report pro-inflammatory [78, 79] while others report anti-inflammatory responses upon MR ligation [77, 239].

As our experiments with MR-KO cells prove that the MR accounts for the main uptake of enforced glycosylated  $\beta$ -gal and NST-GFP, it is no longer surprising that these proteins do not influence DC-maturation. Instead, it seems likely that the discrepancies to reported stimulatory effects of yeast-derived proteins in other studies are due to the targeting of receptors other than the MR. Mincle and Dectin-2, for example, engage immuno-receptor tyrosine-based activation motif (ITAM)-containing molecules like the Fc receptor  $\gamma$ -chain (FcR $\gamma$ ) for inflammatory signaling [240, 241]. The targeting of such receptors could happen if the chosen proteins simply bear other glycan structures such as hypermannosylated N-glycans or O-glycosylation. Different glycosylation by *P. pastoris* might be a result of either expression conditions or intrinsic protein properties like potential glycosylation sites. For example, it was reported that hypermannosylation is favored by the sequon NNTT [242]. But also mild induction conditions were suggested to promote higher mannose amounts on the glycans, as the protein lasts longer in the secretory pathway, which in turn increases the probability of further mannosyltransferase activity [243]. Neither our model proteins nor our strong induction conditions with the AOX1 promoter meet these criteria for hypermannosylation.

Besides unintended targeting of other receptors, it is even conceivable that one and the same receptor is ligated in the different studies, but polyvalent or strong ligands such as hypermannosylated proteins might promote a different receptor response in comparison to the monovalent or weak ligands. Such a bimodal signaling triggered in the one or the other direction by strong or weak ligation has been demonstrated by Pasquier et al. for Fc $\alpha$ RI via the ITAM-containing FcR $\gamma$  [244].

In addition, it is possible that other signaling competent receptors may be activated by contaminations with yeast-derived PAMPs that were co-purified.  $\beta$ -glucans, for example, are main cell wall components of many yeasts [245], including *P. pastoris* [246, 247] and target Dectin-1 [248, 249], which initiates secretion of inflammatory cytokines *in vivo* [250]. Dectin-1 was also shown to trigger TNF- $\alpha$  release by BM-DCs *in vitro* upon  $\beta$ -glucan binding to a level similar to LPS treatment [251]. We could not measure TNF- $\alpha$  release after incubation with recombinant  $\beta$ -gal, suggesting no considerable  $\beta$ -glucan contamination in our purified protein (see Figure 4.16 A).

Of course, though BM-DCs possess a huge set of PRRs, we cannot exclude that another receptor that signals upon binding to *P. pastoris*-derived glycans is simply not expressed

by these cells. However, nearly all *in vivo* studies use adjuvants like Freund's complete adjuvant (FCA) [222] or aluminium hydroxide [223] to boost immunostimulatory effects of *P. pastoris*-derived vaccines, suggesting that the fungal glycans are not immunogenic enough to serve as their own adjuvant.

## 5.6 The influence of *Pichia pastoris*-derived N-glycans on the cellular and humoral response *in vivo*

Besides the potential to induce DC maturation, many C-type lectin receptors are known as endocytic receptors that engage in antigen uptake leading to MHC-restricted presentation [197, 252–254]. Accordingly, several *in vivo* studies report increased CD8<sup>+</sup> cytotoxic T cell and humoral responses when targeting C-type lectin receptors [53, 57, 221, 255–257] including mannose-specific lectins like DC-SIGN [258] or the MR [109, 259]. Due to their potential to target such receptors and the promising *in vitro* data on increased immunogenicity after glycosylation by *P. pastoris* [120] Ahlen et al. intentionally used *P. pastoris* to express a highly mannosylated carrier protein bearing excessive O-glycans to target C-type lectin receptors on DCs *in vivo* [121]. Additionally, several studies used *P. pastoris* to produce subunit vaccines that elicit neutralizing antibodies [222, 223] or both a humoral and a cellular response [116, 260]. However, none of these studies investigated the sole effect of *P. pastoris*-derived N-glycans and hence the contribution of N-glycans to improved cellular and humoral immune response *in vivo* remained elusive.

To answer this question, we directly compared purified glycosylated versus enzymatically deglycosylated proteins to circumvent the expression of the deglycosylated protein in bacteria, as previously described [120]. Since  $\beta$ -gal from *E. coli* strongly activated DCs (Figure 4.16), we chose the enzymatic approach to exclude interference of possible contaminants like LPS that would make it impossible to determine the effect of N-glycans separately.

After the immunization of mice with glycosylated  $\beta$ -gal, we observed a CD8<sup>+</sup> T cell response that was decreased after deglycosylation as visualized by both cytotoxicity and IFN- $\gamma$  secretion (Figure 4.18 C, D). Since  $\beta$ -gal did not show a strong DC activation *in vitro* irrespective of its glycosylation state (Figure 4.16 and Figure 4.17), this suggests that the increased antigen uptake of glycosylated  $\beta$ -gal by APCs leads to

an improved MHC I presentation *in vivo*. However, N-glycosylation had no beneficial effect on NST-GFP-S8L-related cytotoxicity (Figure 4.18 E), though both NST-GFP and  $\beta$ -gal showed a clear glycan and MR-dependent uptake by BM-DCs (Figure 4.7, Figure 4.8 and Figure 4.12). Instead, NST-GFP-S8L-related cytotoxicity was even significantly increased after deglycosylation, suggesting a negative influence of N-glycans on the cross-presentation of this particular protein. The reason for this discrepancy remains speculative. One explanation could be the presence of subtle O-glycosylations that were not detected by our MR-CTLD blots. The amount of such glycans could differ between both antigens and play only a decisive role as soon as the N-glycans are removed, for example by engagement of other C-type lectins that contribute to MR-independent binding or uptake *in vivo*.

In addition, differences in valency between  $\beta$ -gal and NST-GFP-S8L through different numbers in N-glycans, O-glycans or both may lead to receptor-cross linking by one or the other protein. Cross-linking can alter the trafficking of one and the same receptor towards either recycling endosomes or lysosomes, as has been shown for Dectin-1 [261], thereby favoring different presentation pathways. As receptor cross-linking is associated with lysosomal targeting [262], this would imply that either  $\beta$ -gal is only cross-linked after the removal of its N-glycans, which seems rather unlikely, or that the single N-glycan in NST-GFP-S8L participates in cross-linking together with undetected O-glycans, which is abrogated upon the removal of that N-glycan.

When we investigated the humoral response against the recombinant proteins, we surprisingly observed a significantly higher response after the immunization with deglycosylated proteins in both cases (Figure 4.19). In particular, in the case of  $\beta$ -gal, there was hardly any response measurable for the N-glycosylated protein at all. This suggests that N-glycosylation has no beneficial influence on a humoral response in either case. There are several possible explanations that might solely or in combination account for this result. First, B-cells might get negatively selected if they express a BCR against certain high-mannose N-glycans that also occur naturally in the bone marrow [237], as BCR affinity against such glycans would cause auto-immunity. In accordance with this, antibodies generated by vaccination with glycosylated NST-GFP-S8L recognized their cognate antigens mainly independent of N-glycosylation (Figure 4.19 B). Second, it has been shown that glycosylation is able to decrease protein susceptibility to proteolytic degradation [263–265]. Such an inhibition could prevent efficient processing of N-glycosylated antigens by lysosomal proteases, which would result in less MHC II-

restricted presentation and hence a decreased humoral response. Third, OVA that is internalized by the MR is predominantly processed for cross-presentation [51]. Uptake by receptors like the MR could decrease the pool of pinocytosable antigens by capturing glycosylated antigens and delivering them towards early endosomal compartments related to cross-presentation. Lastly, it was shown that glycans within MHC II epitopes can either prevent the binding of such epitopes to the MHC molecule or the recognition of the MHC-peptide complex by the TCR [160].  $\beta$ -gal with its 4 putative glycosylation sites would be particularly susceptible to such an effect.

Of course, N-glycans could also block proteolytic processing, MHC I-binding or TCR recognition during cross-presentation. Indeed, we found that the asparagine within the MHC I-restricted  $\beta$ -gal epitope  $\beta$ -gal<sub>96-103</sub> (DAPIYTNV) is likely to be N-glycosylated and that the unglycosylated DAPIYTNV peptide is not recognized by CD8<sup>+</sup> cytotoxic T cells after immunization with *P. pastoris*-derived  $\beta$ -gal (Figure 4.20). Importantly, such blocking of MHC-restricted epitopes is not unique to enforced N-glycosylation, but could potentially happen in any targeting strategy that uses covalent linkage of carrier-molecules like antibodies, aptamers or glycans to the antigens, which is frequently done by chemical cross-linking [59, 221, 233].

Two other critical points that will have impact on the overall immune response to *P. pastoris*-derived N-glycosylated proteins are the choice of the adjuvant and the route of vaccine delivery. As shown above, *P. pastoris*-derived glycans did not induce DC maturation. Since DC maturation is a prerequisite for MR-dependent cross-presentation of OVA [52], we used LPS as an adjuvant *in vivo*. Similarly, other groups used FCA [222] or aluminium hydroxide [223] to boost immunogenicity *in vivo*. However, the choice of the adjuvant formulation might strongly bias the immune response. Accordingly, adjuvants targeting endosomal TLRs that are associated with the recognition of intracellular pathogens (e.g. TLR3, TLR7/8 or TLR9) have been shown to act as strong activators of CD8<sup>+</sup> cytotoxic T cell responses [266] and might be better suited in combination with MR-targeted vaccines.

The influence of the application route on the success of a vaccine might be explained mainly by the presence of different DC subsets with differing receptor profiles [267]. In comparison to intraperitoneal (i.p.) or intravenous (i.v.) virus administration, intradermal (i.d.) and subcutaneous (s.c.) delivery were shown to predominantly induce cytotoxic T-cell responses via cross-presentation, which suggests that DCs within these tissues are suitable targets for vaccines aiming to induce cross-presentation [268]. How-

ever, the cross-presentation of mannosylated synthetic long peptides (SLPs) proved to be even more efficient after i.d. administration in comparison to s.c. [269], most likely due to the different expression of the MR within these tissues [270]. Finally, the i.v. injection of mannosylated proteins is not advisable due to clearance by liver sinusoidal endothelial cells (LSECs) that also express the MR [87, 271].

## 5.7 Outlook and concluding remarks

We could demonstrate that *P. pastoris* is a valuable expression system to tag unglycosylated proteins with glycans that are recognized by the C-type lectin part of the MR. Like MR-internalized OVA, such modified proteins were readily delivered to early endosomal compartments within BM-DCs that are associated with cross-presentation. As *P. pastoris*-derived high-mannose glycans bear the potential to target C-type lectin receptors of the immune system, they are commonly considered immunostimulatory. However, we could not observe that N-glycans in particular do expose any immunostimulatory capacity per se. In addition, we showed that beneficial effects on the induction of a cytotoxic CD8<sup>+</sup> T cell response depend on the nature of the antigen and the epitope chosen for MHC I-restricted presentation. This suggests that the influence of N-glycans on cytotoxicity is hardly predictable and that each antigen subjected to enforced N-glycosylation will have to be evaluated individually by experimentation. Beside the use of its glycans to target C-type lectins and improve cytotoxicity, *P. pastoris* is generally considered to be a potent expression system to generate high amounts of recombinant subunit vaccines. Our data on humoral responses, however, suggest negative effects of N-glycosylation on antibody production and strongly argue against the use of N-glycosylated proteins expressed in *P. pastoris* for such purposes. Together, these findings have major implications on the use of *P. pastoris* as an expression system for recombinant subunit vaccines.

Beyond antigen presentation, endo- and phagocytosis by MR-family C-type lectin receptors also play a role in diverse other disease-related processes, including the entry of intracellular pathogens like mycobacteria [272, 273], cancer progression [219], or lysosomal storage diseases [274]. In this respect, our presented enforced N-glycosylation strategy with *P. pastoris* might even be exploited in addition to classical therapies to block pathogen entrance, to prevent matrix turnover, or to restore lysosomal enzymes.

## 6 References

- [1] A. P. Dobson and E. R. Carper. “Infectious Diseases and Human Population History”. *BioScience* **46** (1996), pp. 115–126.
- [2] C. Mathers et al. *The global burden of disease: 2004 update*. Geneva, Switzerland: World Health Organization., 2008.
- [3] R. Rappuoli et al. “Vaccines, new opportunities for a new society”. *Proc. Natl. Acad. Sci. U.S.A.* **111** (2014), pp. 12288–12293.
- [4] G. L. Armstrong. “Trends in Infectious Disease Mortality in the United States During the 20th Century”. *JAMA* **281** (1999), pp. 61–66.
- [5] S. W. Roush. “Historical Comparisons of Morbidity and Mortality for Vaccine-Preventable Diseases in the United States”. *JAMA* **298** (2007), pp. 2155–2163.
- [6] E. Jenner. *An Inquiry into the Causes and Effects of Variolae Vaccinae, a Disease Discovered in Some Western Counties of England*. London: Sampson Low, 1798.
- [7] S. Plotkin. “History of vaccination”. *Proc. Natl. Acad. Sci. U.S.A.* **111** (2014), pp. 12283–12287.
- [8] T. A. Röhn and M. F. Bachmann. “Vaccines against non-communicable diseases”. *Curr. Opin. Immunol.* **22** (2010), pp. 391–396.
- [9] M. F. Bachmann and G. T. Jennings. “Therapeutic vaccines for chronic diseases: successes and technical challenges”. *Philos. T. Roy. Soc. B.* **366** (2011), pp. 2815–2822.
- [10] L. H. Butterfield. “Cancer vaccines”. *BMJ* **350** (2015), h988–h988.
- [11] R. Rappuoli et al. “Vaccines for the twenty-first century society.” *Nat. Rev. Immunol.* **11** (2011), pp. 865–72.
- [12] S. Sadanand. “Vaccination: The Present and the Future.” *The Yale Journal of Biology and Medicine.* **84** (2011), pp. 353–359.
- [13] J. Berzofsky, J. Ahlers, and I. Belyakov. “Strategies for designing and optimizing new generation vaccines.” *Nat. Rev. Immunol.* **1** (2001), pp. 209–19.
- [14] J. Parkin and B. Cohen. “An overview of the immune system”. *The Lancet* **357** (2001), pp. 1777–1789.
- [15] S. Akira, S. Uematsu, and O. Takeuchi. “Pathogen Recognition and Innate Immunity”. *Cell* **124** (2006), pp. 783–801.
- [16] J. M. González-Navajas, M. P. Corr, and E. Raz. “The immediate protective response to microbial challenge”. *Eur. J. Immunol.* **44** (2014), pp. 2536–2549.

- [17] M. D. Cooper. “The early history of B cells”. *Nat. Rev. Immunol.* **15** (2015), pp. 191–197.
- [18] S. L. Nutt et al. “The generation of antibody-secreting plasma cells”. *Nat. Rev. Immunol.* **15** (2015), pp. 160–171.
- [19] D. L. Woodland and R. W. Dutton. “Heterogeneity of CD4+ and CD8+ T cells”. *Curr. Opin. Immunol.* **15** (2003), pp. 336–342.
- [20] M. Barry and R. Bleackley. “Cytotoxic T lymphocytes: all roads lead to death.” *Nat. Rev. Immunol.* **2** (2002), pp. 401–9.
- [21] D. L. Farber, N. A. Yudanin, and N. P. Restifo. “Human memory T cells: generation, compartmentalization and homeostasis”. *Nat. Rev. Immunol.* **14** (2013), pp. 24–35.
- [22] N. Schmitt and H. Ueno. “Regulation of human helper T cell subset differentiation by cytokines”. *Curr. Opin. Immunol.* **34** (2015), pp. 130–136.
- [23] S. Crotty. “A brief history of T cell help to B cells”. *Nat. Rev. Immunol.* **15** (2015), pp. 185–189.
- [24] J. D. Siliciano and R. Siliciano. “A long-term latent reservoir for HIV-1: discovery and clinical implications”. *J. Antimicrob. Chemother.* **54** (2004), pp. 6–9.
- [25] H.-C. Yang and J.-H. Kao. “Persistence of hepatitis B virus covalently closed circular DNA in hepatocytes: molecular mechanisms and clinical significance”. *Emerg Microbes Infect* **3** (2014), e64.
- [26] J. Banchereau and R. M. Steinman. “Dendritic cells and the control of immunity”. *Nature* **392** (1998), pp. 245–252.
- [27] H. Wan and M. Dupasquier. “Dendritic cells in vivo and in vitro.” *Cell. Mol. Immunol.* **2** (2005), pp. 28–35.
- [28] R. Medzhitov. “Recognition of microorganisms and activation of the immune response”. *Nature* **449** (2007), pp. 819–826.
- [29] C. Maisonneuve et al. “Unleashing the potential of NOD- and Toll-like agonists as vaccine adjuvants”. *Proc. Natl. Acad. Sci. U.S.A.* **111** (2014), pp. 12294–12299.
- [30] L. A. J. O’Neill, C. E. Bryant, and S. L. Doyle. “Therapeutic Targeting of Toll-Like Receptors for Infectious and Inflammatory Diseases and Cancer”. *Pharmacol. Rev.* **61** (2009), pp. 177–197.
- [31] R. Medzhitov, P. Preston-Hurlburt, and C. J. Jr. “A human homologue of the Drosophila Toll protein signals activation of adaptive immunity.” *Nature* **388** (1997), pp. 394–7.
- [32] M. S. Trent et al. “Diversity of endotoxin and its impact on pathogenesis”. *J. Endotoxin Res.* **12** (2006), pp. 205–223.
- [33] S. Tsuji et al. “Maturation of Human Dendritic Cells by Cell Wall Skeleton of Mycobacterium bovis Bacillus Calmette-Guerin: Involvement of Toll-Like Receptors”. *Infect. Immun.* **68** (2000), pp. 6883–6890.
- [34] C. D. Trez et al. “TLR4 and Toll-IL-1 Receptor Domain-Containing Adapter-Inducing IFN- $\beta$ , but Not MyD88, Regulate Escherichia coli-Induced Dendritic Cell Maturation and Apoptosis In Vivo”. *The Journal of Immunology* **175** (2005), pp. 839–846.

- [35] N. Bertho et al. “Efficient migration of dendritic cells toward lymph node chemokines and induction of TH1 responses require maturation stimulus and apoptotic cell interaction”. *Blood* **106** (2005), pp. 1734–1741.
- [36] S. Gröbner et al. “Lipopolysaccharide induces cell volume increase and migration of dendritic cells”. *Microbiol. Immunol.* **58** (2014), pp. 61–67.
- [37] J. Villadangos, P. Schnorrer, and N. Wilson. “Control of MHC class II antigen presentation in dendritic cells: a balance between creative and destructive forces.” *Immunol. Rev.* **207** (2005), pp. 191–205.
- [38] M. L. Toribio et al. “Interleukin-2-dependent autocrine proliferation in T-cell development”. *Nature* **342** (1989), pp. 82–85.
- [39] L. M. Sedger and M. F. McDermott. “TNF and TNF-receptors: From mediators of cell death and inflammation to therapeutic giants - past, present and future”. *Cytokine & Growth Factor Reviews* **25** (2014), pp. 453–472.
- [40] F. Schaper and S. Rose-John. “Interleukin-6: Biology, signaling and strategies of blockade”. *Cytokine & Growth Factor Reviews* **26** (2015), pp. 475–487.
- [41] G. Trinchieri. “Interleukin-12 and the regulation of innate resistance and adaptive immunity”. *Nat. Rev. Immunol.* **3** (2003), pp. 133–146.
- [42] K. J. L. Jackson et al. “The Shape of the Lymphocyte Receptor Repertoire: Lessons from the B Cell Receptor”. *Front Immunol* **4** (2013).
- [43] A. M. Avalos and H. L. Ploegh. “Early BCR Events and Antigen Capture, Processing, and Loading on MHC Class II on B Cells”. *Front Immunol* **5** (2014).
- [44] H. N. Eisen. “Affinity Enhancement of Antibodies: How Low-Affinity Antibodies Produced Early in Immune Responses Are Followed by High-Affinity Antibodies Later and in Memory B-Cell Responses”. *Cancer Immunology Research* **2** (2014), pp. 381–392.
- [45] F. D. Batista and N. E. Harwood. “The who, how and where of antigen presentation to B cells”. *Nat. Rev. Immunol.* **9** (2009), pp. 15–27.
- [46] K. Zhang. “Accessibility control and machinery of immunoglobulin class switch recombination”. *J. Leukocyte Biol.* **73** (2003), pp. 323–332.
- [47] E. Harlow and D. Lane. *Antibodies: A Laboratory Manual*. Cold Spring Harbor Laboratory, 1988.
- [48] S. Hulpke and R. Tampé. “The MHC I loading complex: a multitasking machinery in adaptive immunity”. *Trends Biochem. Sci.* **38** (2013), pp. 412–420.
- [49] O. P. Joffre et al. “Cross-presentation by dendritic cells”. *Nat. Rev. Immunol.* **12** (2012), pp. 557–569.
- [50] C. Kreer et al. “Cross-presentation: how to get there - or how to get the ER”. *Front Immunol* **2** (2012).
- [51] S. Burgdorf et al. “Distinct pathways of antigen uptake and intracellular routing in CD4 and CD8 T cell activation.” *Science* **316** (2007), pp. 612–6.
- [52] S. Burgdorf and C. Kurts. “Endocytosis mechanisms and the cell biology of antigen presentation.” *Curr. Opin. Immunol.* **20** (2008), pp. 89–95.



- [53] L. Bonifaz et al. "Efficient targeting of protein antigen to the dendritic cell receptor DEC-205 in the steady state leads to antigen presentation on major histocompatibility complex class I products and peripheral CD8+ T cell tolerance." *J. Exp. Med.* **196** (2002), pp. 1627–38.
- [54] A. Moris et al. "DC-SIGN promotes exogenous MHC-I-restricted HIV-1 antigen presentation." *Blood* **103** (2004), pp. 2648–54.
- [55] R. W. Carter et al. "Induction of CD8+ T cell responses through targeting of antigen to Dectin-2". *Cell. Immunol.* **239** (2006), pp. 87–91.
- [56] L. Bozzacco et al. "DEC-205 receptor on dendritic cells mediates presentation of HIV gag protein to CD8+ T cells in a spectrum of human MHC I haplotypes". *Proc. Natl. Acad. Sci. U.S.A.* **104** (2007), pp. 1289–1294.
- [57] D. Sancho et al. "Tumor therapy in mice via antigen targeting to a novel, DC-restricted C-type lectin". *J. Clin. Invest.* **118** (2008), pp. 2098–2110.
- [58] J. Idoyaga et al. "Cutting Edge: Langerin/CD207 Receptor on Dendritic Cells Mediates Efficient Antigen Presentation on MHC I and II Products In Vivo". *The Journal of Immunology* **180** (2008), pp. 3647–3650.
- [59] S. Singh et al. "Targeting glycan modified OVA to murine DC-SIGN transgenic dendritic cells enhances MHC class I and II presentation." *Mol. Immunol.* **47** (2009), pp. 164–74.
- [60] E. Klechevsky et al. "Cross-priming CD+ T cells by targeting antigens to human dendritic cells through DCIR". *Blood* **116** (2010), pp. 1685–1697.
- [61] K. Drickamer and M. E. Taylor. "Recent insights into structures and functions of C-type lectins in the immune system". *Curr. Opin. Struct. Biol.* **34** (2015), pp. 26–34.
- [62] W. Weis, K. Drickamer, and W. Hendrickson. "Structure of a C-type mannose-binding protein complexed with an oligosaccharide." *Nature* **360** (1992), pp. 127–34.
- [63] K. Drickamer. "C-type lectin-like domains". *Curr. Opin. Struct. Biol.* **9** (1999), pp. 585–590.
- [64] Y. Liu et al. "Preparation of high-activity whole cell biocatalysts by permeabilization of recombinant yeasts with alcohol." *Journal of bioscience and bioengineering* **89** (2000), pp. 554–8.
- [65] C. Leteux et al. "The Cysteine-Rich Domain of the Macrophage Mannose Receptor Is a Multispecific Lectin That Recognizes Chondroitin Sulfates a and B and Sulfated Oligosaccharides of Blood Group Lewis<sub>a</sub> and Lewis<sub>x</sub> Types in Addition to the Sulfated N-Glycans of Lutropin". *J. Exp. Med.* **191** (2000), pp. 1117–1126.
- [66] L. Martinez-Pomares et al. "Carbohydrate-independent recognition of collagens by the macrophage mannose receptor." *Eur. J. Immunol.* **36** (2006), pp. 1074–82.
- [67] C. E. Napper, K. Drickamer, and M. E. Taylor. "Collagen binding by the mannose receptor mediated through the fibronectin type II domain". *Biochem. J.* **395** (2006), pp. 579–586.
- [68] M. Taylor, K. Bezouska, and K. Drickamer. "Contribution to ligand binding by multiple carbohydrate-recognition domains in the macrophage mannose receptor." *J. Biol. Chem.* **267** (1992), pp. 1719–26.

- [69] M. Taylor and K. Drickamer. "Structural requirements for high affinity binding of complex ligands by the macrophage mannose receptor." *J. Biol. Chem.* **268** (1993), pp. 399–404.
- [70] V. Kéry et al. "Ligand recognition by purified human mannose receptor". *Arch. Biochem. Biophys.* **298** (1992), pp. 49–55.
- [71] S. Munro. "What can yeast tell us about N-linked glycosylation in the Golgi apparatus?" *FEBS Lett.* **498** (2001), pp. 223–7.
- [72] D. Harvey et al. "Composition of N-linked carbohydrates from ovalbumin and co-purified glycoproteins." *J. Am. Soc. Mass Spectrom.* **11** (2000), pp. 564–71.
- [73] P. Stahl et al. "Receptor-mediated pinocytosis of mannose glycoconjugates by macrophages: characterization and evidence for receptor recycling." *Cell* **19** (1980), pp. 207–15.
- [74] C. Tietze, P. Schlesinger, and P. Stahl. "Mannose-specific endocytosis receptor of alveolar macrophages: demonstration of two functionally distinct intracellular pools of receptor and their roles in receptor recycling." *J. Cell Biol.* **92** (1982), pp. 417–24.
- [75] T. Wileman et al. "Monensin inhibits recycling of macrophage mannose-glycoprotein receptors and ligand delivery to lysosomes." *Biochem. J.* **220** (1984), pp. 665–75.
- [76] A. Schweizer, P. D. Stahl, and J. Rohrer. "A Di-aromatic Motif in the Cytosolic Tail of the Mannose Receptor Mediates Endosomal Sorting". *J. Biol. Chem.* **275** (2000), pp. 29694–29700.
- [77] M. Chieppa et al. "Cross-linking of the mannose receptor on monocyte-derived dendritic cells activates an anti-inflammatory immunosuppressive program." *J. Immunol.* **171** (2003), pp. 4552–60.
- [78] Y. Shibata, W. Metzger, and Q. Myrvik. "Chitin particle-induced cell-mediated immunity is inhibited by soluble mannan: mannose receptor-mediated phagocytosis initiates IL-12 production." *J. Immunol.* **159** (1997), pp. 2462–7.
- [79] Y. Yamamoto, T. Klein, and H. Friedman. "Involvement of mannose receptor in cytokine interleukin-1beta (IL-1beta), IL-6, and granulocyte-macrophage colony-stimulating factor responses, but not in chemokine macrophage inflammatory protein 1beta (MIP-1beta), MIP-2, and KC responses, caused by attachment of *Candida albicans* to macrophages." *Infect. Immun.* **65** (1997), pp. 1077–82.
- [80] U. Gazi and L. Martinez-Pomares. "Influence of the mannose receptor in host immune responses." *Immunobiology* **214** (2009), pp. 554–61.
- [81] C. G. Figdor, Y. van Kooyk, and G. J. Adema. "C-type lectin receptors on dendritic cells and Langerhans cells." *Nat. Rev. Immunol.* **2** (2002), pp. 77–84.
- [82] E. McKenzie et al. "Mannose receptor expression and function define a new population of murine dendritic cells." *J. Immunol.* **178** (2007), pp. 4975–83.
- [83] T Mokoena and S Gordon. "Human macrophage activation. Modulation of mannosyl, fucosyl receptor activity in vitro by lymphokines, gamma and alpha interferons, and dexamethasone." *J. Clin. Invest.* **75** (1985), pp. 624–631.

- [84] M. Stein et al. "Interleukin 4 potently enhances murine macrophage mannose receptor activity: a marker of alternative immunologic macrophage activation". *J. Exp. Med.* **176** (1992), pp. 287–292.
- [85] M. Kato et al. "Expression of multilectin receptors and comparative FITC-dextran uptake by human dendritic cells". *Int. Immunol.* **12** (2000), pp. 1511–1519.
- [86] D. H. Madsen et al. "The Non-phagocytic Route of Collagen Uptake". *J. Biol. Chem.* **286** (2011), pp. 26996–27010.
- [87] I. Malovic et al. "The mannose receptor on murine liver sinusoidal endothelial cells is the main denatured collagen clearance receptor". *Hepatology* **45** (2007), pp. 1454–1461.
- [88] S. Lee et al. "Mannose receptor-mediated regulation of serum glycoprotein homeostasis." *Science* **295** (2002), pp. 1898–901.
- [89] F. Marttila-Ichihara et al. "Macrophage mannose receptor on lymphatics controls cell trafficking." *Blood* **112** (2008), pp. 64–72.
- [90] K. W. Moremen, M. Tiemeyer, and A. V. Nairn. "Vertebrate protein glycosylation: diversity, synthesis and function". *Nat. Rev. Mol. Cell Biol.* **13** (2012), pp. 448–462.
- [91] M. Aebi. "N-linked protein glycosylation in the ER." *Biochim. Biophys. Acta* **1833** (2013), pp. 2430–7.
- [92] P. Stanley. "Golgi Glycosylation". *Cold Spring Harbor Perspect. Biol.* **3** (2011), a005199–a005199.
- [93] P. Van den Steen et al. "Concepts and Principles of O-Linked Glycosylation". *Crit. Rev. Biochem. Mol. Biol.* **33** (1998), pp. 151–208.
- [94] A. Varki. "Biological roles of oligosaccharides: all of the theories are correct". *Glycobiology* **3** (1993), pp. 97–130.
- [95] A. Cambi and C. Figdor. "Levels of complexity in pathogen recognition by C-type lectins." *Curr. Opin. Immunol.* **17** (2005), pp. 345–51.
- [96] A. P. Corfield and M. Berry. "Glycan variation and evolution in the eukaryotes". *Trends Biochem. Sci.* **40** (2015), pp. 351–359.
- [97] R. Bretthauer and F. Castellino. "Glycosylation of *Pichia pastoris*-derived proteins." *Biotechnol. Appl. Biochem.* **30** (1999), pp. 193–200.
- [98] D. Bosch et al. "N-Glycosylation of Plant-produced Recombinant Proteins". *Curr. Pharm. Des.* **19** (2013), pp. 5503–5512.
- [99] D. R. Branch. "Anti-A and anti-B: what are they and where do they come from?" *Transfusion (Paris)* **55** (2015), S74–S79.
- [100] E. C. Gotschlich, T. Liu, and M. Artenstein. "Human immunity to the meningococcus. 3. Preparation and immunochemical properties of the group A, group B, and group C meningococcal polysaccharides." *J. Exp. Med.* **129** (1969), pp. 1349–1365.
- [101] E. C. Gotschlich. "HUMAN IMMUNITY TO THE MENINGOCOCCUS: IV. IMMUNOGENICITY OF GROUP A AND GROUP C MENINGOCOCCAL POLYSACCHARIDES IN HUMAN VOLUNTEERS". *J. Exp. Med.* **129** (1969), pp. 1367–1384.

- [102] A. B. Sabin. “STUDIES ON VARIANTS OF POLIOMYELITIS VIRUS: I. EXPERIMENTAL SEGREGATION AND PROPERTIES OF AVIRULENT VARIANTS OF THREE IMMUNOLOGIC TYPES”. *J. Exp. Med.* **99** (1954), pp. 551–576.
- [103] M. R. Hilleman et al. “Live, Attenuated Mumps-Virus Vaccine”. *N. Engl. J. Med.* **278** (1968), pp. 227–232.
- [104] D. Salmon and T. Smith. “One method of producing immunity from contagious diseases”. *Am. J. Vet. Rev.* **10** (1886), 63–9.
- [105] S. Liljeqvist and S. Ståhl. “Production of recombinant subunit vaccines: protein immunogens, live delivery systems and nucleic acid vaccines”. *J. Biotechnol.* **73** (1999), pp. 1–33.
- [106] R. L. Coffman, A. Sher, and R. A. Seder. “Vaccine Adjuvants: Putting Innate Immunity to Work”. *Immunity* **33** (2010), pp. 492–503.
- [107] S. A. Plotkin. “Vaccines: past, present and future”. *Nat. Med.* **10** (2005), S5–S11.
- [108] R. M. Bill. “Recombinant protein subunit vaccine synthesis in microbes: a role for yeast?” *J. Pharm. Pharmacol.* **67** (2014), pp. 319–328.
- [109] L. He et al. “Antigenic targeting of the human mannose receptor induces tumor immunity.” *J. Immunol.* **178** (2007), pp. 6259–67.
- [110] S. L. Lambert et al. “A Novel Respiratory Syncytial Virus (RSV) F Subunit Vaccine Adjuvanted with GLA-SE Elicits Robust Protective TH1-Type Humoral and Cellular Immunity In Rodent Models”. *PLoS ONE* **10** (2015). Ed. by S. M. Varga, e0119509.
- [111] J. M. Cregg et al. “*Pichia pastoris* as a host system for transformations.” *Mol. Cell. Biol.* **5** (1985), pp. 3376–3385.
- [112] J. Cregg et al. “Recombinant protein expression in *Pichia pastoris*.” *Mol. Biotechnol.* **16** (2000), pp. 23–52.
- [113] M. W. T. Werten et al. “High-yield secretion of recombinant gelatins by *Pichia pastoris*”. *Yeast* **15** (1999), pp. 1087–1096.
- [114] O. Farnós et al. “The recombinant rabbit hemorrhagic disease virus VP60 protein obtained from *Pichia pastoris* induces a strong humoral and cell-mediated immune response following intranasal immunization in mice.” *Vet. Microbiol.* **114** (2006), pp. 187–95.
- [115] C. Su et al. “Heterologous expression of FMDV immunodominant epitopes and HSP70 in *P. pastoris* and the subsequent immune response in mice.” *Vet. Microbiol.* **124** (2007), pp. 256–63.
- [116] M. Wang, S. Jiang, and Y. Wang. “Recombinant VP1 protein expressed in *Pichia pastoris* induces protective immune responses against EV71 in mice.” *Biochem. Biophys. Res. Commun.* **430** (2013), pp. 387–93.
- [117] R. Daly and M. Hearn. “Expression of heterologous proteins in *Pichia pastoris*: a useful experimental tool in protein engineering and production”. *J. Mol. Recognit.* **18** (2005), pp. 119–38.

- [118] M. Bollok et al. “Recent Patents on the *Pichia Pastoris* Expression System: Expanding the Toolbox for Recombinant Protein Production”. *Recent Pat Biotechnol* **3** (2009,), pp. 192–201.
- [119] S. R. Hamilton and T. U. Gerngross. “Glycosylation engineering in yeast: the advent of fully humanized yeast”. *Curr. Opin. Biotechnol.* **18** (2007), pp. 387–392.
- [120] J. Lam et al. “A model vaccine exploiting fungal mannosylation to increase antigen immunogenicity.” *J. Immunol.* **175** (2005), pp. 7496–503.
- [121] G. Ahlén et al. “Mannosylated mucin-type immunoglobulin fusion proteins enhance antigen-specific antibody and T lymphocyte responses.” *PLoS ONE* **7** (2012), e46959.
- [122] J. Lam, H. Huang, and S. Levitz. “Effect of differential N-linked and O-linked mannosylation on recognition of fungal antigens by dendritic cells.” *PLoS ONE* **2** (2007), e1009.
- [123] J. Gustafsson et al. “*Pichia pastoris*-produced mucin-type fusion proteins with multivalent O-glycan substitution as targeting molecules for mannose-specific receptors of the immune system.” *Glycobiology* **21** (2011), pp. 1071–86.
- [124] P. Taylor, S. Gordon, and L. Martinez-Pomares. “The mannose receptor: linking homeostasis and immunity through sugar recognition.” *Trends Immunol.* **26** (2005), pp. 104–10.
- [125] M. Zehner et al. “Intraendosomal flow cytometry: A novel approach to analyze the protein composition of antigen-loaded endosomes”. *Eur. J. Immunol.* **42** (2012), pp. 2187–2190.
- [126] G. Schönrich et al. “Down-regulation of T cell receptors on self-reactive T cells as a novel mechanism for extrathymic tolerance induction.” *Cell* **65** (1991), pp. 293–304.
- [127] K. Hogquist et al. “T cell receptor antagonist peptides induce positive selection.” *Cell* **76** (1994), pp. 17–27.
- [128] S. R. Clarke et al. “Characterization of the ovalbumin-specific TCR transgenic line OT-I: MHC elements for positive and negative selection”. *Immunol. Cell Biol.* **78** (2000), pp. 110–117.
- [129] M. J. Barnden et al. “Defective TCR expression in transgenic mice constructed using cDNA-based alpha- and beta-chain genes under the control of heterologous regulatory elements”. *Immunol. Cell Biol.* **76** (1998), pp. 34–40.
- [130] D. Hanahan. “Studies on transformation of *Escherichia coli* with plasmids.” *J. Mol. Biol.* **166** (1983), pp. 557–80.
- [131] K. Inaba et al. “Generation of large numbers of dendritic cells from mouse bone marrow cultures supplemented with granulocyte/macrophage colony-stimulating factor”. *J. Exp. Med.* **176** (1992), pp. 1693–1702.
- [132] M. Lutz et al. “An advanced culture method for generating large quantities of highly pure dendritic cells from mouse bone marrow.” *J. Immunol. Methods* **223** (1999), pp. 77–92.
- [133] J. Xue et al. “Transcriptome-Based Network Analysis Reveals a Spectrum Model of Human Macrophage Activation”. *Immunity* **40** (2014), pp. 274–288.

- [134] J. M. Cregg et al. *Chapter 13 Expression in the Yeast Pichia pastoris*. Elsevier BV, 2009, pp. 169–189.
- [135] E. Gasteiger et al. “ExPASy: the proteomics server for in-depth protein knowledge and analysis”. *Nucleic Acids Res.* **31** (2003), pp. 3784–3788.
- [136] U. K. Laemmli. “Cleavage of Structural Proteins during the Assembly of the Head of Bacteriophage T4”. *Nature* **227** (1970), pp. 680–685.
- [137] M. Roederer. “Interpretation of cellular proliferation data: avoid the panglossian.” *Cytometry A* **79** (2011), pp. 95–101.
- [138] T. Schwandt et al. “Expression of type I interferon by splenic macrophages suppresses adaptive immunity during sepsis”. *The EMBO Journal* **31** (2011), pp. 201–213.
- [139] S. Burgdorf, V. Lukacs-Kornek, and C. Kurts. “The mannose receptor mediates uptake of soluble but not of cell-associated antigen for cross-presentation.” *J. Immunol.* **176** (2006), pp. 6770–6.
- [140] T. Hilmenyuk et al. “Effects of glycation of the model food allergen ovalbumin on antigen uptake and presentation by human dendritic cells.” *Immunology* **129** (2010), pp. 437–45.
- [141] N. Mullin, K. Hall, and M. Taylor. “Characterization of ligand binding to a carbohydrate-recognition domain of the macrophage mannose receptor.” *J. Biol. Chem.* **269** (1994), pp. 28405–13.
- [142] D. Juers et al. “A structural view of the action of Escherichia coli (lacZ) beta-galactosidase.” *Biochemistry* **40** (2001), pp. 14781–94.
- [143] Y. Gavel and G. von Heijne. “Sequence differences between glycosylated and non-glycosylated Asn-X-Thr/Ser acceptor sites: implications for protein engineering.” *Protein Eng.* **3** (1990), pp. 433–42.
- [144] S. Ben-Dor et al. “Biases and complex patterns in the residues flanking protein N-glycosylation sites.” *Glycobiology* **14** (2004), pp. 95–101.
- [145] S. Shakin-Eshleman, S. Spitalnik, and L. Kasturi. “The amino acid at the X position of an Asn-X-Ser sequon is an important determinant of N-linked core-glycosylation efficiency.” *J. Biol. Chem.* **271** (1996), pp. 6363–6.
- [146] J. Mellquist et al. “The amino acid following an asn-X-Ser/Thr sequon is an important determinant of N-linked core glycosylation efficiency.” *Biochemistry* **37** (1998), pp. 6833–7.
- [147] O. Shimomura, F. Johnson, and Y. Saiga. “Extraction, purification and properties of aequorin, a bioluminescent protein from the luminous hydromedusan, Aequorea.” *J Cell Comp Physiol* **59** (1962), pp. 223–39.
- [148] D. Prasher et al. “Primary structure of the Aequorea victoria green-fluorescent protein.” *Gene* **111** (1992), pp. 229–33.
- [149] R. Heim, A. Cubitt, and R. Tsien. “Improved green fluorescence.” *Nature* **373** (1995), pp. 663–4.
- [150] S. Routledge et al. “Antifoam addition to shake flask cultures of recombinant Pichia pastoris increases yield.” *Microb Cell Fact.* **10** (2011).

- [151] F. Yang, L. Moss, and G. Phillips. “The molecular structure of green fluorescent protein.” *Nat. Biotechnol.* **14** (1996), pp. 1246–51.
- [152] E. Böhm et al. “Differences in N-glycosylation of recombinant human coagulation factor VII derived from BHK, CHO, and HEK293 cells.” *BMC Biotechnol.* **15** (2015), p. 87.
- [153] J. Llopis et al. “Measurement of cytosolic, mitochondrial, and Golgi pH in single living cells with green fluorescent proteins.” *Proc. Natl. Acad. Sci. U.S.A.* **95** (1998), pp. 6803–8.
- [154] S. Gringhuis et al. “Carbohydrate-specific signaling through the DC-SIGN signalosome tailors immunity to Mycobacterium tuberculosis, HIV-1 and Helicobacter pylori.” *Nat. Immunol.* **10** (2009), pp. 1081–8.
- [155] P. Hernanz-Falcón et al. “Internalization of Dectin-1 terminates induction of inflammatory responses.” *Eur. J. Immunol.* **39** (2009), pp. 507–13.
- [156] F. Albert et al. “Interactions between MHC-encoded products and cloned T-cells. I. Fine specificity of induction of proliferation and lysis.” *Immunogenetics* **16** (1982), pp. 533–49.
- [157] A. Guimezanes et al. “Identification of endogenous peptides recognized by in vivo or in vitro generated alloreactive cytotoxic T lymphocytes: distinct characteristics correlated with CD8 dependence”. *Eur. J. Immunol.* **31** (2001), pp. 421–432.
- [158] B. J. McFarland et al. “Energetics and Cooperativity of the Hydrogen Bonding and Anchor Interactions that Bind Peptides to MHC Class II Protein”. *J. Mol. Biol.* **350** (2005), pp. 170–183.
- [159] E. T. Abualrous et al. “The Carboxy Terminus of the Ligand Peptide Determines the Stability of the MHC Class I Molecule H-2Kb: A Combined Molecular Dynamics and Experimental Study”. *PLoS ONE* **10** (2015). Ed. by S. Sadegh-Nasseri, e0135421.
- [160] G. Ishioka et al. “MHC interaction and T cell recognition of carbohydrates and glycopeptides.” *J. Immunol.* **148** (1992), pp. 2446–51.
- [161] T. Jensen et al. “T cell recognition of Tn-glycosylated peptide antigens”. *Eur. J. Immunol.* **26** (1996), pp. 1342–1349.
- [162] W. Overwijk et al. “Identification of a Kb-restricted CTL epitope of beta-galactosidase: potential use in development of immunization protocols for “self” antigens.” *Methods* **12** (1997), pp. 117–23.
- [163] B. Bolinger et al. “A new model for CD8+ T cell memory inflation based upon a recombinant adenoviral vector.” *J. Immunol.* **190** (2013), pp. 4162–74.
- [164] P. J. Tacken et al. “Dendritic-cell immunotherapy: from ex vivo loading to in vivo targeting”. *Nat. Rev. Immunol.* **7** (2007), pp. 790–802.
- [165] M. Luong et al. “Effects of fungal N- and O-linked mannosylation on the immunogenicity of model vaccines.” *Vaccine* **25** (2007), pp. 4340–4.
- [166] R. M. Bill. “Playing catch-up with Escherichia coli: using yeast to increase success rates in recombinant protein production experiments”. *Front. Microbiol.* **5** (2014).

- [167] S. C. Spohner et al. “Expression of enzymes for the usage in food and feed industry with *Pichia pastoris*”. *J. Biotechnol.* **202** (2015), pp. 118–134.
- [168] B. Byrne. “*Pichia pastoris* as an expression host for membrane protein structural biology”. *Curr. Opin. Struct. Biol.* **32** (2015), pp. 9–17.
- [169] I. Braakman and N. Balleid. “Protein folding and modification in the mammalian endoplasmic reticulum.” *Annu. Rev. Biochem.* **80** (2011), pp. 71–99.
- [170] R. B. Trimble et al. “Characterization of N- and O-linked glycosylation of recombinant human bile salt-stimulated lipase secreted by *Pichia pastoris*”. *Glycobiology* **14** (2003), pp. 265–274.
- [171] K. Ito and N. Matsudomi. “Structural characteristics of hen egg ovalbumin expressed in yeast *Pichia pastoris*.” *Biosci. Biotechnol. Biochem.* **69** (2005), pp. 755–61.
- [172] E. Kopera et al. “Expression, purification and characterization of glycosylated influenza H5N1 hemagglutinin produced in *Pichia pastoris*.” *Acta Biochim. Pol.* **61** (2014), pp. 597–602.
- [173] H. Muller-Steffner et al. “Identification of the N-glycosylation sites on recombinant bovine CD38 expressed in *Pichia pastoris*: Their impact on enzyme stability and catalytic activity”. *Protein Expression Purif.* **70** (2010), pp. 151–157.
- [174] R. Fonseca-Maldonado et al. “Biochemical properties of glycosylation and characterization of a histidine acid phosphatase (phytase) expressed in *Pichia pastoris*”. *Protein Expression Purif.* **99** (2014), pp. 43–49.
- [175] R. García et al. “Concanavalin A- and Wheat Germ Agglutinin-Conjugated Lectins as a Tool for the Identification of Multiple N-Glycosylation Sites in Heterologous Protein Expressed in Yeast”. *Anal. Biochem.* **231** (1995), pp. 342–348.
- [176] K. Kukk, S. Kasvandik, and N. Samel. “N-glycosylation site occupancy in human prostaglandin H synthases expressed in *Pichia pastoris*”. *SpringerPlus* **3** (2014), p. 436.
- [177] T. Suzuki et al. “Site-specific de-N-glycosylation of diglycosylated ovalbumin in hen oviduct by endogenous peptide: N-glycanase as a quality control system for newly synthesized proteins.” *Proc. Natl. Acad. Sci. U.S.A.* **94** (1997), pp. 6244–9.
- [178] D. H. Juers, B. W. Matthews, and R. E. Huber. “LacZ  $\beta$ -galactosidase: Structure and function of an enzyme of historical and molecular biological importance”. *Protein Sci.* **21** (2012), pp. 1792–1807.
- [179] M. Shelikoff, A. J. Sinskey, and G. Stephanopoulos. “A modeling framework for the study of protein glycosylation”. *Biotechnol. Bioeng.* **50** (1996), pp. 73–90.
- [180] Y. Doyon et al. “Effect of C-domain N-glycosylation and deletion on rat pancreatic alpha-amylase secretion and activity”. *Biochem. J.* **362** (2002), pp. 259–264.
- [181] C. E. Mire et al. “A Recombinant Hendra Virus G Glycoprotein Subunit Vaccine Protects Nonhuman Primates against Hendra Virus Challenge”. *J. Virol.* **88** (2014), pp. 4624–4631.
- [182] D. Govindarajan et al. “Preclinical development of a dengue tetravalent recombinant subunit vaccine: Immunogenicity and protective efficacy in nonhuman primates”. *Vaccine* **33** (2015), pp. 4105–4116.



- [183] T. Shibayama et al. “Characterization of seven genotypes (A to E, G and H) of Hepatitis B virus recovered from Japanese patients infected with human immunodeficiency virus type 1”. *J. Med. Virol.* **76** (2005), pp. 24–32.
- [184] Juniastuti et al. “Another novel subgenotype of hepatitis B virus genotype C from papuans of Highland origin”. *J. Med. Virol.* **83** (2010), pp. 225–234.
- [185] R. Y. Tsien. “The green fluorescent protein”. *Annu. Rev. Biochem.* **67** (1998), pp. 509–544.
- [186] G. T. Hanson et al. “Investigating Mitochondrial Redox Potential with Redox-sensitive Green Fluorescent Protein Indicators”. *J. Biol. Chem.* **279** (2004), pp. 13044–13053.
- [187] M. Bañó-Polo et al. “N-glycosylation efficiency is determined by the distance to the C-terminus and the amino acid preceding an Asn-Ser-Thr sequon”. *Protein Sci.* **20** (2010), pp. 179–186.
- [188] C. M. J. Sagt et al. “Introduction of an N-Glycosylation Site Increases Secretion of Heterologous Proteins in Yeasts”. *Appl. Environ. Microbiol.* **66** (2000), pp. 4940–4944.
- [189] M. Kaup et al. “Construction and analysis of a novel peptide tag containing an unnatural N-glycosylation site.” *FEBS Lett.* **585** (2011), pp. 2372–6.
- [190] R. A. Brierley. “Secretion of Recombinant Human Insulin-Like Growth Factor I (IGF-I)”. In: *Pichia Protocols*. Springer Science + Business Media, 1998, pp. 149–178.
- [191] S. Mochizuki et al. “Expression and Characterization of Recombinant Human Antithrombin III in *Pichia pastoris*”. *Protein Expression Purif.* **23** (2001), pp. 55–65.
- [192] T. Wileman, M. Lennartz, and P. Stahl. “Identification of the macrophage mannose receptor as a 175-kDa membrane protein.” *Proc. Natl. Acad. Sci. U.S.A.* **83** (1986), pp. 2501–5.
- [193] M. Lennartz, T. Wileman, and P. Stahl. “Isolation and characterization of a mannose-specific endocytosis receptor from rabbit alveolar macrophages.” *Biochem. J.* **245** (1987), pp. 705–11.
- [194] G. S. Canton J Neculai D. “Scavenger receptors in homeostasis and immunity.” *Nat. Rev. Immunol.* **13** (2013), pp. 621–34.
- [195] L. Martinez-Pomares. “The mannose receptor.” *J Leukoc Biol* **92** (2012), pp. 1177–86.
- [196] M. Aebi et al. “N-glycan structures: recognition and processing in the ER”. *Trends Biochem. Sci.* **35** (2010), pp. 74–82.
- [197] K. Mahnke et al. “The dendritic cell receptor for endocytosis, DEC-205, can recycle and enhance antigen presentation via major histocompatibility complex class II-positive lysosomal compartments.” *J. Cell Biol.* **151** (2000), pp. 673–84.
- [198] S. Wallner et al. “The Role of the E3 Ligase Cbl-B in Murine Dendritic Cells”. *PLoS ONE* **8** (2013). Ed. by M. Platten, e65178.
- [199] S. Viriyakosol et al. “Dectin-1 Is Required for Resistance to *Coccidioidomycosis* in Mice”. *mBio* **4** (2013), e00597–12–e00597–12.
- [200] A. Yonekawa et al. “Dectin-2 Is a Direct Receptor for Mannose-Capped Lipoarabinomannan of *Mycobacteria*”. *Immunity* **41** (2014), pp. 402–413.

- [201] C. Platt et al. “Mature dendritic cells use endocytic receptors to capture and present antigens.” *Proc. Natl. Acad. Sci. U.S.A.* **107** (2010), pp. 4287–92.
- [202] E. Amiel et al. “Scavenger receptor-A functions in phagocytosis of *E. coli* by bone marrow dendritic cells”. *Exp. Cell Res.* **313** (2007), pp. 1438–1448.
- [203] C. C. Norbury et al. “Constitutive macropinocytosis allows TAP-dependent major histocompatibility complex class I presentation of exogenous soluble antigen by bone marrow-derived dendritic cells”. *Eur. J. Immunol.* **27** (1997), pp. 280–288.
- [204] M. B. West et al. “Detection of distinct glycosylation patterns on human  $\gamma$ -glutamyl transpeptidase 1 using antibody-lectin sandwich array (ALSA) technology”. *BMC Biotechnol.* **14** (2014).
- [205] J. Garcia-Vallejo and Y. van Kooyk. “The physiological role of DC-SIGN: a tale of mice and men.” *Trends Immunol.* **34** (2013), pp. 482–6.
- [206] A. Powlesland et al. “Widely divergent biochemical properties of the complete set of mouse DC-SIGN-related proteins.” *J. Biol. Chem.* **281** (2006), pp. 20440–9.
- [207] K. Nagaoka et al. “Expression of C-type lectin, SIGNR3, on subsets of dendritic cells, macrophages, and monocytes”. *J. Leukocyte Biol.* **88** (2010), pp. 913–924.
- [208] K. Takahashi and R. A. B. Ezekowitz. “The Role of the Mannose-Binding Lectin in Innate Immunity”. *Clin. Infect. Dis.* **41** (2005), S440–S444.
- [209] L. East and C. Isacke. “The mannose receptor family.” *Biochim. Biophys. Acta* **1572** (2002), pp. 364–86.
- [210] J. Valladeau et al. “Langerin, a Novel C-Type Lectin Specific to Langerhans Cells, Is an Endocytic Receptor that Induces the Formation of Birbeck Granules”. *Immunity* **12** (2000), pp. 71–81.
- [211] E. P. McGreal et al. “The carbohydrate-recognition domain of Dectin-2 is a C-type lectin with specificity for high mannose”. *Glycobiology* **16** (2006), pp. 422–430.
- [212] R. T. Lee et al. “Survey of immune-related, mannose/fucose-binding C-type lectin receptors reveals widely divergent sugar-binding specificities”. *Glycobiology* **21** (2010), pp. 512–520.
- [213] K. Bloem et al. “Ligand Binding and Signaling of Dendritic Cell Immunoreceptor (DCIR) Is Modulated by the Glycosylation of the Carbohydrate Recognition Domain”. *PLoS ONE* **8** (2013). Ed. by M. Lahmann, e66266.
- [214] S. A. F. Jégouzo et al. “A Novel Mechanism for Binding of Galactose-terminated Glycans by the C-type Carbohydrate Recognition Domain in Blood Dendritic Cell Antigen 2”. *J. Biol. Chem.* **290** (2015), pp. 16759–16771.
- [215] A. Persson, D. Chang, and E. Crouch. “Surfactant protein D is a divalent cation-dependent carbohydrate-binding protein.” *J. Biol. Chem.* **265** (1990), pp. 5755–60.
- [216] E. C. Crouch. *Respir. Res.* **1** (2000), p. 93.
- [217] H. Sheikh et al. “Endo180, an endocytic recycling glycoprotein related to the macrophage mannose receptor is expressed on fibroblasts, endothelial cells and macrophages and functions as a lectin receptor.” *J. Cell Sci.* **113** (2000), pp. 1021–32.

- [218] M. Melander et al. “The collagen receptor uPARAP/Endo180 in tissue degradation and cancer (Review)”. *Int. J. Oncol.* (2015).
- [219] L. H. Engelholm et al. “Targeting a novel bone degradation pathway in primary bone cancer by inactivation of the collagen receptor uPARAP/Endo180”. *J. Pathol.* **238** (2015), pp. 120–133.
- [220] A. Dzionek et al. “BDCA-2, a Novel Plasmacytoid Dendritic Cell-specific Type II C-type Lectin, Mediates Antigen Capture and Is a Potent Inhibitor of Interferon  $\alpha/\beta$  Induction”. *The Journal of Experimental Medicine* **194** (2001), pp. 1823–1834.
- [221] L. Bonifaz et al. “In vivo targeting of antigens to maturing dendritic cells via the DEC-205 receptor improves T cell vaccination.” *J. Exp. Med.* **199** (2004), pp. 815–24.
- [222] T. Athmaram et al. “Yeast expressed recombinant Hemagglutinin protein of novel H1N1 elicits neutralising antibodies in rabbits and mice.” *Viol. J.* **8** (2011), p. 524.
- [223] S. Murugan et al. “Recombinant haemagglutinin protein of highly pathogenic avian influenza A (H5N1) virus expressed in *Pichia pastoris* elicits a neutralizing antibody response in mice.” *J. Virol. Methods* **187** (2013), pp. 20–5.
- [224] H. Yan et al. “Targeting C-Type Lectin Receptors for Cancer Immunity.” *Front Immunol* **6:408**. (2015), doi: 10.3389/fimmu.2015.00408. eCollection 2015.
- [225] R. Shrimpton et al. “CD205 (DEC-205): a recognition receptor for apoptotic and necrotic self.” *Mol. Immunol.* **46** (2009), pp. 1229–39.
- [226] M. Lahoud et al. “DEC-205 is a cell surface receptor for CpG oligonucleotides.” *Proc. Natl. Acad. Sci. U.S.A.* **109** (2012), pp. 16270–5.
- [227] G. Lambeau, P. Ancian, and M. Barhanin J. Lazdunski. “Cloning and expression of a membrane receptor for secretory phospholipases A2.” *J. Biol. Chem.* **269** (1994), pp. 1575–8.
- [228] P. Ancian et al. “The human 180-kDa receptor for secretory phospholipases A2. Molecular cloning, identification of a secreted soluble form, expression, and chromosomal localization.” *J. Biol. Chem.* **270** (1995), pp. 8963–70.
- [229] J.-P. Nicolas, G. Lambeau, and M. Lazdunski. “Identification of the Binding Domain for Secretory Phospholipases A2 on Their M-type 180-kDa Membrane Receptor”. *J. Biol. Chem.* **270** (1995), pp. 28869–28873.
- [230] M. Darmostuk et al. “Current approaches in SELEX: An update to aptamer selection technology”. *Biotechnol. Adv.* **33** (2015), pp. 1141–1161.
- [231] T. S. Johnson et al. “Inhibition of Melanoma Growth by Targeting of Antigen to Dendritic Cells via an Anti-DEC-205 Single-Chain Fragment Variable Molecule”. *Clin. Cancer Res.* **14** (2008), pp. 8169–8177.
- [232] C. Cheong et al. “Improved cellular and humoral immune responses in vivo following targeting of HIV Gag to dendritic cells within human anti-human DEC205 monoclonal antibody”. *Blood* **116** (2010), pp. 3828–3838.
- [233] B. C. Wengerter et al. “Aptamer-targeted Antigen Delivery”. *Mol. Ther.* **22** (2014), pp. 1375–1387.

- [234] A. N. Zelensky and J. E. Gready. “The C-type lectin-like domain superfamily”. *FEBS J.* **272** (2005), pp. 6179–6217.
- [235] E. Hartung et al. “Induction of Potent CD8 T Cell Cytotoxicity by Specific Targeting of Antigen to Cross-Presenting Dendritic Cells In Vivo via Murine or Human XCR1”. *The Journal of Immunology* **194** (2014), pp. 1069–1079.
- [236] M. M. C. van Beers and M. Bardor. “Minimizing immunogenicity of biopharmaceuticals by controlling critical quality attributes of proteins”. *Biotechnol. J.* **7** (2012), pp. 1473–1484.
- [237] A. Heiskanen et al. “Glycomics of bone marrow-derived mesenchymal stem cells can be used to evaluate their cellular differentiation stage”. *Glycoconj J* **26** (2008), pp. 367–384.
- [238] H. J. An et al. “Extensive Determination of Glycan Heterogeneity Reveals an Unusual Abundance of High Mannose Glycans in Enriched Plasma Membranes of Human Embryonic Stem Cells”. *Molecular & Cellular Proteomics* **11** (2011), pp. M111.010660–M111.010660.
- [239] P. Allavena et al. “Engagement of the Mannose Receptor by Tumoral Mucins Activates an Immune Suppressive Phenotype in Human Tumor-Associated Macrophages”. *Clin. Dev. Immunol.* **2010** (2010), pp. 1–10.
- [240] K. Sato et al. “Dectin-2 Is a Pattern Recognition Receptor for Fungi That Couples with the Fc Receptor  $\gamma$  Chain to Induce Innate Immune Responses”. *J. Biol. Chem.* **281** (2006), pp. 38854–38866.
- [241] S. Yamasaki et al. “Mincle is an ITAM-coupled activating receptor that senses damaged cells”. *Nat. Immunol.* **9** (2008), pp. 1179–1188.
- [242] M. Wang et al. “Single-chain Fv with manifold N-glycans as bifunctional scaffolds for immunomolecules”. *Protein Engineering Design and Selection* **11** (1998), pp. 1277–1283.
- [243] R. Montesino et al. “Variation in N-Linked Oligosaccharide Structures on Heterologous Proteins Secreted by the Methylophilic Yeast *Pichia pastoris*”. *Protein Expression Purif.* **14** (1998), pp. 197–207.
- [244] B. Pasquier et al. “Identification of Fc $\alpha$ RI as an inhibitory receptor that controls inflammation: dual role of FcR $\gamma$  ITAM.” *Immunity* **22** (2005), pp. 31–42.
- [245] G. D. Brown and S. Gordon. “Fungal beta-Glucans and Mammalian Immunity”. *Immunity* **19** (2003), pp. 311–315.
- [246] B. Guan et al. “Absence of Yps7p, a putative glycosylphosphatidylinositol-linked aspartyl protease in *Pichia pastoris*, results in aberrant cell wall composition and increased osmotic stress resistance”. *FEMS Yeast Res.* **12** (2012), pp. 969–979.
- [247] B. Chagas et al. “Chbeta-glucan complex production by *Komagataella* (*Pichia*) *pastoris*: impact of cultivation pH and temperature on polymer content and composition”. *New Biotechnol.* **31** (2014), pp. 468–474.
- [248] G. D. Brown and S. Gordon. “Immune recognition: A new receptor for beta-glucans”. *Nature* **413** (2001), pp. 36–37.

- [249] G. D. Brown et al. “Dectin-1 Is A Major beta-Glucan Receptor On Macrophages”. *The Journal of Experimental Medicine* **196** (2002), pp. 407–412.
- [250] P. R. Taylor et al. “Dectin-1 is required for beta-glucan recognition and control of fungal infection”. *Nat. Immunol.* **8** (2006), pp. 31–38.
- [251] T. Harada et al. “Highly Expressed Dectin-1 on Bone Marrow-Derived Dendritic Cells Regulates the Sensitivity to beta-Glucan in DBA/2 Mice”. *Journal of Interferon & Cytokine Research* **28** (2008), pp. 477–486.
- [252] A. Engering et al. “The mannose receptor functions as a high capacity and broad specificity antigen receptor in human dendritic cells.” *Eur. J. Immunol.* **27** (1997), pp. 2417–25.
- [253] A. Engering et al. “The dendritic cell-specific adhesion receptor DC-SIGN internalizes antigen for presentation to T cells.” *J. Immunol.* **168** (2002), pp. 2118–26.
- [254] M. M. Weck et al. “hDectin-1 is involved in uptake and cross-presentation of cellular antigens”. *Blood* **111** (2008), pp. 4264–4272.
- [255] S. B. Boscardin et al. “Antigen targeting to dendritic cells elicits long-lived T cell help for antibody responses”. *J. Exp. Med.* **203** (2006), pp. 599–606.
- [256] A. Donadei et al. “Rational Design of Adjuvant for Skin Delivery: Conjugation of Synthetic  $\beta$ -Glucan Dectin-1 Agonist to Protein Antigen.” *Mol. Pharm.* **12** (2015), pp. 1662–1672.
- [257] J. Li et al. “Antibodies targeting Clec9A promote strong humoral immunity without adjuvant in mice and non-human primates”. *Eur. J. Immunol.* **45** (2015), pp. 854–864.
- [258] C. Hesse et al. “In vivo targeting of human DC-SIGN drastically enhances CD8+ T-cell-mediated protective immunity”. *Eur. J. Immunol.* **43** (2013), pp. 2543–2553.
- [259] L.-Z. He et al. “Toll-like receptor agonists shape the immune responses to a mannose receptor-targeted cancer vaccine”. *Cell. Mol. Immunol.* **12** (2014), pp. 719–728.
- [260] M. Wang et al. “Expression and immunogenic characterization of recombinant gp350 for developing a subunit vaccine against Epstein-Barr virus”. *Appl. Microbiol. Biotechnol.* **100** (2015), pp. 1221–1230.
- [261] J. Herre et al. “Dectin-1 uses novel mechanisms for yeast phagocytosis in macrophages”. *Blood* **104** (2004), pp. 4038–4045.
- [262] P. R. Moody et al. “Receptor Crosslinking: A General Method to Trigger Internalization and Lysosomal Targeting of Therapeutic Receptor:Ligand Complexes”. *Mol. Ther.* **23** (2015), pp. 1888–1898.
- [263] T. S. Raju and B. J. Scallon. “Glycosylation in the Fc domain of IgG increases resistance to proteolytic cleavage by papain”. *Biochem. Biophys. Res. Commun.* **341** (2006), pp. 797–803.
- [264] D. Russell, N. J. Oldham, and B. G. Davis. “Site-selective chemical protein glycosylation protects from autolysis and proteolytic degradation”. *Carbohydr. Res.* **344** (2009), pp. 1508–1514.

- [265] H. Hayashi and Y. Yamashita. “Role of N-glycosylation in cell surface expression and protection against proteolysis of the intestinal anion exchanger SLC26A3”. *AJP: Cell Physiology* **302** (2011), pp. C781–C795.
- [266] F. Steinhagen et al. “TLR-based immune adjuvants”. *Vaccine* **29** (2011), pp. 3341–3355.
- [267] L. Cohn and L. Delamarre. “Dendritic Cell-Targeted Vaccines”. *Front Immunol* **5** (2014).
- [268] X. Shen et al. “Direct Priming and Cross-Priming Contribute Differentially to the Induction of CD8+ CTL Following Exposure to Vaccinia Virus Via Different Routes”. *The Journal of Immunology* **169** (2002), pp. 4222–4229.
- [269] J. Rauen et al. “Enhanced cross-presentation and improved CD8+ T cell responses after mannosylation of synthetic long peptides in mice.” *PLoS ONE* **9** (2014), e103755.
- [270] T. Keler, V. Ramakrishna, and M. Fanger. “Mannose receptor-targeted vaccines.” *Expert Opin. Biol. Ther.* **4** (2004), pp. 1953–62.
- [271] K. Elvevold et al. “Liver sinusoidal endothelial cells depend on mannose receptor-mediated recruitment of lysosomal enzymes for normal degradation capacity”. *Hepatology* **48** (2008), pp. 2007–2015.
- [272] C. Astarie-Dequeker et al. “The mannose receptor mediates uptake of pathogenic and nonpathogenic mycobacteria and bypasses bactericidal responses in human macrophages.” *Infect. Immun.* **67** (1999), pp. 469–77.
- [273] P. B. Kang et al. “The human macrophage mannose receptor directs Mycobacterium tuberculosis lipoarabinomannan-mediated phagosome biogenesis”. *The Journal of Experimental Medicine* **202** (2005), pp. 987–999.
- [274] G. Grabowski. “Gaucher disease and other storage disorders.” *Hematology Am Soc Hematol Educ Program.* (2012), pp. 13–8.

# Abbreviations

<b>ABTS</b> 2,2'-Azino-bis(3-ethylbenzothiazoline-6-sulfonic acid)	<b>EEA1</b> early endosome antigen-1
<b>ANOVA</b> analysis of variance	<b>ELISA</b> enzyme-linked immunosorbent assay
<b>AP</b> alkaline phosphatase	<b>Endo H</b> Endoglycosidase H
<b>APC</b> antigen presenting cell	<b>ER</b> endoplasmic reticulum
<b>APS</b> ammonium persulfate	<b>EtOH</b> ethanol
<b>BCA</b> bicinchoninic acid	<b>FACS</b> fluorescence-activated cell sorting
<b>BCR</b> B cell receptor	<b>FCA</b> Freund's complete adjuvant
<b>BES</b> N,N-Bis-(2-hydroxyethyl)-2-aminoethane sulphonic acid	<b>FCS</b> fetal calf serum
<b>BM-DC</b> bone marrow-derived dendritic cell	<b>FNII</b> fibronectin II
<b>BSA</b> bovine serum albumin	<b><math>\beta</math>-gal</b> $\beta$ -galactosidase
<b>CD</b> cluster of differentiation	<b>GFP</b> green fluorescent protein
<b>CFSE</b> carboxyfluorescein succinimidyl ester	<b>GM-CSF</b> granulocyte-macrophage colony-stimulating factor
<b>CHO</b> chinese hamster ovary	<b>HBV</b> hepatitis B virus
<b>CR</b> cysteine-rich	<b>HEK</b> human embryonic kidney
<b>CRD</b> carbohydrate recognition domain	<b>HEPES</b> N-2-Hydroxyethyl piperazine-N'-2-ethane sulphonic acid
<b>CTL</b> cytotoxic T lymphocyte	<b>HIV</b> human immunodeficiency virus
<b>CTLD</b> C-type lectin-like domain	<b>HRP</b> horseradish peroxidase
<b>DAPI</b> 4,6-diamidino-2-phenylindole	<b>HSD</b> honestly significant difference
<b>DC</b> dendritic cell	<b>i.d.</b> intradermal
<b>DCIR</b> dendritic cell immunoreceptor	<b>IFN-<math>\gamma</math></b> Interferon gamma
<b>DC-SIGN</b> dendritic cell-specific ICAM-3 grabbing non-integrin	<b>Ig</b> immunoglobulin
<b>DLEC or BDCA-2</b> dendritic cell lectin	<b>IL-12</b> interleukin-12
<b>DMEC</b> dermal microvascular endothelial cell	<b>IL-2</b> interleukin-2
<b>DMEM</b> Dulbecco's Modified Eagle's medium	<b>IL-4</b> interleukin-4
<b><i>E. coli</i></b> <i>Escherichia coli</i>	<b>IL-6</b> interleukin-6
<b>EDTA</b> ethylenediaminetetraacetic acid	<b>IMAC</b> immobilized metal affinity chromatography
	<b>IMDM</b> Iscove's Modified Dulbecco's medium
	<b>i.p.</b> intraperitoneal

<b>IRES</b> internal ribosome entry site	<b>PBMC</b> peripheral blood mononuclear cell
<b>ITAM</b> immuno-receptor tyrosine-based activation motif	<b>PBS</b> Phosphate-buffered saline
<b>i.v.</b> intravenous	<b>PCR</b> polymerase chain reaction
<b>LAMP-1</b> lysosomal-associated membrane protein 1	<b>PFA</b> paraformaldehyde
<b>LN</b> lymph node	<b>PMSF</b> Phenylmethylsulfonyl fluoride
<b>LPS</b> lipopolysaccharide	<b>PNGase F</b> Peptide-N-Glycosidase F
<b>LSEC</b> liver sinusoidal endothelial cell	<b>PRR</b> pattern recognition receptor
<b>MΦ</b> macrophage	<b>RPMI</b> Roswell Park Memorial Institute
<b>MACS</b> magnetic-activated cell sorting	<b>RT</b> room temperature
<b>ManLAM</b> mannose-capped lipoarabino-mannan	<b>S8L</b> SIINFEKL
<b>MBL</b> mannose-binding lectin	<b>s.c.</b> subcutaneous
<b>MCL</b> macrophage C-type lectin	<b>SDS</b> sodium dodecyl sulfate
<b>MCS</b> multiple cloning site	<b>SDS-PAGE</b> sodium dodecyl sulfate polyacrylamide gel electrophoresis
<b>M-CSF</b> macrophage colony-stimulating factor	<b>SELEX</b> systematic evolution of ligands by exponential enrichment
<b>MeOH</b> methanol	<b>SEM</b> standard error of the mean
<b>MF</b> mating factor alpha prepro leader sequence	<b>SLP</b> synthetic long peptide
<b>MFI</b> mean fluorescence intensity	<b>SP-D</b> surfactant protein D
<b>MHC</b> major histocompatibility complex	<b>TAE</b> Tris-acetate-EDTA
<b>Mincle</b> macrophage-inducible C-type lectin	<b>TBS</b> Tris buffered saline
<b>MOPS</b> 3-(N-Morpholino) propane sulfonic acid	<b>TCR</b> T cell receptor
<b>MR</b> mannose receptor	<b>TEMED</b> N,N,N',N'-Tetramethylethylenediamine
<b>Mw</b> molecular weight	<b>T<sub>h</sub> cell</b> T helper cell
<b>NCD</b> non-communicable disease	<b>TLR</b> toll-like receptor
<b>Ni-NTA</b> nickel-nitrilo-triacetic acid	<b>TNF-α</b> tumor necrosis factor alpha
<b>OVA</b> ovalbumin	<b>Trf</b> transferrin
<b>OVA-647</b> Alexa Fluor 647-labeled ovalbumin	<b>Tris</b> tris(hydroxymethyl)-aminomethane
<b><i>P. pastoris</i></b> <i>Pichia pastoris</i>	<b>Triton X-100</b> Polyethylene glycol alkylphenyl ether
<b>PAMP</b> pathogen-associated molecular pattern	<b>Tween 20</b> Polyoxyethylene-20-sorbitan monolaurate
	<b>XCL1</b> chemokine (C motif) ligand
	<b>YNB</b> yeast nitrogen base



# Glossary

**DesTCR** CD8<sup>+</sup> T cells that recognize three endogenous peptides in the Kb context

**HEK-MR** HEK cells expressing the MR

**hNST-GFP** NST-GFP expressed bei HEK293T cells

**hQST-GFP** QST-GFP expressed bei HEK293T cells

**MR-CTLD** Fc chimeric protein of MR CRDs 4–7 and the Fc part of human IgG1

**MR-Nterm** Fc chimeric protein of MR N-terminal part (CR, FNII, and CRDs 1–2) and the Fc part of human IgG1

**NST-GFP** A GFP derivative with an N-terminal *NST* sequon

**NST-GFP-S8L** NST-GFP with a C-terminal S8L sequence

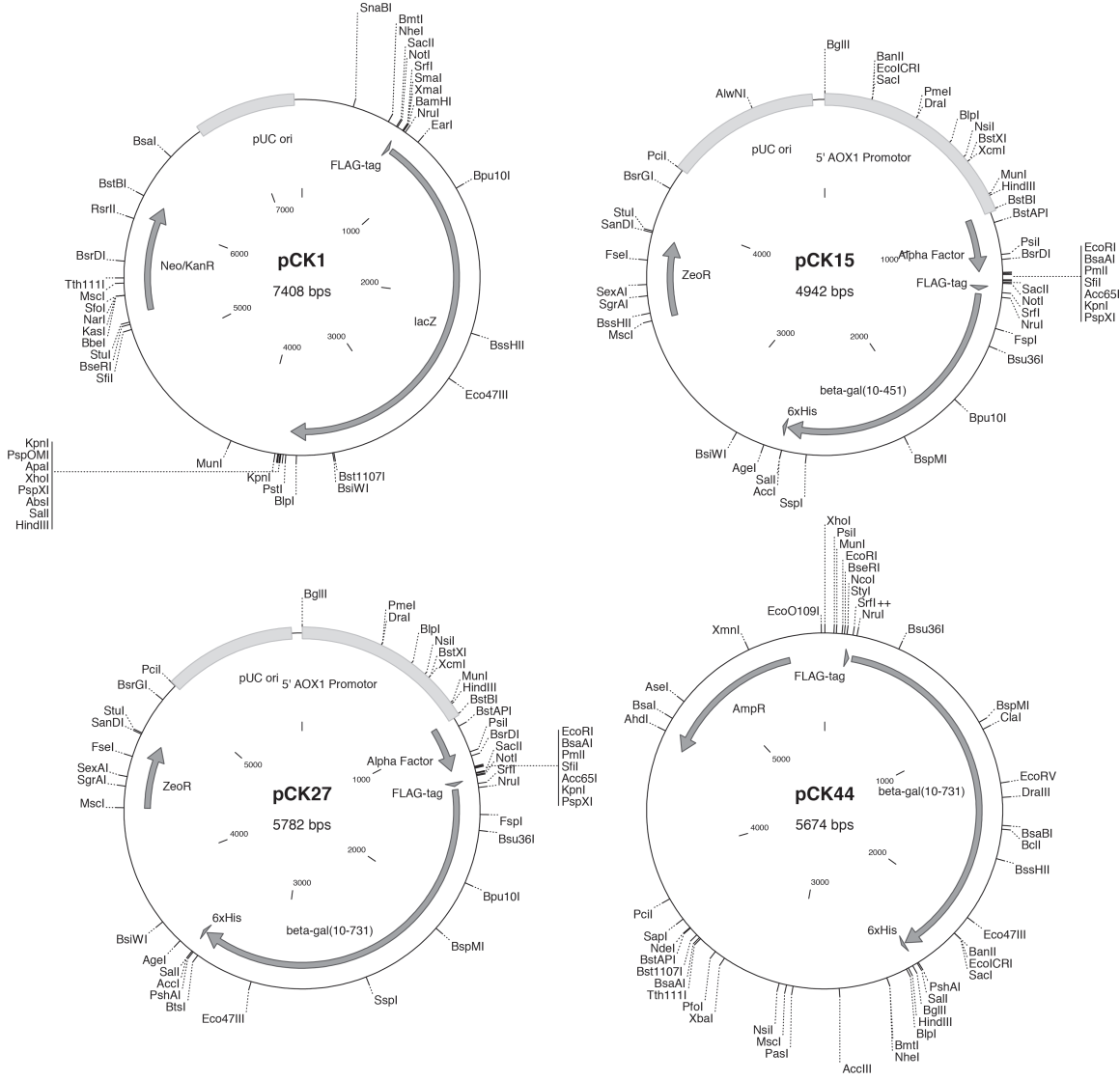
**OT-I** CD8<sup>+</sup> T cells that recognize the ovalbumin peptide OVA<sub>257–264</sub>

**OT-II** CD4<sup>+</sup> T cells that recognize the ovalbumin peptide OVA<sub>323–339</sub>

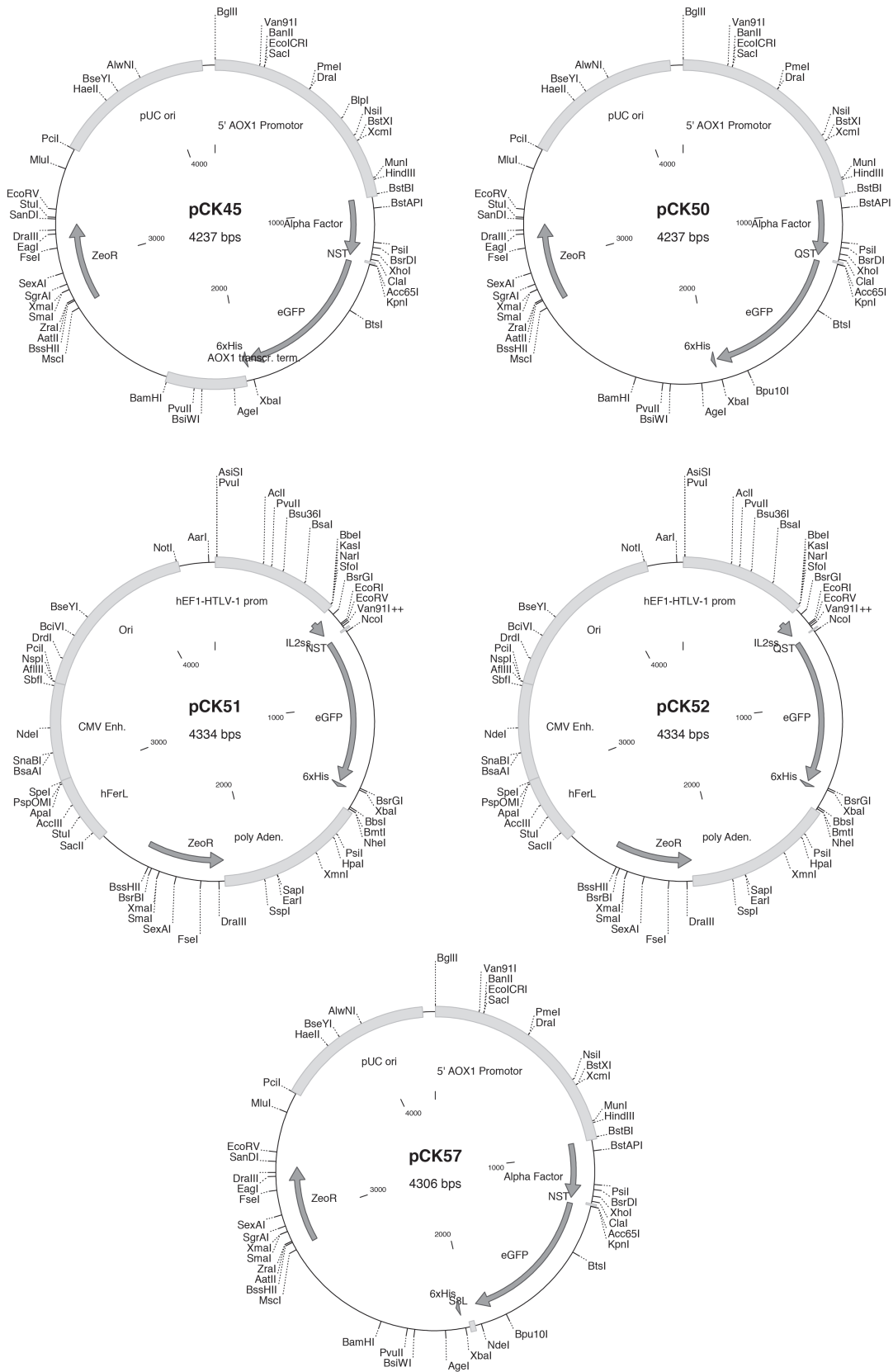
**QST-GFP** A GFP derivative with the N-terminal control sequence *QST*

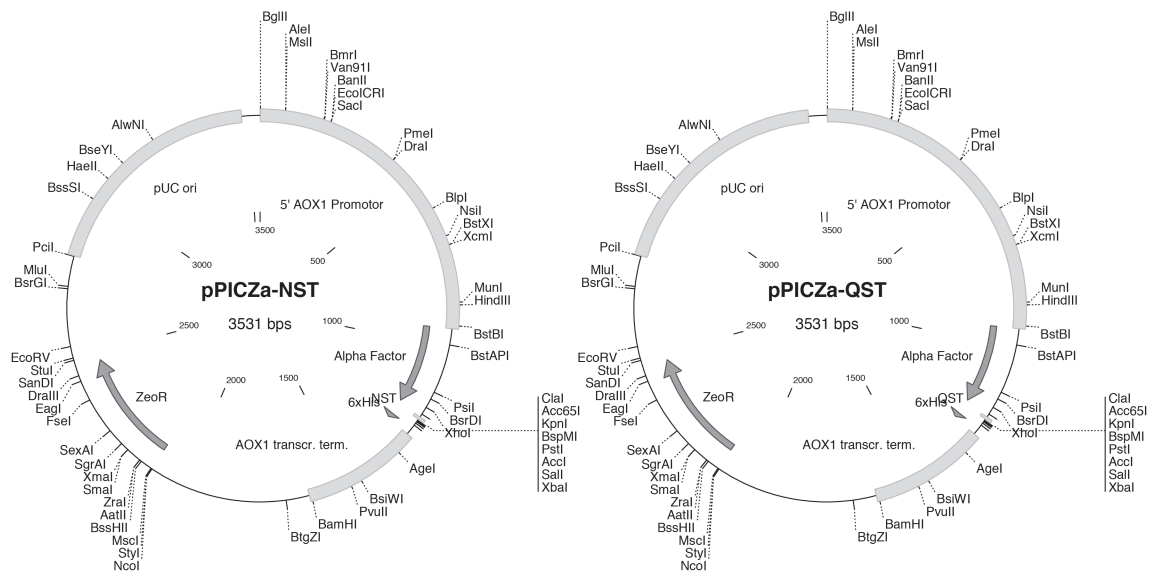
# A Plasmid maps

All plasmid maps were generated with CloneManager 5 software (Sci-Ed).



# A PLASMID MAPS





## B Acknowledgments

Firstly, I would like to thank my supervisor Prof. Dr. Sven Burgdorf, who gave me all the freedom to ask those questions that I was interested in, who was patient with me when I lost myself in details, and who was always open-minded for discussing all my ideas, concerns and questions.

Besides my advisor, I would like to thank the remaining members of my examination board for the time they have spent to evaluate this work.

Next, I would like to thank Beatrix Schumak and her group for the constructive input and for facilitating the *in vivo* experiments. In particular, I need to thank Janina Küpper, who put a lot of time and work into helping me with the *in vivo* experiments.

My sincere thanks also go to Prof. Hans Wandall for the inspiring discussion at the EMBO workshop on Glycobiology and Glycochemistry in 2014, to Prof. Dr. Erwin Galinski and Marlene Hecker for providing their resources and expertise in fermentation and finally to Prof. Dr. Andreas Meyer for sharing great tools, even though they did not make it into this thesis.

Many thanks to Guido Lüchters, who inspired me to critically think about data assessment and to tell significance from relevance.

I thank my labmates Maria, Verena and Judith for taking care of Matthias and me and for never giving up educating us in terms of tidiness. Special thanks to Matthias for the stimulating discussions, for taking good care of my yeasts in my absence, for the spontaneous cloak-and-dagger operations, and for all the fun we had in the lab. I also thank my colleagues from the LIMES Institute for a strong cooperativeness and team spirit, in particular AG Thiele, AG Lang, AG Schultze, AG Kolanus and AG Hoch for sharing critical equipment and expertise. I am exceptionally grateful to Rita, Elvira and Jenny from the scullery, who always supplied me with autoclaved medium on short notice.

Finally, I would like to thank my parents, my brother, and my sister for always believing in me and supporting me throughout my life. I would like to thank my mother-in-law for fighting her way through all these scientific terms and proofreading the manuscript, and last but not least I want to thank my wonderful wife Britta for all her patience, her love, and for backing me up to accomplish this thesis.